UNIVERSITÀ
DEGLI STUDI
DI PADOVA

Sede Amministrativa: Università degli Studi di Padova
Dipartimento di Biologia

SCUOLA DI DOTTORATO DI RICERCA IN: BIOSCIENZE E BIOTECNOLOGIE
INDIRIZZO: GENETICA E BIOLOGIA MOLECOLARE DELLO SVILUPPO
CICLO: XXV

TRANSCRIPTIONAL REPROGRAMMING OF MUSCLE FIBERS BY CHRONIC ELECTRICAL STIMULATION

Direttore della Scuola : Ch.mo Prof. Giuseppe Zanotti
Coordinatore d'indirizzo: Ch.mo Prof. Paolo Bonaldo
Supervisore : Ch.mo Prof. Gerolamo Lanfranchi

Dottorando : Giorgia Busolin

INDEX

ABSTRACT

Background: Skeletal muscle fibers have a remarkable capacity to adjust their molecular, functional, and metabolic properties in response to developmental and environmental stimuli. A central role for neuromuscular activity in determining skeletal muscle fibers composition was demonstrated by cross-innervation and electrical stimulation experiments in adult skeletal muscle. A fast to slow transition can be induced by chronic low-frequency electrical stimulation (CLFS). In literature, CLFS studies have focused on the effects produced after days or weeks of stimulation. Here, I present the first transcriptome study that identifies the earliest genetic changes in this process.

Methods. The fast EDL muscle was subjected to CLFS for 6 and 12 hours. First, microarray experiments were performed using whole EDL muscle. Then, in order to reduce biological noise caused by different cell types, I applied microgenomic analyses at the level of single fibers (SF), isolated according to the protocol recently developed in my laboratory. Microarray experiments have been produced with updated platforms (Agilent SurePrint G3 Mouse GE 8x60K).

Results and discussion. The expression profiles of whole muscle after 6 and 12 hours of electrical stimulation identified about two hundred differentially expressed (DE) genes. The functional categories of blood vessel development and transcription regulation were most enriched. Genomic analyses of isolated fibers identified more than a thousand DE genes after 12 hours of stimulation. The functional category of blood vessel development was enriched also at the SF level, suggesting that myofibers are able to interact with other cell types in order to stimulate the angiogenesis process. In general, muscle structural genes were equally expressed between stimulated and unstimulated muscles, indicating that changes in fiber type require prolonged stimulation. On the contrary, genes involved in transcription, chromatin-remodeling genes and several myofibril genes acting as signaling molecule were early activated after CLFS.

ABSTRACT (IN ITALIANO)

Introduzione: Le fibre del muscolo scheletrico possiedono una notevole capacità di modificare le loro proprietà molecolari, funzionali e metaboliche in risposta a stimoli di crescita e ambientali. Esperimenti di cross-innervazione e stimolazione elettrica hanno dimostrato il ruolo fondamentale dell'attività neuromuscolare nel determinare il tipo di fibra. La stimolazione cronica a bassa frequenza (CLFS) è in grado di indurre il processo di trasformazione di una fibra veloce verso un fenotipo lento. Fino ad ora, questi processi sono stati studiati dopo lunghi periodi di stimolazione. In questo lavoro, mi sono proposta di identificare i cambiamenti trascrizionali precoci di questo processo.

Metodi. Il muscolo veloce EDL di topo è stato sottoposto a CLFS per 6 e 12 ore. Inizialmente ho utilizzato il muscolo intero per produrre i profili di espressione Successivamente, per ovviare al problema dell'eterogenea composizione del muscolo, ho utilizzato l'approccio microgenomico, producendo profili di espressione a livello di una singola fibra, isolata utilizzando il protocollo sviluppato nel mio laboratorio. Tutti i profili sono stati ottenuti mediante l'utilizzo di piattaforme Agilent (SurePrint G3 Mouse GE 8x60K).

Risultati e discussione. I profili di espressione con il muscolo intero hanno identificato circa 200 geni differenzialmente espressi (DE). Lo sviluppo dei vasi sanguigni e la regolazione della trascrizione sono risultate le categorie funzionali più arricchite. Le analisi genomiche a livello di singola fibra hanno identificato più di mille geni DE dopo 12 ore di stimolazione. La categoria funzionale riguardante lo sviluppo dei vasi sanguigni risulta arricchita anche con questo approccio, suggerendo un'interazione tra le fibre muscolari e gli altri tipi cellulari al fine di stimolare il processo di angiogenesi. La maggiorparte dei geni strutturali risulta essere ugualmente espressa, suggerendo che i cambiamenti nel tipo di fibra richiedono un tempo prolungato. Al contrario, i geni coinvolti nella trascrizione, nel rimodellamento della cromatina e alcuni geni miofibrillari che agiscono come molecule di segnale, si attivano rapidamente in risposta a CLFS.

1. Introduction

1.1 Skeletal muscle fibers

1.1.1 Skeletal Muscle

Skeletal muscle comprises 40% of the body mass and is an effective transformer of electrical energy (from the nerve impulse), through chemical energy (by the breakdown of adenosine triphosphate) to mechanical energy, supporting respiration, movement and biochemical homeostasis (Helliwell T.R., 1999).

The basic functional units of skeletal muscle are the muscle fibers (Figure 1.1). Each muscle fiber is formed during development by the fusion of mononucleated cells known as myocytes. Myocytes are the postmitotic daughters of myoblasts, the stem cells of developing muscle. Myotubes, multinucleated skeletal muscle cells, originate from myocyte fusions. During maturation of the myotube, the centrally positioned nuclei move to the periphery and the myotubes lose their interconnecting junctions. These myotubes become adult muscle fibers, each with its innervation.

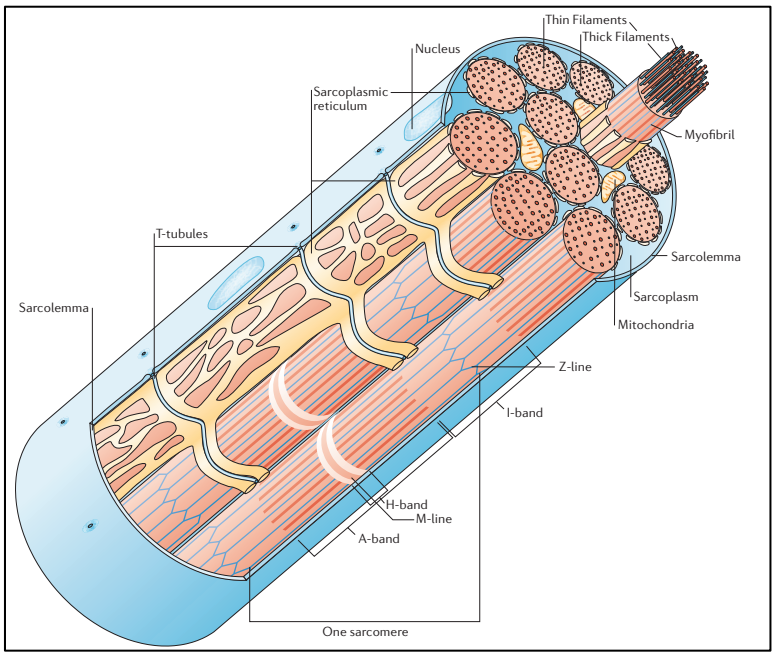

Figure 1.1: Myofibers structure. Skeletal muscle fibers are single and cylindrical cells. They have multiple nuclei, which are located on the periphery of the cell (Figure from Davies K.E. & Nowak K.J. 2006, with permission from Nature Publishing Group).

Myofibers may be several millimeters long and range in diameter from 10 to 100 µm. In longitudinal section the nuclei are located at the edge of the fiber and the cytoplasm is occupied by the contractile filaments, which show a regular pattern of cross-striation, under light microscope. Two type of nuclei are present within the fibers: the sarcolemmal nuclei, which control the functions of the fibers generating mRNA for protein synthesis, and satellite cell nuclei, which remain in a non-proliferative quiescent state. Myofibers posses a complicate membrane system: the basement membrane surrounds each muscle fiber and is covered by a network of type IV collagen which is linked to other proteins. The plasma membrane of the fiber, i.e. the sarcolemma, is situated immediately under the basement membrane. The fibers are packed with numerous myofibrils, about 1 to 3 µm diameter, each enveloped by the sarcoplasmic reticulum membrane. Myofibrils are themselves striated, and the striation pattern repeats with a periodicity of about 2 to 3 µm. The repeating unit, known as a sarcomere, is a contractile unit of the skeletal muscle (Figure 1.2). The sarcomere is bordered at each end by dense line known as the Z line. Each Z line bisects in two parts a lighter I band. In the middle of each sarcomere lies the dense A band, dissected by a less dense H zone. At the center of H zone is collocated a band of higher density, called M line (Craig R.W. & Padron R., 2003). The thick filaments, that comprised myosin and myosin binding protein, are located in A-band and run parallel to the fibril axis. Each half I band contains the thin filaments: actins, troponins, and tropomyosins. One end of each thin filament is anchored at the Z line, whereas the other end overlaps a portion of the thick filaments into the A band.

Skeletal muscle is a complex organ composed by several cell types in addition to myofibers. Each muscle contains various connective tissue components that contribute to the mechanical properties of muscle, promote myogenesis, and organize muscle regeneration. It is composed by three anatomical parts. A collagenous epimysium covers the entire surface of the muscle and separates it from other muscles. Smaller bundles of collagen extend inward from the epimysium to form the perimysium, which divides the muscle into groups of

fibers (fascicles). Nerves, blood vessels, and fat cells lie within the perimysium. Finally, endomysium envelops each muscle fiber and contains capillaries, nerves, fibroblast, macrophages, and a network of extracellular fibrils (Sanes J.R., 2003).

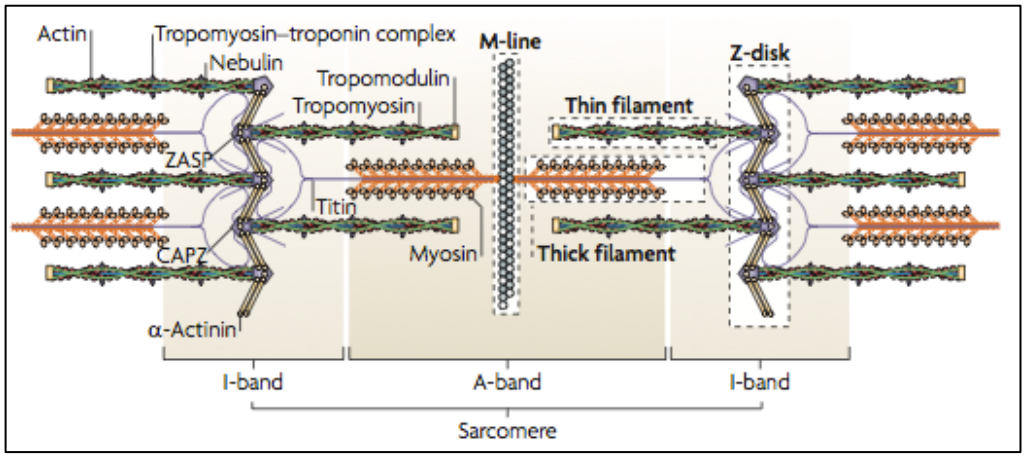

Figure 1.2: Sarcomere structure. The typical striated pattern is due to the complex structure of the sarcomere, the contractile unit of muscle (Figure from Sparrow J.C. & Schöck F., 2009, with permission from Nature Publishing Group).

1.1.2 Muscle fiber type with different myosin composition

Skeletal muscle is composed of heterogeneous specialized myofibers that enable the body to maintain posture and perform a wide range of movements and motions. (Bassel-Duby R. et al, 2006). Myofibers differ in size, metabolism, and contractile function. The overall properties of a muscle result from a combination of the individual properties of the different fiber types and their proportion (Pette D. et al, 2001).

During the last 50 years, several nomenclatures of fiber types have been followed. Ranvier proposed the first classification in 1873. He identified two major types of skeletal muscles: slow red muscles, involved in continuous tonic activity, and fast white muscles, with phasic activity. From 1960, histochemical staining showed that fibers of red muscle are rich in myoglobin and mitochondria, and exhibit oxidative metabolism, and fibers of white muscle are poor in mitochondria and exhibit glycolytic metabolism (Dubowitz V. & Pearse A.G., 1960; Gauthier G.F. & Padykula, 1966). The second classification started around 1970, when several studies led to the classification of slow oxidative type

1, fast-twitch oxidative glycolytic type 2A and fast-twitch glycolytic type 2B muscle fibers (Brooke M.H. & Kaiser K.K., 1970; Schiaffino S. et al, 1970; Peter J.B. et al, 1972). After the identification of a correlation between histochemical differences in myosin ATPase activity and myosin heavy chain (MyHC) isoform expression (Staron R.S. & Pette D., 1986), the ATPase staining procedure became the standard method for muscle fiber typing. The final step was characterized by the discovery of another fast type myosin heavy chain, called 2X, with intermediate properties between 2A and 2B (Schiaffino S. et al, 1989). In situ hybridization and immunohistochemical analysis of muscle sections (De Nardi C. et al, 1993; Gorza L. et al, 1990) and physiological studies (Bottinelli R. et al, 1994) confirmed the existence of a spectrum of fiber type, including pure and hybrid MyHC composition, according to the scheme: 1⇔1/2A⇔2A⇔2A/2X⇔2X⇔2X/2B⇔2B. This fiber type profile has been observed in different mammalian species, including mouse, rat, rabbit and guinea pig (Gorza L. et al, 1990); however, human muscle contain a more restricted repertoire of MyHC isoform, due to the absence of the 2B component (Smerdu V. et al., 1994).

The four fiber types identified on the basis of specific MyHC isoform expression are distributed in body muscles of mammals, and the relative proportion vary according to species and anatomical site. Slow type I myofibers are characterized by slow contraction, high content in mitochondria, high number of capillaries surrounding each fiber, and exhibit oxidative metabolism and resistance to fatigue. They are recruited for postural support and tasks involving endurance. Fast type II fibers comprise a wide spectrum of fibers with variable properties: at one extreme 2A fibers, more similar to type 1, and at the other side 2B fibers, that exhibit glycolytic metabolism, contract rapidly, and have low resistance to fatigue. 2B myofibers are required for movements involving strength and speed (Figure 1.3).

Although MyHC isoforms appear the best available marker for fiber typing, specific programs of gene expression also exist for other myofibrillar proteins

and their isoforms (Schiaffino S. & Reggiani C., 1996). Furthermore, the expression levels of some proteins and metabolic enzymes vary in fiber type manner, adding a further level of complexity to the concept of muscle fiber heterogeneity.

MyHC	Metabolism	Contraction speed	Resistance to fadigue	Cross-sectional area	Capillary density
1	oxidative	slow	high	small	high
2A	⇕	⇕	⇕	⇕	⇕
2X	⇕	⇕	⇕	⇕	⇕
2B	glycolitic	fast	low	large	low

Figure 1.3: The properties of fiber types in mammalian skeletal muscle.

1.1.3 Role of nerve in fiber type heterogeneity

In mammals, the neuromuscular system is organized into motor units, which are composed of a motor neuron and a group of muscle fibers with similar structural and functional properties. Each branch of a motor neuron forms a specialized synapse with a muscle fiber, called neuromuscular junction. The region of the sarcolemma that contributes to the neuromuscular junction is known as motor end plate.

The selective recruitment of motor units and the heterogeneity of muscle fibers is the base of the flexibility which enables the same muscle to respond to different functional demands, from continuous low-intensity activity (e.g., posture), to long-lasting and repetitive activities like respiration or locomotion, and to fast and strong maximal contractions (e.g. jumping, kicking). The connection of the various fiber types with motor neurons with specific activity (discharge pattern or firing pattern) is also important for fiber type remodeling in adult muscles.

Motor neurons display great differences in the firing patterns. 50 years ago, two classes of motor neurons, “tonic” and “phasic,” have been described (Granit R. et al, 1956). Studies in rat, using continuous electromyography (EMG) recording of

single motor units, have made possible the identification of three distinct firing patterns (Henning R. & Lomo T., 1985). The first pattern is typical of slow fibers. It is characterized by high amount of impulse activity (300,000–500,000 over 24 h), with long-lasting trains (300–500 s) and low frequency of firing (about 20 Hz). The slow motor neurons are active almost continuously because the slow motor units are utilized constantly to maintain posture and antagonize gravity. The second pattern, corresponding to 2B fibers, shows very modest amount of activity per day (3,000–10,000 impulses), high discharge frequency (70–90 Hz), and short duration of the trains (<3 s). Finally, the third pattern, corresponds to 2A and 2X fibers, has similar discharge frequency respect 2B (50–80 Hz), but has much greater activity per day (90,000–250,000 impulses) and relatively long train duration (60–140 s) (Schiaffino S. & Reggiani C., 2011). Those different patterns of activity have a profound influence on characteristics of different fiber types, such as contractile machinery, calcium shuttling mechanisms, structure of the cytoskeleton, and energy metabolism.

1.1.4 Excitation-Contraction Coupling

In skeletal muscle fibers the interaction of contractile proteins is responsible for the shortening and the production of force. Skeletal muscle fibers use the changes in intracellular calcium concentration ($[Ca^{2+}]_i$) to control the interaction of the contractile proteins. An increase in $[Ca^{2+}]_i$ will cause shortening, and a decrease of $[Ca^{2+}]_i$ will result in relaxation. Excitation–contraction (EC) coupling is the process in which an electrical depolarization of the plasma membrane causes the mechanical activation of the contractile myofibrils lying within the membrane (Sandow A, 1965).

The process starts with the arrival of an action potential at the motor end plate of the axon causing the release of acetylcholine from storage vesicles into neuromuscular junction. Acetylcholine molecules bind to nicotinic acetylcholine receptors on the end plate of the muscle fiber membrane causing an instantaneous increase in sodium and potassium conductance. End-plate

potentials lead to generation of action potentials along the sarcolemmal membrane and into invaginations of the sarcolemma, called transverse tubules (T-tubules; Figure 1.4). Each T-tubule is tightly associated with the sarcoplasmic reticulum (SR), in a region called terminal cisternae (Payne A.M. & Delbono O., 2006). The close association of one T-tubule with two terminal cisternae on both sides of the tubule is called the triad (Felder E. et al., 2002). Membrane depolarization activates the dihydropyridine-sensitive L-type Ca^{2+} channel in T-tubule membrane, also called dihydropyridine receptor (DHPR) (Rios E. & Brum G., 1987). A single DHPR is a protein complex consisting of 5 subunits: α1, α2, β, γ, and δ. The α1 subunit is able to function alone as a voltage gated Ca^{2+} channel, while the other subunits have modulatory functions (Catteral W.A., 1991). After activation, the DHPR α1 subunit interacts with the ryanodine receptor (RyR) to evoke Ca^{2+} release from the SR terminal cisternae (Marty I. et al., 1994). RyRs are the intracellular Ca^{2+} release channels and they are homotetramers, composed by four identical subunits forming a structure with rotation symmetry (Serysheva I.I. et al., 1999). Several isoforms of RyRs exist: RyR1 is the skeletal muscle type (Takeshima H. et al., 1989). Ca^{2+} released from RyR1s binds to diverse targets, including troponin C. After removing tropomyosin blockade of actin binding sites. Now, MyHC heads can bind actin to form cross-bridges and produce active shortening of muscle fibers (Melzer W. et al., 1995, Payne A.M. & Delbono O., 2006).

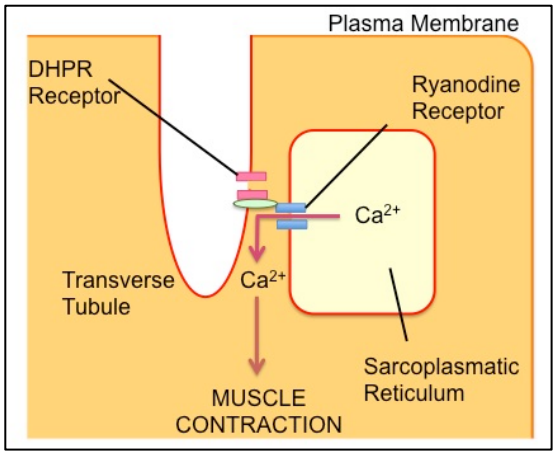

Figure 1.4: Schematic diagram of EC coupling. The depolarization of an action potential is detected by the DHPR voltage sensors in the T-tubules, which directly control the opening and closure of RyR in the adjacent SR.

In contrast to the passive entry of Ca^{2+} following its electrochemical gradient, removal of Ca^{2+} from the cytoplasm requires the expenditure of chemical energy and has a fixed stoichiometry of two Ca^{2+} ions transported per ATP hydrolyzed. The active re-uptake of calcium into SR is carried out by sarco(endo)plasmic reticulum calcium ATPase (SERCA) (Barton K.N. & MacLennan D.H., 2003). SERCA proteins are encoded by three different genes with alternative splicing variants (Periasamy M & Kalyanasundaram A., 2007). SERCA1a is expressed in fast-twitch skeletal fibers, while Serca1b is an alternative-splicing variant expressed in fetal and neonatal muscle. SERCA2a is expressed in slow skeletal fibers and in cardiac muscle, and SERCA2b is expressed in smooth muscles. SERCA3 is found in non-muscle cells, such as platelets, lymphoid and endothelial cells (Lytton J. et al., 1992). The density of the pump is much greater (5- to 7-fold) in fast than in slow fibers (Everts M.E. et al., 1989; Wu K.D. & Lytton J., 1993). Fast fibers have a more efficient system to removal of Ca^{2+} from the cytoplasm, so they relax faster than slow fibers. Calcium ions pumped into SR by SERCAs are transferred to calcium binding proteins localized within SR. Calsequestrin (CASQ) is the most important calcium binding protein inside SR, and is located in the terminal cysternae near to RyR. CASQ works as calcium buffer and as modulator of calcium release, interacting with RyR (Beard N.A. et al., 2004). Calsequestrin has two isoforms: CASQ1 and CASQ2. Both isoforms can be found in slow fibers, whereas only CASQ1 is expressed in fast fibers (Damiani E. & Margreth A., 1994). Furthermore, the content of CASQ protein is greater in fast than in slow fibers (Leberer E. et al., 1988). Another calcium binding protein is parvalbumin, which is expressed in fast fibers, but is absent in slow fibers in normal condition (Campbell W.G. et al., 2001). The important role of parvalbumin in regulating the speed of relaxation is supported by studies in parvalbumin knockout mice, which show a marked prolongation of the calcium transient (Schwaller B. et al., 1999).

1.1.5 Myofibrillar Protein Diversity

Striated muscles are organs specialized for the rapid generation of movement and force. So, skeletal muscle fibers are highly organized and composed of myofibrils, resulting from repeating units arranged in series, the sarcomeres (Figure 1.2). The sarcomere is a complex structure containing, in vertebrate muscle, at least 28 different proteins. These proteins show multiple isoforms, due to specific tissue distribution, and can be used as markers for fiber types (Schiaffino S. & Reggiani C., 1996). Myofibrillar proteins can be divided in three functional classes: contractile, regulatory, and structural (Craig R.W. & Padron R., 2003). Myosin and actin are the contractile proteins, which assemble into polymeric filaments (the thick and thin myofilaments), and are responsible for the transduction of chemical energy into mechanical work when a muscle contracts. Myosin and actin comprised more that 70% of myofibrillar proteins (Huxley H.E., 1957). Troponin and tropomyosin are the major regulatory proteins, binding actin and regulating contraction in a Ca2+ dependent manner. Finally the structure of the sarcomere is completed using several structural proteins that associate with the actin and the myosin filaments.

Thick filaments are composed of myosin, myosin-binding proteins (C, H, and X), myomesin, M protein, and creatine kinase. The large superfamily of myosins is grouped into 18 classes of evolutionary related motor proteins. Sarcomeric myosins are referred to class myosin II, or conventional myosin (Berg J.S. et al., 2001). Muscle myosin is a hexamer containing two heavy chains (MyHC, molecular mass 220 kDa) and two pair of light chains (MyLC, molecular mass 20kDa), referred to as essential light chain and regulatory light chains (Figure 1.5; Clark K.A. et al., 2002). The entire myosin molecule is often characterized into two functional regions: the head and the tail. The head domain, which forms the catalytic motor domain, comprise the N-terminal region of each MyHC and two light chains and contains the binding sites for actin and nucleotides (Rayment I. et al., 1996). After hydrolysis of each ATP molecule, the head domain undergoes a large angular rotation, and myosin binds to the thin filaments. After completion

of this power stroke, ADP is dissociated and the actomyosin complex returns to the relaxed state. Each myosin head can repeats this cycle several times in a single twitch (Vale R.D. & Milligan R.A., 2000). The C-terminal regions of the two MyHC form the tail. The C-terminal end of the tail contains coiled-coil domains involved in myosin polymerization. The other portion of the tail connects the myosin heads to the thick filament core. Myosin heavy chains, essential light chain, and regulatory light chains are encoded by multigene families and comprise several isoforms. Various combinations of these subunits form a large number of isomyosins (Pette D. & Staron R.S., 1990). At least ten muscle MHC isoforms have been identified in mammals: embryonic, neonatal, cardiac alpha, cardiac beta or slow type 1, fast 2A, fast 2X, fast 2B, extraocular, mandibular, and slow tonic (Haddad F. et al., 2006). The two cardiac heavy-chains genes (α or Myh6, and β or Myh7, respectively) are located in tandem on chromosome 15 (rat) and 14 (mouse and human). Myh6 is expressed only in cardiac muscle, while Myh7 is the major isoform expressed in slow fiber type (Schiaffino S. and Reggiani C., 1996). All fast skeletal MyHC genes are found as a part of a multigene locus on chromosome 10 (rat), 11 (mouse), and 17 (human). The fast skeletal locus is composed of six distinct heavy chain genes: embryonic Myh3, perinatal Myh8, fast type 2A (Myh2), fast type 2X (Myh1), fast type 2B (Myh4), and extraocular Myh13. The embryonic and neonatal isoforms are expressed in developing skeletal muscle, but also in adult regenerating fibers (Haddad F. et al., 2006). Also MyLC family is composed by several isoforms. Fast skeletal muscle fibers contain two isoforms of regulatory MyLC: MyLC-1f and MyLC-3f, which originate from a single gene (Myl1) by different transcription initiation sites and alternative splicing. Slow skeletal muscle fibers also contain two isoforms: MyLC-1sa (Myl6b or slow-α), which is also expressed in smooth muscle and non-muscle tissues and MyLC-1sb (Myl3 or slow-β), which is expressed in ventricular myocardium. Two isoforms of regulatory MyLC are present in mammalian skeletal muscle: MyLC-2fast (Mylpf) and MyLC-2slow (Myl2; Schiaffino S. and Reggiani C., 1996).

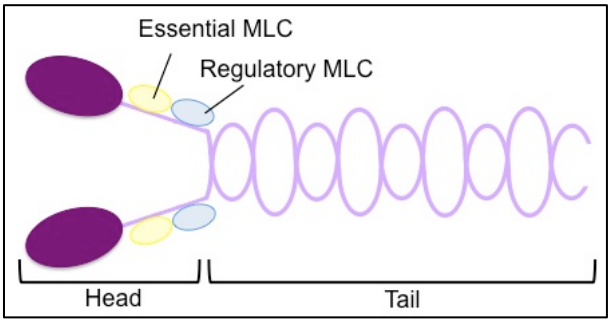

Figure 1.5: Myosin protein structure. Myosin is a hexamer composed by 2 MyHC, 2 essential MyLC, and 2 regulatory MyLC. Each MHC can be divided in two parts: the head, to which essential and regulatory MLCs are bound, and the tail, where the 2 MyHC intertwine to form an a-helical coiled coil.

Myosin binding proteins (MyBPs) bind to myosin along the thick filament. MyBP-C (molecular mass 140 kDa) and MyBP-H (molecular mass is 58 kDa) are myosin-binding proteins that contain several FN and Ig domains. Three MyBP-C isoforms have been characterized in adult muscle: skeletal fast, skeletal slow (previously identified as MyBP-X), and cardiac, each of which is encoded by separate genes (Bennett P.M. et al., 1999). In contrast, only one isoform of MyBP-H has been identified, which is expressed in fast skeletal fibers. The MyBPs play at least three roles in muscle: 1) is essential to filament formation in myofibrillogenesis; 2) has a structural role, helping to stabilize the organization of myosin molecules (Bennett PM et al., 1999); and 3) is involved in modulating contractility of cardiac muscle (Craig RW & Padron R, 2003).

The other three components of thick filament, myomesin, M protein, and creatine kinase, are localized at the level of the M-line. Creatine kinase is a dimeric globular protein which buffers cellular ATP and ADP concentration by regenerating ATP from ADP produced during contraction (Kushmerick M.J., 1998). Myomesin and M protein are both modular proteins. Myomesin is present in both fast and slow fibers; the major role of this protein is to link titin molecules to the thick filament (Obermann W.M. et al., 1996). M protein is present only in cardiac and fast skeletal fibers, and interacts with myosin (Fürst D.O. et al., 1999).

The thin filaments are anchored in the Z-disc, span the I-band, and extend toward the middle of the sarcomere. In the A-band they interact with the thick filaments. Actin, tropomyosin and the troponin complex compose the thin filaments. Actin is the major component of the thin filaments, and it is a globular protein (G actin), which self-associates to form a helical polymer known as the filamentous actin (F actin). The muscle contraction is controlled by Ca^{2+} ions surrounding the myofilaments. At low Ca^{2+} levels muscle is relaxed, while at high levels it contracts. Tropomyosin and troponin form a complex that ultimately regulates contraction in vertebrates. Tropomyosin is composed by two α-helical chains arranged as a coiled-coil tail that associate with actin filaments. Troponin is a complex of three subunits (TnI, TnC, and TnT) that attaches to a specific site of each tropomyosin. Troponin is the Ca^{2+} binding component of the complex. When Ca2+ concentration increases, troponin binds Ca^{2+}, releasing the inhibitory effect and allowing actin and myosin to interact (Craig RW & Padron R, 2003).

The thin and thick filaments are also associated with two proteins that constitute a third set of filaments: nebulin and titin. The C-terminal part of nebulin is partially inserted into the Z-lines, while its N-terminal part is associated with the thin filaments. Nebulin could act as a molecular ruler for specifying the precise lengths of the thin filaments. Indeed, alternative splicing variants of nebulin correlate with the different thin filament lengths present in various muscle fibers (Kruger M. et al. 1991). Titin filaments are closely associated with thick filaments. The N-terminal ends of titin, from adjacent sarcomeres, overlap in the Z-line. The proteins span the I- and A-bands, and their C-terminal ends overlap in the M-line, thus forming a continuous filament system in myofibrils (Clark K.A. et al., 2002). Its primary function in adult muscle is to act as an elastic element that maintains sarcomere integrity and filament order in the relaxed and active states (Horowits R, 1999).

The striking regularity of the thin filaments in the sarcomere is a result of specific interactions with the Z-disc, which is located at the borders of the sarcomere, forming the junction between one sarcomere and the next. The size of the Z-disc

is a useful indicator of fiber type: fast fibers have narrow (≈30-50 nm) Z-discs, while slow and cardiac fibers have wide (≈100-140 nm) Z-discs (Luther PK et al., 2003). The Z-line contains numerous other proteins, including FATZ (myozenin), ZASP, myopalladin, and telethonin (Faulkner G et al., 2001).

1.2 Skeletal muscle plasticity

1.2.1 Concept of muscle plasticity

Skeletal muscle fibers are dynamic structures capable to undergo adaptive changes in response to various conditions, ranging from stimuli modifying the contractile activity (endurance exercise, electrical stimulation, denervation), stimuli modifying imposed load (resistance training, microgravity), changes of substrate supply or environmental factors such as hypoxia and thermal stress. Furthermore, skeletal muscle tissue undergoes gradual modifications with ageing (Flück M. & Hoppeler H., 2003). The term “plasticity of muscle” describes and summarizes this adaptive responsiveness (Pette D., 2001).

The adaptation of muscle fibers to altered functional demands is cause of quantitative and qualitative changes at molecular and cellular levels. The quality, intensity and duration of the adaptive stimulus determine a wide degree of transformation on elements of energy metabolism and myofibrillar apparatus. Quantitative modifications in myofibrillar protein levels lead to change in fiber size (atrophy/hypertrophy). Qualitative changes in the type of contractile and regulatory proteins end up in fiber type transformations (Pette D., 2006).

1.2.2 Muscle plasticity studies

The term muscle plasticity was introduced to describe the first experiment of cross reinnervation in cats. After week of denervation, slow muscles become faster when reinnervated by a fast nerve and fast muscles become slower when reinnervated by a slow nerve (Buller A.J. et al., 1960). The model of cross reinnervation has been applied in other species, such us rat (Hoh J.F.; 1975), and

the distinct responses of different muscle types have been analyzed (Buller A. et al., 1987).

Subsequently, studies based on electrical stimulation validated the cross reinnervation data, showing that impulse patterns, applied directly on the nerve or on denervated muscles, and mimicking the firing pattern of slow and fast motor neurons, were able to induce changes in muscle fiber-type composition (Pette D. & Vrbova G., 1992). A fast-to-slow switch in the direction 2B⇔2X⇔2A⇔1 can be induced by tonic low-frequency electrical stimulation, mimicking the firing pattern of slow motor neurons. A slow-to-fast switch in the opposite direction 1⇔2A⇔2X⇔2B can be induced by phasic high-frequency electrical stimulation, resembling the firing pattern of fast motor neurons (Schiaffino S. & Reggiani C., 2011).

Since then, several studies have been focused on the effects of neuromuscular activity on muscle phenotype. Exercise training, functional overload and chronic low-frequency stimulation (CLFS) are major experimental models for studying the effects produced by an increase of neuromuscular activity, and result in transformation of pre-existing fast fibers into slow-oxidative fibers (Baldwin K.M. & Haddad F., 2001; Sugiura T. et al., 1993; Pette D. & Vrbovà G., 1992). In several studies using endurance exercise training the major adaptive responses regard an increases in enzyme activities of aerobic-oxidative metabolism (Booth F.W. & Baldwin K.M., 1996). The increases in enzyme levels are preceded by alterations in the transcriptional rate of specific mRNAs (Wu H. et al., 2003). Similarly, mechanical loading produced by immobilization of fast muscles cause an increase in the fraction of slow fibers (Pattullo et al. 1992) and fast-to-slow MyHC transitions (Goldspink et al., 1992). Conversely, decreased neuromuscular activity induced by tenotomy, immobilization of the muscle in a shortened position, hind limb suspension, and microgravity causes the shift of slow oxidative into fast glycolytic fibers (Booth F.W. & Baldwin K.M., 1996). This fiber type switching is associated with an increased use of glucose and a corresponding decreased use of lipid as energy source (Grichko V.P. et al., 2000).

The phenotypic properties of myofibers are also controlled by hormones. In particular, thyroid hormones have a great influence. In general, hypothyroidism causes fast-to-slow fiber shifts, while hyperthyroidism causes slow-to-fast transitions (Izumo S. et al., 1986). Also testosterone has a significant effect on the fiber type composition of guinea pig temporalis muscle (Gutmann E. et al., 1970) and rabbit masseter muscle (English A.W. et al., 1999). Furthermore, testosterone differences contribute to the gender differences in skeletal muscle mass. MyHC muscle composition is similar in men and women, but there is a greater ratio of type 2 to type 1 fiber mass in men, probably due to hypertrophy of type 2 fibers induced by testosterone (Welle S. et al., 2008).

1.2.3 Chronic Low Frequency Stimulations

Unilateral, Chronic Low-Frequency Stimulation (CLFS) is an experimental model able to induce specific changes in biochemical and physiological muscle properties (Pette D. & Vrbovà G., 1992). This method was first developed in rabbits using bipolar platinum stainless steel electrodes insulated except for the tip. The electrodes were fixed to the surrounding tissue at each side of the nerve. The impulse pattern imposed to stimulate extensor digitorum longus (EDL) and tibialis anterior (TA) muscles mimics the impulse pattern normally found in slow motoneurons (10 Hz) (Salmons S. & Vrbovà G., 1969). This type of stimulation was called CLFS, and converts fast-twitch muscles into muscles with a slow-twitch phenotype.

The model of CLFS has been subsequently applied in the hindlimb muscle of cats (Salmons S. & Vrbovà G., 1969), mice, rats, guinea pigs (Simoneau J-A & Pette D., 1988) and chickens (Barnard E.A. et al., 1986). Generally, CLFS protocol is applied to peroneal nerve of the hindlimb. This is done unilaterally, and the contralateral unstimulated muscle can be used as a valid control tissue. The peroneal nerve innervates TA and EDL muscles: both are fast twitch muscles, but TA muscles have a distribution of fiber type from 2B to 2A, while EDL muscles are composed prevalently of 2B and 2X fibers.

Although electrical stimulation causes muscle contraction, it differs from voluntary training for several reasons. First, during exercise, the motor units are recruited according to size, because the number of fibers recruited is dependent on the force required. Second, these motor units are activated asynchronously and with different frequency. Both of these activation patterns are cancelled by supramaximal electrical stimulation, which activates all motor units and with the same impulse pattern. Despite these differences, electrically induced contractile activity has several advantages. First, all motor units can be simultaneously activated by the same pattern of stimulation, including also the fibers that normally are not recruited during exercise. Second, the standardized regimen of stimulation gives the possibility to investigate the plasticity responses in reproducible manner. Third, the fibers can be activated for long period of time, greater than any exercise regimen. Fourth, imposed activity is restricted to the target muscle and has minimal secondary systemic effect. Finally, high levels of activity can be imposed from the beginning of stimulation, because nervous and cardiovascular system will not interfere with the amount of activity.

The effects caused by chronic stimulation were first obtained from rabbit EDL and TA muscles. After long term stimulation, a slowing of the time-courses of contraction and relaxation and an increased in fatigue resistance were observed. Furthermore, a decrease of maximum rate of tetanic tension and a decrease of muscle fibers diameter were observed (Brown M.D. et al., 1976; Pette D. et al, 1973; Simoneau J.A. et al., 1993). Several functional changes of chronic stimulated muscle were caused by a change in gene expression, in order to modify muscle fibers phenotype.

- Calcium regulatory system

The Ca^{2+} system of fast-twitch muscle can be altered by CLFS. Ca^{2+} uptake of SR and the amount of cytosolic Ca^{2+} binding protein both are modified by CLFS. These include the upregulation of the slow SERCA2a isoform (Leberer E. et al., 1989), and the downregulation of fast SERCA1 isoform, parvalbumin and calsequestrin (Huber B. & Pette D., 1996; Ohlendieck K. et al., 1999; Hicks A. et

al., 1997). Alterations in the slow direction are also observed in the proteins involved in EC coupling: in particular DHPR and fast RyR1 proteins are greatly reduced, and slow RyR2 is induced (Froemming G.R. et al., 2000). These adaptations result in higher level of cytosolic Ca^{2+} and a reduced rate of intracellular Ca^{2+} decay, causing a prolonged relaxing profile (Sreter F.A. et al., 1987).

- Metabolic adaptation

CLFS produces an increase in enzyme activities involved in oxidative pathways (e.g., citric acid cycle, fatty acid oxidation, respiratory chain), while the glycolytic enzyme activities decline (Pette D. & Vrbovà G., 1992). Within the glycolytic pathway, CLFS induced downregulation of muscle specific isoforms (M-LDH), and upregulation of heart specific isoforms (H-LDH), thus favoring pyruvate resynthesis from lactate (Hood D.A. & Pette D., 1989). Furthermore, one of the earliest changes is the increase of GLUT4 and hexokinase II (HK2) activity, indicating rises both in glucose uptake and glucose phosphorylation (Hoffmann S. & Pette D., 1994). Then, CLFS causes an increase of fatty acid oxidation (Hudlicka O. et al., 1977). These changes cause an increased aerobic metabolism of fatty acids and glucose. In parallel, there is an increase in mitochondrial density and enzymatic composition of mitochondria (Reichmann H. et al., 1985). This process recruits both mitochondrial and nuclear encoded mitochondrial proteins, in particular the subunits of cytochrome c oxidase (Hood D.A. et al., 1989). In addition, CLFS stimulates the expression of other proteins involved in oxidative phosphorylation, for example ALA synthase (Takahashi et al., 1993).

- Myofibrillar proteins

Several studies have demonstrated that CLFS induces MyHC isoforms transitions from fast to slow in rabbit TA muscle within 14-24 days (Pette D. & Vrbovà G., 1992; 1999). However, CLFS usually produces an incomplete transformation of the muscle fiber type: a fast muscle can adapt in the range 2B ⇔ 2X ⇔ 2A and slow muscle in the range 1⇔2A⇔2X (Ausoni S. et al., 1990). This limit is caused by long time required for the change in protein levels, that require weeks or

months (Pette D. & Staron R.S., 1997). These transformations in MyHC expression are accompanied by a remodeling of the isoform patterns of regulatory myofibrillar proteins, including myosin light chain (Leeuw T. & Pette D., 1993), troponin (Hartner K.T. et al., 1989), tropomyosin and α-actinin (Schachat F.H. et al., 1988).

- Angiogenesis

After CLFS, fast-twitch TA and EDL muscles display a red color as compared to white, unstimulated contralateral muscles. This change is a consequence of stimulation-induced increases in capillary density (Brown M.D. et al., 1976) and in myoglobin content (Kaufmann M. et al., 1989).

1.3 Signaling pathway mediating by nerve activity

1.3.1 Calcineurin/NFAT signaling

Calcineurin (Cn), also called protein phosphatase 2B, is a Ca^{2+}/calmodulin-regulated serine-threonine protein phosphatase localized to the cytoplasm. Cn is a heterodimer composed of a 59 kDa catalytic subunit (CnA) and a 19 kDa Ca^{2+}-binding regulatory subunit (CnB). The first observation that calcineurin plays a role in the control of slow genes was obtained in cultured muscle cells with the overexpression of activated calcineurin (Chin E.R. et al., 1998). The slow specific gene program was activated; conversely, the calcineurin inhibitor cyclosporine A (CsA) caused again a slow to fast fiber transition. Furthermore, in vivo studies on adult rat muscles revealed that calcineurin inhibition induced a partial slow-to-fast conversion. Since then, several studies based on transgenic mice overexpressing calcineurin, on calcineurin knockout mice, and on transfection experiments in adult muscles, have confirmed the notion that activated calcineurin upregulates slow gene program and downregulates fast gene program (Schiaffino S. & Serrano A., 2002).

Calcineurin activity is regulated not only by calmodulin, but also by several physiological inhibitory proteins, for example RCAN1 (also known as

DSCR1/MCIP1/calcipressin) and calsarcins (also known as FATZ and myozenin). Overexpression of RCAN1 inhibits Cn signaling (Fuentes J.J. et al., 2000) through direct binding of its COOH-terminal domain to the enzyme active site (Chakkalakal J.V. et al., 2003). Transgenic mice line overexpressing RCAN1 specifically in skeletal muscle from embryonic day 8 have normal phenotype at birth, with the same muscle fiber type composition of controls (Oh M. et al., 2005). However, slow fibers in transgenic mice begin a transformation process at postnatal day 7, and by day 14, all slow type 1 fibers have switched to type 2A. This result suggests that calcineurin signaling is not required for the initial diversification of fiber types but is necessary for the nerve activity-dependent maintenance of slow fibers in adult. Also calsarcin proteins are important for skeletal muscle fiber type diversification. These proteins colocalize with calcineurin at the Z-disc, and their expression pattern is fiber type specific: calsarcin1 is expressed in slow fibers and calsarcin2 and calsarcin3 are expressed in fast fibers. Calsarcin1 KO mice show an increase in calcineurin activity and in the number of slow fibers (Frey N. et al, 2004), while calsarcin2 KO mice show an increase of type 2A fibers in fast muscles (Frey N. et al, 2008).

Cn influences gene expression in the myofibers by dephosphorylating nuclear factor of activated T cells (NFAT) family, inducing their translocation to the nucleus and transcriptional activation (Crabtree G.R. & Olson E.N., 2002). Several studies using gain-of-function and loss-of-function approaches confirm a major role of the calcineurin-NFAT pathway in activity-dependent fiber type plasticity (Figure 1.6). Fast muscles from transgenic mice overexpressing activated Cn under the control of muscle creatine kinase promoter have an increased number of type 1 and 2A fibers (Naya F.J. et al., 2000) and a decreased proportion of type 2B fibers (Chakkalakal J.V. et al., 2004). On the other hand, Cn null mice show a down-regulation of the slow gene program (Parson S.A. et al, 2004).

NFAT gene family is composed of 5 members: NFATc1, -c2, -c3, -c4, -c5. All the members are regulated by calcineurin, except NFATc5. The interaction of NFAT with calcineurin depends on a specific consensus sequence at the N-terminus of

NFAT, PxIxIT, where x can be any amino acid. This consensus sequence has been used to create VIVIT peptide, which is used as an inhibitor of NFAT signaling because blocks the interaction of all NFATs with calcineurin (Aramburu J. et al., 1999). In vivo studies showed that NFAT proteins have cytoplasmic localization in the fast tibialis anterior muscle, while in the slow soleus muscle NFAT exhibited nuclear localization. NFAT nuclear import is induced in fast muscle fibers by CLFS, whereas nuclear export in slow soleus muscle fibers is caused by inactivity (Tothova J. et al., 2006). NFAT nuclear import follows dephosphorylation of a serine-rich region near its amino-termini, which unmasks two nuclear localization sequences. Once in the nucleus, NFAT can be phosphorylated again by several kinases. Glycogen synthase kinase 3β (GSK3β), casein kinase (CK) 1 and 2, and dual-specificity tyrosine phosphorylation regulated kinase 1A (DYRK1A) are the major kinases that regulate NFATc1 nuclear export (Shen T. et al., 2007). When NFAT is located in the nucleus, it binds to DNA thought the REL homology region and cooperates with several transcriptional partners (Schiaffino S. et al., 2006), including MEF2, which is also implicated in muscle gene regulation (see below). In vivo transfection with a constitutively active mutant of NFATc1 activates MyHC1, while inhibits MyHC 2B promoter activity (McCullagh K.J. et al., 2004). Furthermore, NFAT can bind the fast troponin I intronic regulatory element, causing transcriptional repression of this gene (Rana Z.A. et al., 2008).

NFATc1-4 are all expressed in skeletal muscle, but only NFATc1 shows slow fiber type specificity and translocates in the nucleus after slow electrical stimulations. NFATc2 and -3 are also show activity dependent translocation in the nucleus, but the pattern of stimulation is not clear. On the contrary, NFAT-4 is always localized in the nucleus (Calabria E. et al., 2009).

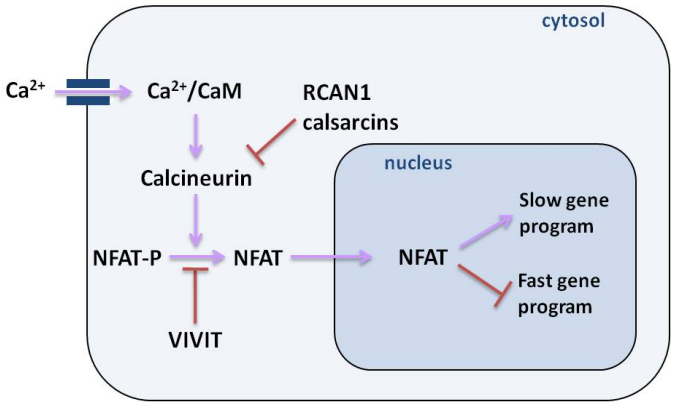

Figure 1.6: Role of the calcineurin-NFAT pathway in activity-dependent fiber type plasticity. Calcineurin is activated by calcium/calmodulin response to increased Ca^{2+} concentration and dephosphorylates NFAT, which enters in the nucleus and activates slow gene program. RCAN1 and calsarcin are able to inhibit calcineurin, while VIVIT is able to block NFAT in phosphorylated state.

1.3.2 MEF-2, HDAC and CaMK

The myocyte enhancer factor 2 (MEF2) transcription factors are major regulators during early muscle development and are involved in activity-dependent muscle fiber type remodeling. Four different genes (MEF2a, -2b, -2c, -2d) compose the MEF2 transcription family, each of which shows different splicing variants (Black B. & Olson E., 1998). In adults, MEF2 proteins are expressed at similar levels in fast and slow muscles (Potthoff M.J. et al., 2007). In order to investigate MEF2 activity, a transgenic mouse was developed, where three tandem MEF2 binding sites from the desmin gene promoter were linked to lacZ reporter. In adult mice, no lacZ expression was detected, except in some soleus fibers, suggesting that MEF2 activity was higher in slow than in fast muscles. When the transgenic mice were subjected to running exercise the lacZ reporter became strongly activated in the soleus and in some fast muscles. This effect was blocked by injection of the calcineurin inhibitor CsA, suggesting a direct interaction of calcineurin with MEF2 (Wu H. et al., 2001). These findings led to the suggestion that activation of calcineurin in slow muscles dephosphorylates and activates MEF2 (Wu H. et al., 2000). In vivo experiments supported a role of MEF2 genes in the regulation of fiber type profile: in particular, in mice with muscle specific knockout of MEF2c or MEF2d the proportion of type 1 fibers was decreased, while the number of slow fibers increased with the overexpression of an activated Mef2c (Potthoff

M.J. et al., 2007). MEF2 is inactivated by class II histone deacetylases (HDACs), while calcium- and calmodulin-dependent protein kinase (CaMK) activate MEF by phosphorylation and nuclear export of HDAC (McKinsey T.A. et al., 2000a; figure1.7).

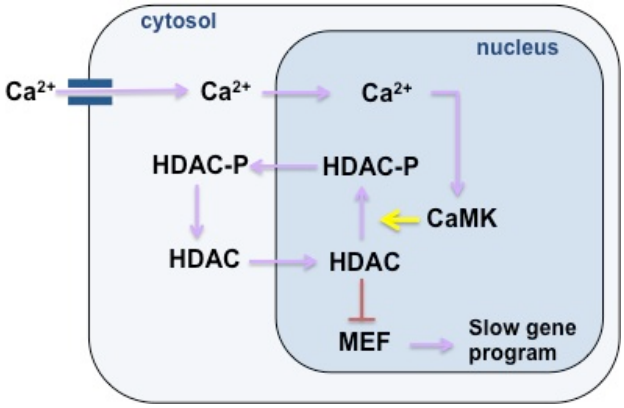

Figure 1.7: MEF2/HDAC/CaMK pathway. CamK is activated by increased Ca^{2+} concentration and phosphorylates HDAC, which exit from the nucleus. After this event, MEF2 is able to activate slow gene program.

There are two classes of histone deacetylases (HDAC) that have the ability to deacetylate a variety of proteins, not only histones but also several transcription factors, and can influence gene expression. HDAC4, −5, −7 and 9 have the highest expression in brain and muscle and form the class II HDAC, with low deacetylase activity. Class IIa HDACs function as co-repressors of transcription, interact with transcription factors and regulate histone acetylation together with class I HDACs (Mejat A. et al., 2005). The class IIa HDACs is regulated not only transcriptionally but also by ubiquitination, which leads to degradation, and phosphorylation, which causes nuclear export. In adult muscle, RNA levels of class II HDACs are higher in slow than fast muscles, while protein levels are higher in fast muscles, because these proteins are rapidly degraded by the proteasome in slow fibers (Potthoff M.J. et al., 2007). Knockout mice lacking individual class IIa HDACs displayed no changes in muscle fiber profile, but mice with a double knockouts of two HDAC IIa genes showed increased numbers of slow fibers and elevated mRNA levels of MyHC1 and -2A (Potthoff et al., 2007). On the other hand, adult mice overexpressing HDAC5 from an inducible promoter did not show any increase in type 1 and 2A fibers after treadmill running (Potthoff et al., 2007).

These experiments suggest that HDAC activity maintains the fast phenotype, while reduced HDAC signaling facilitates fast-to-slow transformation.

Ca^{2+}/calmodulin-dependent protein kinase (CaMK) also has a role in muscle fiber type plasticity. In particular, CaMKIV phosphorylates MEF2-HDAC complexes causing nuclear export of HDAC and synergizes with calcineurin during the differentiation of cultured myocytes (McKinsey T.A. et al., 2000b). Furthermore, the overexpression of an active CaMKIV selectively in skeletal muscle causes mitochondrial biogenesis and upregulation of oxidative enzymes (Wu H. et al., 2002). In adult skeletal muscle, however, CaMKIV is not expressed, while CaMKII is present and is stimulated by muscle activity (Rose A.J. et al., 2006). HDAC4 nuclear export, MEF2 reporter activation, and autophosphorylation and nuclear translocation of CaMKII have been observed after electrostimulation of adult isolated fibers with low-frequency 10-Hz trains (Liu Y. et al., 2005).

1.3.3 PPARs and PGC1α

The peroxisome proliferator-activated receptors (PPARs) are members of the nuclear receptor superfamily that form dimers with retinoid X receptors (RXRs) and bind DNA. In mammals, three mammalian subtypes of PPARs, -α, -γ, and -δ, have been identified (Kliewer et al., 1994). All PPARs are activated by lipids and affect lipid metabolism in different tissues. PPARα is predominantly expressed in liver and PPARγ in adipose tissue, while PPARδ is the predominant isoform in heart and skeletal muscle (Braissant et al., 1996). PPARδ is expressed at higher levels in slow/ oxidative compared with fast/glycolytic muscles (Wang Y.X. et al., 2004) and is induced by endurance training in mice (Luquet S. et al., 2003). In transgenic mice, where the PPARδ gene was knocked out, a slow-to fast- shift and decreased levels of oxidative enzymes were observed (Schuler M. et al., 2006). On the other hand, muscle-specific overexpression of wild-type or constitutively active PPARδ gene leads to a more oxidative capacity with increased mitochondrial DNA, type I fibers, and resistance to fatigue (Luquet S. et al., 2003; Wang Y.X. et al., 2004). In rat, CLFS caused an increase of PPARδ

mRNA, while a fast stimulation pattern on denervated slow muscle causes a decrease of PPARδ mRNA (Lunde I.G. et al., 2007). In conclusion, the level of PPARδ is upregulated by slow activity and downregulated by fast activity.

Peroxisome proliferator-activated receptor γ (PPARγ) coactivator-1α (PGC-1α) is a transcriptional coactivator, which does not bind the DNA but interacts with transcription factors in order to stimulate the transcription. The functional domains that mediate the binding of PGC-1α to transcription factors are located throughout the PGC-1α protein: nuclear receptors predominantly bind at the N-terminus whereas other factors such as FoxO1 or MEF2 interact more C-terminally (Puigserver P & Spiegelman BM., 2003). PGC-1α is expressed at higher levels in slow than fast muscles and is induced by exercise in both rodents and humans (Russel A.P. et al., 2003; Terada S. et al., 2002; Figure 1.8). Calcium signaling is involved in increasing the transcription of PGC-1α, via activation of CaMK and CnA (Handschin C. et al., 2003). Both in culture and in vivo PGC-1α concentration is elevated by slow electrical stimulation (Irrcher I. et al., 2003). Exercise can also induce a rapid activation of PGC-1α and its translocation to the nucleus, due to p38 mitogen activated protein kinase (MAPK)-dependent phosphorylation (Wright D.C. et al., 2007). The metabolic demand of exercise causes energy deprivation and AMP-activated protein kinase (AMPK) activation. So, AMPK is able to phosphorylate the PGC-1α protein and to induce PGC-1α gene expression (Jäger S. et al., 2007). Contractile stress causes an increase of reactive oxygen species (ROS), which induce an adaptive response, inducing PGC-1α gene expression and subsequently elevating ROS detoxifying enzyme levels (St-Pierre J. et al., 2006).

Transgenic mice overexpressing PGC-1α show increased mitochondrial content, increased levels of oxidative enzymes and increased type I fibers, making the muscles more resistant to fatigue (Lin J. et al., 2002). Conversely, PGC-1α KO mice have reduced oxidative capacity, but not significant difference in fiber type development (Arany Z. et al., 2005). PGC-1α is implicated in regulating pathways related to mitochondrial oxidative metabolism, and to glucose, lipid and energy

homeostasis (Figure 1.8). Glucose uptake and glycogen synthesis are increased by PGC-1α in muscle whereas glycolysis is inhibited (Michael L.F. et al., 2001). PGC-1α stimulates mitochondrial biogenesis and oxidative metabolism by inducing the expression of nuclear respiratory factors (NRF)-1 and -2, the mitochondrial transcription factor A that is required for the replication of mitochondrial DNA (Tfam), and mitofusin 2, a protein involved in mitochondrial fission and fusion (Wu Z. et al., 1999). PGC-1α is a co-activator not only for PPARγ, but also the other PPARs, including PPARδ (Lin J. et al., 2005). PGC-1α also interacts with forkhead box O1 (FoxO1) for muscle size regulation, and with MEF2, involved in muscle plasticity. Finally, PGC-1α is also able to control angiogenesis (Chinsomboon J. at al., 2009).

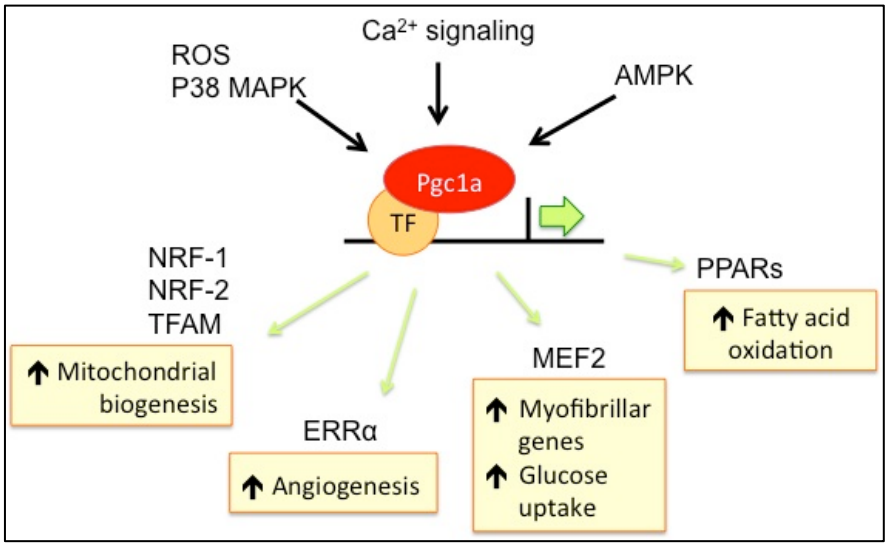

Figure 1.8: Pgc1α regulation. Signaling pathway induced by exercise converge on PGC1α activation. As a consequence, PGC1α binds to transcription factors involved in several functions.

PGC-1β, a homolog of PGC-1α, is expressed at high levels in skeletal muscle and exerts similar functions. Transgenic mice overexpressing PGC-1β have increased mitochondrial biogenesis, oxidative enzymes, and type 2X fibers (Arany Z. et al., 2007).

1.3.4 Other signaling pathways

MAPK. Several MAPKs, including the ERK1/2, the p38 MAPK, and the JNK pathway, are activated during exercise. A role of ERK1/2 in the regulation of slow

gene program was suggested by transfection of denervated muscle with a constitutively active Ras mutant, which is known to selectively activate ERK1/2. During the regeneration process MyHC slow was upregulated and the MyHC fast isoforms were downregulated. Furthermore, when adult muscles were denervated and subjected to CLFS for 24 hours a six-fold increase in MAPK-ERK activity has been observed with respect to denervated unstimulated muscles. In contrast, a fast stimulation did not have any effect. (Murgia M. et al., 2000).

MyoD family. The muscle specific transcription factors of the MyoD family (MyoD, Myf-5, myogenin and MRF4) play a fundamental role in myogenesis, but their role in muscle plasticity is not clear. MyoD and myogenin are differentially expressed in adult muscles, with MyoD most expressed in fast and myogenin in slow muscles. Mice lacking functional MyoD show changes in MyHC composition, and the upregulation of MyHC 2B in the unloaded soleus is decreased in MyoD-null mice (Seward D.J. et al., 2001). Myogenin overexpression in glycolytic fibers causes an increase of oxidative enzymes, but the MyHC expression pattern does not change (Hughes S.M. et al., 1999)

Six1-Eya1. The Six-family of transcription factors has five subtypes (Six1–5) in mice. These factors are implicated in the development of eye and muscle. Eya is a metal-dependent protein tyrosine phosphatase, which functions as a transcription factor or an enzyme. In mammals there are four paralogs (Eya1-4). Eya physically interact with Six and those factors are enriched in the nuclei of fast glycolytic fibers. When Six1 and Eya1 are overexpressed in adult soleus, MyHC2B, MyHC2X and the genes of the glycolytic metabolic pathway are upregulated (Grifone R. et al., 2004).

FoxO. The FoxO transcription factors control muscle atrophy by activating the ubiquitin-proteasome and the autophagy-lysosome pathways. Several studies show that these transcription factors have a role also in fiber type plasticity. FoxO1 is more abundant in slow muscles and FoxO4 in fast muscles, and a slow-to-fast fiber type switch is produced by muscle-specific FoxO1 KO (Kitamura T. et al., 2007).

1.4 Microarrays and muscle plasticity

In the last 20 years, with the advances in genome sequencing and the development of new molecular tools, the interest for measurement of large-scale gene expression became greater. The analysis of all genes that are expressed in a tissue under certain conditions has become the starting point to understand the physiology of cells and tissues. Since muscle plasticity is at least in part based on transcriptional regulation of structural and regulatory genes, many studies have applied high throughput approaches to study how the whole mRNA population changes in response to a given stimulus (Kandarian S.C., 2006). cDNA microarrays expression technology has been applied in muscle to study differentiation (Bean C. et al., 2005), effect of exercise (Pattison JS et al., 2003), aging (Welle S. et al., 2003), and physiopathological disorders (Campanaro S et al. 2002, Raffaello A. et al., 2006). The basic procedure of microarray analysis is to deposit a very small amount of DNA each one corresponding to a gene (the "probes") on a solid surface (the array), and then perform the hybridization of "target" mRNA populations that have been labeled with fluorescent dye. The amount of fluorescent mRNA target found in each probe spot is proportional to the abundance of the transcript in the sample. However, microarray technology lacks the ability to measure the absolute abundance of transcripts and can only be used to compare differences between samples. So, microarray analysis provided the first step in characterizing muscle gene expression; then, the expression changes are verified by other methods, such as Northern blotting and quantitative RT-PCR. Another problem of microarray data is the origin of mRNA pools. When a tissue, such as skeletal muscle, is composed of more than one cell type, the results of microarray experiment reflect this heterogeneous composition. So differences in gene expression could reflect altered cell content within the tissue or distinct cell–cell interaction. Usually in these cases, the expression changes are verified by mRNA in situ hybridization and protein immunohistochemistry (Reggiani C. & Kronnie G.T., 2004).

The first result of microarrays is a list of genes that are up- or down- regulated during the adaptive response. To identify the biological context where the differentially expressed genes act is necessary to perform a GO analysis, which assign genes to one or more molecular functions, biological processes, and cellular components. However, this approach is limited to looking up existing annotations and is not able to discover new function. Furthermore, several studies have found lists of differentially expressed genes that in GO analysis appears involved in a wide range of biological processes. In this case, GO is not able to select the more relevant one by using the context of the other genes (Khatri P & Draghici S, 2005). Other databases such as the Kyoto Encyclopedia of Genes and Genomes (KEGG) and BioCarta allow placing the genes in a biological pathway. However, the pathway analysis presents exactly the same limitations of GO analysis.

Expression profiling of muscle fiber transformation has largely been performed in rabbit and rodent muscles, and many of these transcriptional changes have been individually validated at the protein level. Recently, the application of high-throughput mass spectroscopy assays to chronically stimulated fast muscle has added proteomics data of the myofiber transition process to the fiber type plasticity database (Donoghue P. et al., 2007). While these study have focused on myofiber changes after days or months of stimulation, little is known about the onset of this process, especially the early molecular events associated with the initiation of the fast to slow transition. The unique study that analyzed transcriptional changes after 4 hour of chronic stimulation was published in 2009. The results obtained in this study revealed that 10-Hz stimulation of the mouse hindlimb for 4 hour produced the onset of fast to slow myofiber transformation, with decreased transcripts for fast muscle contractile proteins (MyHC2B, MyHC2X, fast MyLC, fast troponin I and T3), and increased slow muscle specific transcripts (MyHC1 and slow troponin C and T1). There was also a concomitant decline in transcripts encoding glycolytic enzymes, all in absence of muscle damage or satellite cell activation. Furthermore, they found an increase

of transcription factors previously implicated in myofiber phenotype conversion, such as EYA1, NFAT, and Ppargc1a (LaFramboise W.A. et al., 2009).

1.4.1 Microgenomics in skeletal muscle

Microgenomics is the “omics” analysis at single cell level. All the cells of an organism have the same genomic information, but differ in their transcriptome. So, the quantitative measurement of expression in a single cell is essential for the understanding of properties or states of cells in any biological context (Kurimoto K & Saitou M, 2010). A lot of methods have been described as “omic" analysis in single cell (Wang D & Bodovitz S, 2010). Among these, microarray platforms provide major opportunities for quantitative, genome-wide transcriptional analyses. Three critical steps are present in producing good quality and reproducible microarray data from a single cell. First, cells should be collected in the shortest time to avoid change in gene expression. Second, RNA extraction should be performed with great care to avoid degradation of the small amount of RNA into one cell. Finally, this technology requires large amounts of starting materials. So, the RNA/cDNA must be amplified, and this procedure should introduce as minor bias as possible (Kurimoto K & Saitou M, 2010).

Microarray analysis in whole muscle has the limitation of the heterogeneity of this tissue. Each muscle is composed by different fiber types and also by other cell types, as fibroblasts in the connective layers (perimysium and endomysium), endothelial and smooth muscle cells in the vessel walls, Schwann cells around the axons, and blood cells (chapter 1.1.1). So, the mRNA of all cellular components is pooled and interpreted together. Microarray analysis of single, isolated myofibers allow to obtain thousand of the genes differentially expressed between different fiber types, removing any background noise. In the first microgenomic study published in skeletal muscle, slow oxidative (SO) and fast glycolytic (FG) were analyzed (Chemello F. et al., 2011). GO analyses clearly demonstrated the removal of transcripts specific of other cell types; as a consequence, muscle specific genes were identified with a much higher

resolution. The microgenomic technologies permit a better interpretation of the real complexity existing in muscle fibers through identification of specific marker genes. As shown in this work, the microgenomic approach is also well suitable for studies on muscle plasticity, since a change in gene expression is the first reply of muscle to various physiological stimuli.

2. AIMS OF THE EXPERIMENTAL PROJECT

Skeletal muscle fibers are dynamic structures capable to undergo adaptive changes in response to various conditions. The adaptation consist of quantitative and qualitative changes at molecular and cellular levels, in order to change the elements of energy metabolism and myofibrillar apparatus, depending on the quality, intensity and duration of the adaptive stimulus. Unilateral, Chronic Low-Frequency Stimulation (CLFS) mimics the impulse pattern of slow-twitch muscles and is an experimental model widely used to induce a fast to slow transition. So far, CLFS studies have focused on the effects produced in the whole EDL muscle after days or weeks of stimulation. The aim of my work was to identify the earliest genetic changes in this process, since changes in gene expression are the most immediate reply of muscle to physiological stimuli. The contribution of myofibers to the muscle changes may be hidden in transcriptional studies with whole EDL muscle, as a result of the complex anatomy of skeletal muscle and the heterogeneity of myofibers, and therefore I have scaled down the phenotypic analysis to the level of single, isolated muscle fibers. This is the first report of microgenomic technologies applied in a model of muscle plasticity.

3. MATERIALS AND METHODS

3.1 Stimulation protocol and tissue collection

3.1.1 Animals

All experiments were performed using wild-type male CD1 mice (Charles River) at three months age (32-35 g). The animals were maintained in a controlled environment with a 12:12-h light-dark cycle and provided with food and water. The local Animal Care Committee of the University of Padua approved experimental protocols.

3.1.2 Stimulation protocol

To perform electrical stimulation, CD1 mice were anesthetized by intraperitoneal injection of a mixture of Xylor and Zoletil. Surgical preparations comprised a small incision to expose the common peroneal nerve. Teflon-covered stainless steel electrodes were fixed to each side of the common peroneal nerve of one leg and the other one serving as a control. Chronic low-frequency stimulation (CLFS) was applied while the mouse was maintained under anesthesia. The stimulation protocol mimics the slow-twitch pattern and consists of trains of 10-second duration and 20-Hz frequency given every 30 seconds (Tothova J. et al., 2006). Foot dorsal flexion was checked as indication of the correct stimulation. Core body temperature was maintained at 37°C using a temperature-controlled plate. Electrical stimulation was applied for 6 and 12 hours.

3.1.3 Tissue collection

After six and twelve hours of stimulation, the mice were killed by rapid cervical dislocation. Stimulated and contralateral unstimulated EDL muscles were quickly removed by microdissection. The muscles were immersed in 1 ml of TRIzol Reagent (Invitrogen) for RNA extraction from whole muscle, and in 1 ml of high-

glucose Dulbecco's modified Eagle medium (DMEM; Invitrogen-Gibco) for single fibers dissociation.

3.1.4 Enzymatic dissociation of myofibers

To obtain isolated single fibers I used the protocol for enzymatic dissociation (Chemello F. et al, 2011). EDL muscles were incubated for 45 min at 37°C in 1 ml DMEM, containing 10 mg type I collagenase (220 U mg^{-1}; Sigma). After the incubation, muscles were sequentially rinsed for 2 min in 3 ml of DMEM, 3 ml DMEM supplemented with 10% fetal bovine serum (FBS) and 3 ml of DMEM. Finally, muscles were transferred into 50 mm x 18 mm well that contained 3 ml of DMEM with 10% FBS. To release single fibers, the EDL muscles were triturated gently with a plastic Pasteur pipette. This final process was repeated several times in order to obtain about 100 isolated fibers. Then, under stereomicroscope, intact fibers were picked and washed first in DMEM then in phosphate buffered saline (PBS; 137 mM NaCl, 2.7 mM KCl, 10 mM Na_2HPO_4, 1.76 mM KH_2PO_4, pH 7.4). About one-third of each fiber was placed in Laemmli buffer and used for fiber typing (by SDS-PAGE); the remaining part was placed in TRIzol Reagent and used for RNA extraction.

3.1.5 MyHC isoform identification

For separation of myosin heavy chain (MyHC) isoforms, about one-third of each fibers was solubilized in Laemmli buffer solution (62.5 mM Tris, pH 6.8; 10% glycerol, 2.3% SDS and 5% β-mercaptoethanol). Proteins were denaturated in SDS and heat (at 90°C for 5 min) and then analyzed on 4% stacking (4% polyacrylamide 50:1, 30% glycerol, 70 mM Tris pH 6.7, 4 mM EDTA and 0.4% SDS) and 8% resolving gels (8% polyacrylamide 50:1, 30% glycerol, 0.4% SDS, 0.2 M Tris, and 0.1 M glycine). Slabs 18 cm wide, 16 cm high, and 1 mm thick were used. Electrophoresis was carried out at 4°C for 45 h, at 70 V for 1 h and 140 V for the remaining time. Gels were silver stained (Bio-Rad Silver Stain). The bands

of the MyHC isoforms were separated in the 200 KDa region and were identified in according to their migration order.

3.2 RNA purification

3.2.1 RNA extraction from whole muscle

Whole muscle samples were homogenated in 1 ml TRIzol reagent using the ULTRA-TURRAX dispenser (IKA), taking care to maintain the samples in ice. After 15 min of incubation at room temperature (RT), to permit complete dissociation of the nucleoprotein complex, 0.2 ml of chloroform were added, and tubes were vigorously shaken by hand. Samples were incubated for 15 min and then centrifugated at 12,000 x g for 20 min at 4°C. After centrifugation, the samples were separated into a lower red phenol-chloroform phase, containing the protein fraction, an interphase, with the DNA, and a colorless upper aqueous phase, with the RNA. RNA was precipitated by adding an isovolume of isopropyl alcohol, incubating samples at -20°C for 30 min., and centrifuging at 12,000 x g for 20 min. at 4°C. The RNA pellet was washed twice with 1 ml of 75% ethanol vortexing, and centrifuging at 7,500 x g for 10 min. at 4°C. Finally, RNA pellet was air dried and resuspended in 15 µl of RNase free water (Gibco).

3.2.2 RNA extraction from single fibers

Total RNA from single fibers fragments was extracted using 250 µl of TRIzol. After 15 min of incubation at RT, 50 µl of chloroform were added, and tubes were vigorously shaken by hand. Samples were incubated for 15 min and then centrifugated at 12,000 x g for 20 min at 4°C. An isovolume of 70% ethanol was added to the aqueous phase and RNA was purified using the silica membrane technology of RNeasy Micro Kit (Qiagen). To remove any contamination, washes were performed on the column, following the manufacturer instructions. RNA elution was performed with 16 µl of RNase-free water.

3.2.3 RNA quantification and quality control

Total RNA extracted from whole muscle was quantified by spectrophotometry, using the NanoDrop ND1000 (Celbio). Total RNA extracted from single fibers was not quantified, because the quantity is too low (about few nanograms). RNA quality was determinated with the RNA 6000 Pico/Nano LabChip on a 2100 Bioanalyzer (Agilent). All chips were prepared according to the manufacturer instructions, using 1/3 of total RNA extracted from single fibers and 200 ng of RNA from whole muscles. RNA samples were separated electrophoretically; then, the bioanalyzer software generated an electropherogram and gel-like image. For the experiment comparison and repeatability, the program provided the RNA Integrity Number (RIN), with 1 indicated the most degraded profile and 10 the most intact. All poor quality RNA samples were discarded.

3.3 RNA Amplification and labeling

3.3.1 Whole muscle RNA amplification and labeling with One Color Microarray Based Gene Expression Analysis

Whole muscle RNA sample (50 ng) were amplified and labeled using One Color Microarray Based Gene Expression Analysis (Low Input Quick Amp WT Labeling) protocol (Agilent Technology), in accordance with the manufacturer's instructions. Agilent One-Color Spike Mix was added to samples. dsDNA containing T7 promoter was generated with high efficiency by AffinityScript reverse transcriptase, in a solution containing a mixture of oligo dT- and random nucleotide. Then, cyanine labeled cRNA (complimentary RNA) was generated in the same tube using linear amplification protocol. The reaction was performed using T7 RNA Polymerase, which simultaneously amplifies target material and incorporates Cy3-labeled CTP and incubated at 40°C for 2 hr. The labeled cRNAs were purified by RNAeasy Mini Kit (Qiagen), following the manufacturer instructions.

3.3.2 Single fibers RNA amplification with TransPlex Whole Transcriptome Amplification 2 (WTA2) Kit

RNA samples purified from single fibers were exponentially amplified using the TransPlex Whole Transcriptome Amplification 2 (WTA2) Kit (Sigma-Aldrich), according to manufacturer's instructions. Briefly, the TransPlex WTA process involved two steps. In the first step, sample RNA is reverse transcribed with substantially non-self-complementary primers composed of a semi-degenerate 3' end and a universal 5' end. RNA samples in a total volume of 16 µl were reverse transcribed by adding 2.5 µl of Library Synthesis Solution, incubating at 70 °C for 5 min., adding 2.5 µl of Library Synthesis Buffer, 3.9 µl of water and 2 µl of Library Synthesis Enzyme, and incubating following the parameters suggested by the manufacturer. Annealed primers are extended by WTA polymerase and displaced single strands serve as new templates for primer annealing. In the second step, the resultant Omniplex cDNA library is amplified by PCR with the universal primer to produce WTA products. 301 µl of water, 37.5 µl of Amplification Mix, 7.5 µl WTA of dNTP Mix, and 3.75 µl of Amplification Enzyme have been added at the reaction The samples were amplified for 18 cycles, using the recommended cycling parameters. PCR products were purified from the other component in the reaction using GenElute PCR Clean-up Kit (Sigma-Aldrich).

3.3.3 Single fibers RNA labeling with Enzymatic Labeling protocol of Array-Based CGH for Genomic DNA Analysis Kit

Single fibers RNA labeling was performed following the Enzymatic Labeling protocol of Array-Based CGH for Genomic DNA Analysis Kit (Agilent). Briefly, 2 µg of purified cDNA were concentrated to a final volume of 13 µl with a Speed Vac. 2.5 µl of Random Primers were added to the reaction and it was incubated at 95°C for 10 min. and then putted on ice for 5 min. The reaction was mixed with the Labeling Master Mix (5.0 µl of Buffer 5X, 2.5 µl of 10X dNTP, 1.5 µl of Cy3-dUTP [1.0 mM], and 0.5 µl of Exo-Klenow fragment) and incubated first at 37°C

for 2 hours, and then at 65°C for 10 min. This kit uses random primers and the exo-Klenow fragment to label DNA samples with fluorescent-labeled nucleotides. Labeled DNA was purified and concentrated with Amicon Ultra-0.5 mL Centrifugal Filters (Millipore), following the manufacturer instructions.

3.3.4 cRNAs/dsDNAs quantification

The concentration and specific activity of the labeled cRNAs/dsDNAs (picomole of Cy3/microgram of cRNAs/dsDNAs) were measured by Nanodrop ND1000. For whole muscle cRNA yield was about 10 µg and the specific activity of 30 pmol Cy3 per µg cRNA. For single fibers DNA yield was about 4 µg and the specific activity of 30 pmol Cy3 per µg dsDNA.

3.4 Microarray experiments

The Agilent SurePrint G3 Mouse GE 8x60K Microarrays include 39430 Entrez Gene RNAs, 16251 large intergenic non-coding RNAs, 339 x 10 replicates of biological probes, and 128 x 10 positive controls. Probe design is sourced from RefSeq, Ensembl, RIKEN, GenBank, and UniGene database. Each slide contains 8 arrays printed using Agilent's 60-mer SurePrint technology. This technology uses a proprietary non-contact industrial inkjet printing process, in which oligo monomers are deposited uniformly onto specially prepared glass slides. This in situ synthesis process prints 60-mer length oligonucleotide probes, base-by-base, from digital sequence files.

600 ng of whole EDL muscle labeled cRNAs was mixed with 5 µl of 10X Blocking Agent, 1 µl of 25X Fragmentation Buffer, and water to a final volume of 25 µl. The reaction was incubated at 60°C for 30 min. to fragment cRNA. Then, 25 µl of 2X GEx Hybridization Buffer HI-RPM was added to obtain the hybridization mix. 40 µl of Hybridization mix was putted into one of the 8 arrays of SurePrint G3 Mouse GE 8 × 60K Microarrays.

800 ng of single fibers labeled dsDNAs was mixed with 5 µl of 10X Blocking Agent and water to a final volume of 25 µl, and then was denaturated at 95°C for 2 min. Hybridization mix was composed by denaturated dsDNA and 25 µl of 2X GEx Hybridization Buffer HI-RPM. 40 µl of Hybridization mix was putted into one of the 8 arrays of SurePrint G3 Mouse GE 8 × 60K Microarrays.

The slides were incubated into the Agilent SureHyb chamber at 65°C for 17 hours and rotation was set at 10 rpm. At the end, microarray chambers were disassembled into GE Wash Buffer 1 at room temperature. Then microarray slides were washed 1 min into GE Wash Buffer 1 at room temperature and 1 minute GE Wash Buffer 2 at elevated temperature.

3.5 Data analysis

3.5.1 Data pre-processing

The readout from the microarray is captured as an image acquired using a scanner for fluorescent signal detection via a confocal detector or a charge coupled device (CCD) camera. The microarray scanner excites the fluorophores adhered to the spots on the array and acquire data about the intensities of the light emissions from the field of the microarray. The hybridized arrays were scanned using GenePix 4000B scanner (Agilent Technologies) at 3µm resolution. Scanned images were analyzed with Feature Extraction Software (Agilent Technologies), which is an automatic process for the commercial arrays that use platform specific software with defined spot finding algorithms, background subtraction methods and selection of poor quality spots (Elvidge G., 2006). Only arrays with at least 8/9 quality control metrics in range were used for the following data analysis. Then, intensity measurements should be adjusted to minimize several experimental variables, such as differences in labeling, hybridization and detection. This adjustment is referred to as normalization (Chen J.J., 2007). Feature Extraction Software performed intra-array normalization. Inter-arrays quantile normalization was performed with the

Expander software (Sharan R et al., 2003), using the quantile normalization. This method aims at making the distribution of probe intensities for each array in a set of arrays the same by taking the mean quantile and substituting it as the value of the data item in the original dataset (Bolstad BM et al., 2003). After normalization, the intensity from multiple probes that measure the same gene was been combined to generate a single expression level for the gene. Then, normalized data were Log2 transformed, so that the value range is reduced. Finally, data were filtered by removing probes with at least 3 not available (NA) values in the comparison among whole EDL muscles and at least 5 NA values in the comparison between fibers.

3.5.2 Cluster analysis

Clustering analysis sort the data and group genes or samples together on the basis of their separation in expression space. Hierarchical cluster analysis was performed by MultiExperiment Viewer (MeV, v4.6.2), software included in TM4 Microarray Software Suite (Saeed AI et al., 2006), using Euclidean Correlation.

3.5.3 Identification of differentially expressed genes

Significance Analysis of Microarrays (SAM), a non-parametric statistical test, identified differentially expressed genes. (Tusher VG et al., 2001). SAM uses an adjusted t-test, with permutations of repeated measurements to calculate the False Discovery Rate (FRD) value, defined as the percentage of genes falsely identified as differentially expressed. In whole EDL muscle analysis, paired two-class SAM analysis was performed for each stimulation time-point to find differentially expressed genes between stimulated and contralateral unstimulated muscle. In single fibers analysis, unpaired two-class and multiclass SAM analysis were performed to find differentially expressed genes between the three time points. FDR values minor of 5% are commonly recognized as highly significant. SAM analyses were performed by MeV.

3.5.4 Gene functional enrichment analysis

To know the biological mechanism of differentially expressed genes or cluster of genes is necessary to perform a GO analysis, which assign genes to one or more molecular functions, biological processes, and cellular components. Gene Ontology enrichment was performed with Functional Annotation Clustering of the Database for Annotation, Visualization and Integrated Discovery (DAVID; Huang DW et al., 2009; http://david.abcc. ncifcrf.gov/).

To know the biological system where the genes differentially expressed act, is necessary to analyze the microarray data in pathways. Gene enrichment in pathways was performed at the DAVID web server, using KEGG database. In all the analysis entire mouse genome was used as background.

3.5.5 Pavlidis Template Matching

Pavlidis Template Matching (PTM) approach allow to construct a template expression profile (entering values between 0 and 1 corresponding to each experiment); then the data set will be searched for matches to the template, using Pearson Correlation (Hulshizer R. & Blalock E.M., 2007). The threshold for matching can be either the magnitude of the correlation coefficient, or the p-value of the correlation coefficient. PTM analyses were performed by MeV.

3.6 qPCR

I used quantitative real-time PCR (qPCR) for preliminary data in whole muscle and to validate the results obtained from microarray experiments.

Total RNA from whole muscle was extracted using TRIzol reagent (Invitrogen). 1 µg of RNA was reverse transcribed using Superscript III reverse transcriptase (Invitrogen) according to the manufacturer's directions.

Synthesis of cDNA was done from single fibers from stimulated and contralateral unstimulated muscle. I have used SuperScript™ III Cells Direct cDNA Synthesis

System (Invitrogen), which is an optimized kit for synthesizing first strand cDNA directly from single fibers lysate without first isolating the RNA.

Gene-specific primers were selected with Primer 3 software, in order to amplify fragments of 150–250 bp in length, close to the 3' end of the transcript (table 3.1). To avoid the amplification of contaminant genomic DNA, I selected primers lying on distinct exons, separated by a long intron (more than 1000 bp). Gel electrophoresis and the dissociation curve were used to assess the specificity of the amplicon. Experiments were performed in a 7500 Real-Time PCR System (Applied Biosystems), using GoTaq qPCR Master Mix (Promega), following the manufacturer's instructions. Cycling conditions were 10 min at 95°C, followed by 40 cycles of 25 sec. at 95°C and 1 min. at 60°C, and finally 3 min. at 72°C. Relative expression levels were quantified by constructing a standard curve with dilution of the purified PCR product generated for each specific primer pair. Values were normalized to the expression of reference genes (thioredoxin 1 and ribosomal protein L4), with invariant expression level in my experimental conditions.

Gene Symbol	**Primer FOR**	**Primer REV**
Casq2	TTGTGGATTGACCCAGATGA	CCAGTCTTCCAGCTCCTCAG
Egr1	TAATAGCAGCAGCAGCACCA	GGGATAACTCGTCTCCACCA
Myc	TCCTGTACCTCGTCCGATTC	GGTTTGCCTCTTCTCCACAG
Myh4	TAGGGTGAGGGAGCTTGAAA	GTTTGTCCACCAAGTCCTGC
Myh7	AGCAGGAGCTGATTGAGACC	TGTGATAGCCTTCTTGGCCT
MyoZ2	TAACAGGGTTGCCACTCCAT	CAGCTTCCCTCTCACAGGTC
Ppargc1a	TATGGAGTGACATAGAGTGTGCT	CCACTTCAATCCACCCAGAAAG
Rcan1	GTGTGGCAAACGATGATGTC	AGGAACTCGGTCTTGTGCAG
Rpl4	ACAACAGACAGCCCTATGCC	CAGGTTTTGGTTGGTGCAA
Tnnc1	TGCAGGAGATGATTGACGAA	TGTAGCCATCAGCGTTTTTG
Txn1	TCCAATGTGGTGTTCCTTGA	GGCTTCAAGCTTTTCCTTGTT

Table 3.1: Primers for qPCR. Forward (FOR) and reverse (REV) primers used for qPCR experiments.

4. RESULTS AND DISCUSSION

4.1 CLFS on EDL muscle

To study muscle plasticity, and in particular the specific changes induced by a fast-to slow fiber type shift, I chose to use chronic low-frequency stimulation (CLFS). CLFS is by now a well-established method for inducing specific changes in muscle properties, because it mimics the tonic low-frequency impulse pattern normally delivered to a slow-twitch muscle (Pette D. & Vrbovà G., 1992). The stimulation pattern consisted of trains of 10-second duration and 20-Hz frequency given every 30 seconds delivered to specific fast muscles via electrodes implanted lateral to the common peroneal nerve (Tothova J. et al., 2006; Figure 4.1). I used stainless steel electrodes insulated with Teflon except for the tip. The electrodes were placed on either side of the common peroneal nerve and secured to the surrounding tissue, in order to not make disturb to the nerve. The stimulation was applied while the mice were maintained under anesthesia. I checked the presence of foot dorsal flexion as indication of the correct stimulation.

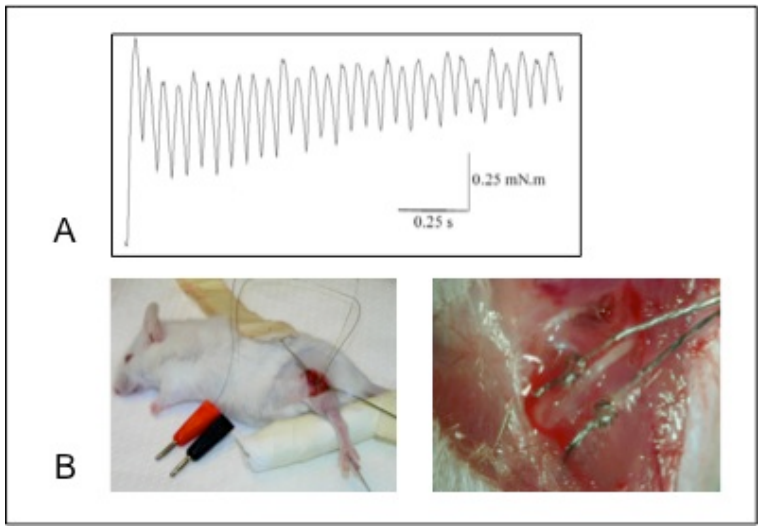

Figure 4.1: CLFS on EDL muscle. The CLFS protocol consists of trains of 10-second duration and 20-Hz frequency given every 30 seconds (A) and delivered to specific fast muscles via electrodes implanted lateral to the common peroneal nerve (B).

In order to study the specific changes induced by a fast-to slow fiber type shift, I chose the extensor digitorum longus (EDL) muscle, which is almost composed of fast fibers (predominantly pure MyHC-2B and hybrid MyHC-2B/2X fibers).

4.1.1 Stimulation time-point selection

Until now, chronic electrical stimulation has been used to study myofiber changes after days or months of stimulation. Here, I wanted to study the changes induced in the onset of this process, especially the early transcriptional changes associated with the initiation of the fast to slow transition. So, I decided to select two time points: 12 hours of stimulation, which is the higher time to maintain the mice under anesthesia; and 6 hours of stimulation, as intermediate time point.

So far, the only study that analyzed transcriptional changes after brief time of stimulation was published in 2009. The results obtained in this study revealed that stimulation of the mouse hindlimb for 4 hour produced the onset of fast to slow myofiber transformation, with decreased transcripts for fast muscle contractile proteins (MyHC2B, MyHC2X, fast MyLC, fast troponin I and T3), and increased slow muscle specific transcripts (MyHC1 and slow troponin C and T1). They found also a concomitant decline in transcripts encoding glycolytic enzymes and an increase of transcription factors previously implicated in myofiber phenotype conversion, such as EYA1, NFAT, Ppargc1a (LaFramboise W.A. et al., 2009). Their stimulation protocol differed from mine for two motifs, and the first was the stimulation pattern. The slow motor neuron generate a large number of impulses grouped in long and short trains with median frequency around 20 Hz (Henning R. & Lomo T., 1985; see introduction 1.1.3), which is twice the 10 Hz that they used in the study. The second motif was the presence of hindlimb immobilization. They stimulated the sciatic nerve and immobilized the hindlimb by positioning the animal prone on a Plexiglas platform fitted with a patellar brace to fix the knee. This type of contraction is defined as isometric, meaning that the length of muscle does not change, though contraction strength may be

varied, because a load is imposed. On the contrary, I stimulated peroneal nerve without imposing a load, so the strength did not change.

In order to compare the two stimulations methods, I analyzed EDL muscles from 3 mice subjected to CLFS for 6 hours and from other 3 mice subjected to CLFS for 12 hours. RNA was extracted from stimulated and contralateral muscle of each mouse and used for qPCR experiments. Then I used qPCR primers specific for Ppargc1a, a transcription cofactor previously implicated in myofiber phenotype conversion and Rcan1, a known target gene of NFAT transcription factors. I also checked the expression of the following structural genes: the slow MyHC 1 (Myh7), the fast MyHC 2B (Myh4) and the slow isoforms of Troponin C (Tnnc1), Calsequestrin (Casq2) and Myozenin (Myoz2). I found that after 6 and 12 hours of CLFS the transcription of regulator genes was activated, while structural genes were equally expressed in stimulated and contralateral muscles (Figure 4.2). Unlike the previous study, these results suggested that this type of stimulation pattern was not able to induce the transcription of structural genes even after 6 and 12 hours of stimulation. So, these two earlier time points could help to understand the initial phases of the muscle reprogramming in response to CLFS, before the changing of structural components.

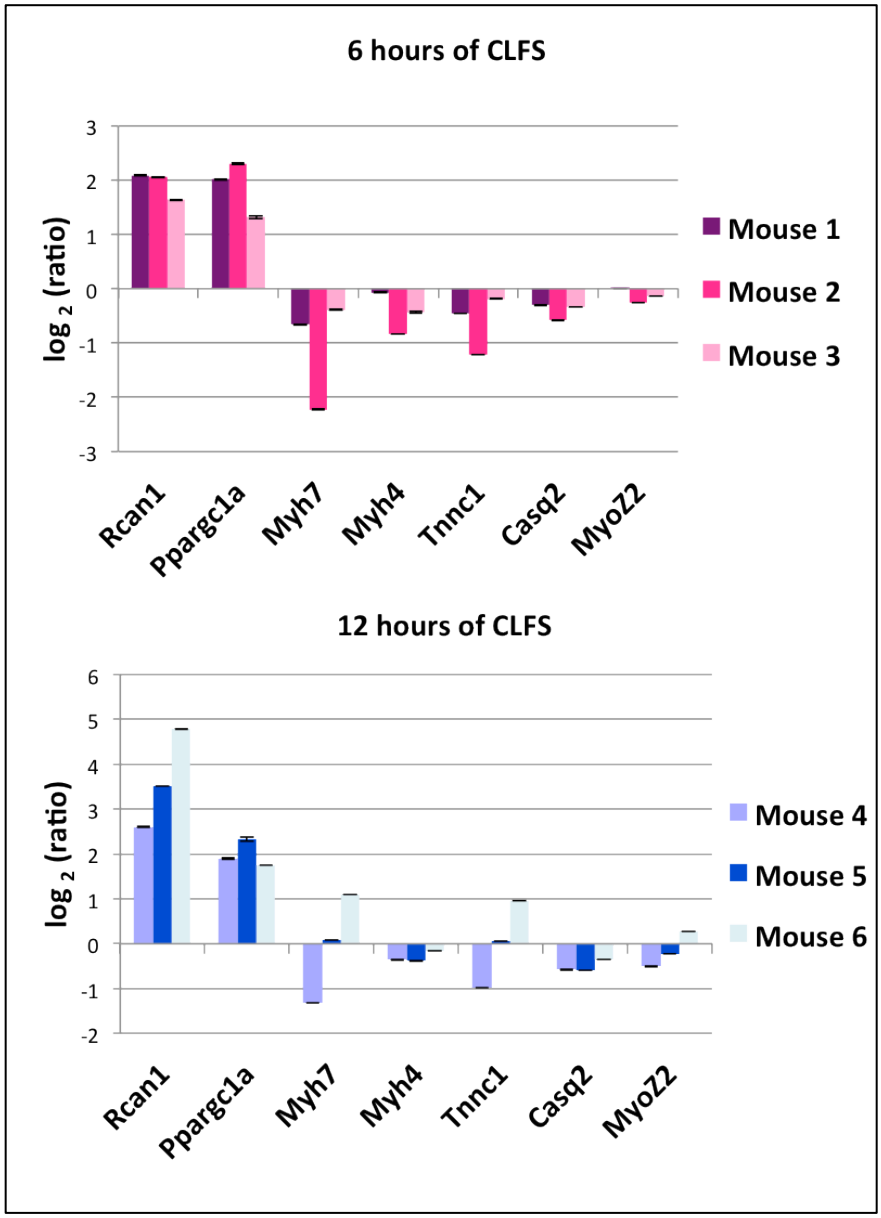

Figure 4.2: Analysis by qPCR of 7 genes involved in fast to slow transition. Signal ratios (log_2 values) were calculated in stimulated EDL whole muscle compared to the contralateral, unstimulated EDL whole. Normalization is relative to the reference gene Txn1.

4.2 Expression profile of stimulated vs contralateral EDL muscles

4.2.1 Experimental design

First, I studied the differences in gene expression between stimulated EDL whole muscle (WM) and the contralateral, unstimulated muscle of the same animal. To this aim, I performed one-color hybridization, using Agilent SurePrint G3 Mouse 8x60K microarray. Total RNA was extracted using TRIzol reagent (Invitrogen).

Linear amplification and labeling of cRNA were then carried out following the standard Agilent protocol, which make use of T7 RNA polymerase. For each sample, starting from 50 ng of total RNA, I obtained 10 μg of amplified RNA on average with a specific activity of about 30 pmol cyanine 3 (Cy3) per μg cRNA. To allow solid statistics of microarray data, I profiled 5 EDL muscle for each condition, and expression profiles were subjected to SAM analysis to determine the statistics relevance of gene expression changes.

Table 4.1 shows the results of two-class SAM paired test: in total, 201 differentially expressed (DE) genes (200 up regulated and 1 down regulated) were identified after 6 hours of stimulation, and 283 DE genes (255 up regulated and 28 down regulated) were identified after 12 hours of stimulation, using a stringent threshold value to minimize the number of false positives (FDR=0%; q-value < 0.001).

DE genes identified in Whole Muscle (WM)						
	FDR 0% (q-value < 0.001)			**FDR 5% (q-value <0.05)**		
	Up	***Down***	***Total***	***Up***	***Down***	***Total***
6 hours of CLFS	200	1	201	644	76	720
12 hours of CLFS	255	28	283	927	637	1564

Table 4.1: DE genes between stimulated and contralateral unstimulated whole muscles. A total number of 213 DE probes (212 up regulated and 1 down regulated) were identified at 6 h and 308 DE probes (277 up regulated and 31 down regulated) at 12 h using a FDR 0%. Since the array contains redundant probes for transcript variants of the same gene, the real number of DE genes is lower, as reported in the table. The analysis was repeated with FDR 5%, to obtain more information for the next functional annotation step.

To test the differences in gene expression between the two time points, I performed a bootstrap cluster analysis with all DE genes identified with FDR 0% (Figure 4.3). The results suggested that a) CLFS induced significant changes at the transcriptional level, since all stimulated muscles formed a distinct group, separated from the contralateral muscles; b) the time points of stimulation are different enough to create two uniform subgroups; c) the contralateral unstimulated muscle used as control showed no significant difference in the two time points.

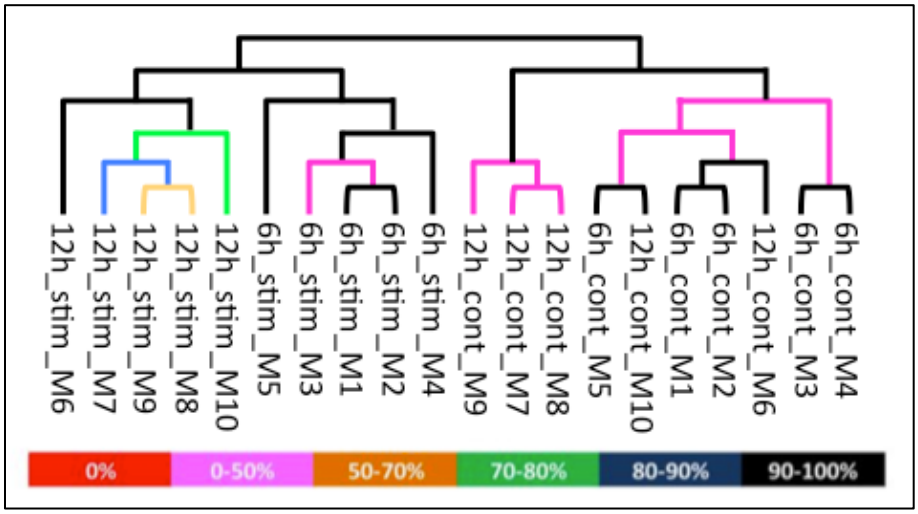

Figure 4.3: Bootstrap cluster analysis with all DE genes (FDR 0%). The stimulated muscles and the contralateral muscles formed two distinct groups. Within the stimulated samples, the two time points of stimulation created two separated subgroups, while the contralateral muscles were mixed together in a unique cluster.

4.2.2 GO enrichment

Skeletal muscle is a complex organ composed by several cell types in addition to myofibers, such as nerves, blood vessels, fat cells, fibroblast, macrophages, and a network of extracellular fibrils. Each of these cell types could respond to CLFS promoting the transcription of particular genes. To gain information about the cellular role of DE genes identified by two-class SAM analysis (FDR 0%), they were sent to the database DAVID (Table 4.2).

The most represented category after 6 hours of stimulation was blood vessel development, which is an essential process to increase the oxidative capacity of skeletal muscle. A great number of genes were involved in regulation of transcription at 12h, and several transcription factors (TF) were already activated after 6 hours of CLFS. I further focused on muscle specific genes included in the categories sarcomere or development of muscle cells. As shown in the next section 4.3, genomic analyses at the single fiber level could better discriminate muscle specific information from processes ongoing in other cell types.

Genes upregulated in WM after 6h of CLFS		
Category	***Number of genes***	***Score***
Blood vessel development	20	3.62
Mesenchymal cell development	12	3.30
Tubulin	23	2.77
Cytoskeleton	31	2.44
Muscle cell development	13	2.28
Nuclear lumen	19	1.95
Transcription regulation	61	1.92
Sarcomere	5	1.91
Genes upregulated in WM after 12h of CLFS		
Category	***Number of genes***	***Score***
Transcription regulation	70	2.08
Negative regulation of transcription	25	1.96
SH2 domain	24	1.79
Muscle cell differentiation	8	1.79
Regulation of cell migration	6	1.47
Regulation of phosphorylation	17	1.45
Nuclear lumen	20	1.41
Regulation of lipid biosynthetic process	3	1.36

Table 4.2: GO analysis of DE identified in WM. Functional Annotation Clustering of DE genes identified in WM was performed at the DAVID database. Clusters formed by enriched categories were ranked according to the relative score number (the higher, the better).

To place the DE genes in the biological system where they act, I then queried a dedicated resource available at KEGG (Tab. 4.3). However, I could obtain significant results only by lowering the threshold of the statistical test to FDR 5% (Table 4.1), thus extending the analysis to 720 and 1564 DE genes after 6h or 12 hours of CLFS, respectively.

Interestingly, more significant pathways were identified at 6h compared to the 12h time point, suggesting that the most important changes occur at the onset of CLFS. In particular, the myofibers could initiate a remodeling process in

response to nerve activity since many genes of actin cytoskeleton were early upregulated. The finding that transcripts of MAPK signaling pathway were also induced is in agreement with reports showing that high-intensity physical exercise and short-term CLFS can stimulate the activity of protein kinases downstream of Ras (Murgia M. et al., 2000).

Only one pathway was statistical significant in the analysis at 12 h, probably because of the cellular heterogeneity of WM. In fact, several processes occurring in myofibers during remodeling of the muscle could be masked by transcriptional changes in other cell types.

Pathway identified by genes upregulated in stimulated muscles after 6h of CLFS		
Term	***Number of genes***	***PValue***
Regulation of actin cytoskeleton	22	1,64E-05
MAPK signaling pathway	24	3,75E-05
Focal adhesion	19	1,52E-04
Chemokine signaling pathway	17	5,20E-04
Pathway identified by genes upregulated in stimulated muscles after 12h of CLFS		
Term	***Number of genes***	***PValue***
Focal adhesion	22	2,40E-04
Pathway identified by genes downregulated in stimulated muscles after 12h of CLFS		
Term	***Number of genes***	***PValue***
ErbB signaling pathway	9	4,76E-04

Table 4.3: Metabolic and signaling pathways identified at the KEGG bioinformatics resource. Pathway analysis of 720 DE genes after 6 hours of CLFS and 1564 DE genes after 12 hours of CLFS identified by two-class SAM analysis using a FDR of about 5% (table 4.1). Due to limitations of pathway analysis (chapter 1.4), only a small portion of these genes had a significant associated pathway. Each pathway was ranked according to the relative P-value (the lower, the better).

4.3 Expression profile of stimulated vs unstimulated EDL muscle fibers

4.3.1 Microgenomic approach

As demonstrated in the previous section, microarray analysis in whole muscle had the limitation that mRNA of all skeletal muscle components are pooled and interpreted together. Recently, my laboratory generated the first list of gene expression in slow-oxidative and fast-glycolytic myofibers (Chemello F. et al., 2011). Microarray analysis from single, isolated myofibers allowed to distinguish the genes differentially expressed between different fiber types and to remove any background noise coming from other cell types or different muscle fibers. So, I wanted to test whether the microgenomic approach could be applied also in models of muscle plasticity. The rationale behind this choice is that changes in gene expression are the first reply of muscle to various physiological stimuli.

To obtain undamaged myofibers, I used the protocol developed in my laboratory (Chemello F. et al., 2011). After CLFS, EDL muscles were quickly removed by microdissection and incubated for 45 min at 37°C with collagenase (Figure 4.4). About 10 dissociated, intact myofibers were collected under stereomicroscope for each muscle and divided in two parts. The shortest one (about 1/3) was used for fiber typing by electrophoretic separation of myosin heavy chain (MyHC) isoforms, and the remaining part was used for RNA purification. I performed organic extraction with TRIzol (Invitrogen) and then I used RNeasy micro Kit (Qiagen) to purify RNA from aqueous phase. The amount of total RNA extracted from a single fiber was very low (in the range of one to few nanograms). So, exponential amplification of purified RNA was necessary before hybridization on Agilent microarrays.

4.3.2 Experimental design

To study the differences in gene expression at the level of isolated single fibers (SF) it is important to have a homogeneous response to the imposed stimulus.

One of the advantages of CLFS is that all motor units of the target muscle are activated by the same impulse pattern under standardized and reproducible conditions. For this reason, each muscle fiber composing the muscle is supposed to be activated in the same manner. However, microgenomics also has the limitation that is very difficult to start from two fibers having exactly the same characteristics in the stimulated and the contralateral muscle. To simplify the experimental design, SF isolated after 6h and 12h CLFS were compared with myofibers isolated from EDL muscle of animals not subjected to any electrical stimulation (time 0). As a consequence, I used a two-class SAM unpaired test and each SF was considered an independent sample.

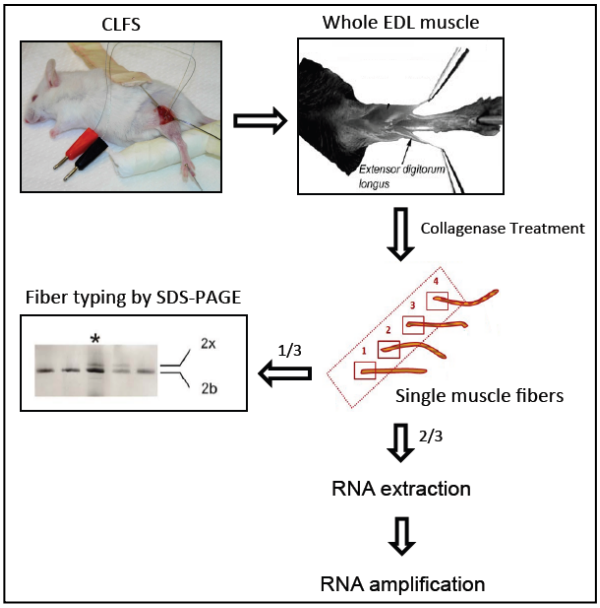

Figure 4.4 Protocol for RNA expression profiling of characterized myofibers. After CLFS, single fibers were dissociated from EDL muscles and cut in two pieces. The smallest part was used for fiber typing, and the remaining part was used for RNA purification.

Total RNA was extracted and then exponentially amplified using the TranPlex Whole Transcriptome Amplification 2 kit (Sigma-Aldrich). Labeling was carried out using incorporated Cy3 dyes and Klenow fragment. On overage about 4 µg of amplified-labeled dsDNA were obtained from a single fiber with a specific activity of 30 pmol Cy3 per µg dsDNA. Five pure fibers 2B and five hybrid fibers 2X/2B were profiled for each condition and microarray experiments were performed with Agilent SurePrint G3 Mouse 8x60K platforms.

Table 4.4 shows the results of the two-class SAM unpaired test in SF: in total, 245 DE genes were identified after 6h and 1301 after 12 h of CLFS, respectively, using the same stringent threshold applied in WM samples (FDR=0%; q-value < 0.001).

DE genes identified in Single Fibers (SF)						
	FDR 0% (q-value < 0.001)			FDR 1% (q-value <0.01)		
	Up	***Down***	***Total***	***Up***	***Down***	***Total***
6 hours of CLFS	207	38	245	430	172	602
12 hours of CLFS	510	791	1301	1532	3233	4765

Table 4.4: DE genes between stimulated and unstimulated EDL single fibers. A total number of 253 DE probes (212 up regulated and 41 down regulated) were identified at 6 h and 1369 DE probes (552 up regulated and 817 down regulated) at 12 h using a FDR 0%. The analysis was repeated with FDR 1%, to obtain more information for the next functional annotation step.

Figure 4.5 shows a bootstrap cluster analysis with all DE genes identified with previous test. In striking contrast with results obtained in WM (Figure 4.3), four 6h-stimulated SF grouped together with the unstimulated fibers, while the other six were more close to 12h-stimulated SF. It is also evident that all SF stimulated for 12h formed a well separate subgroup.

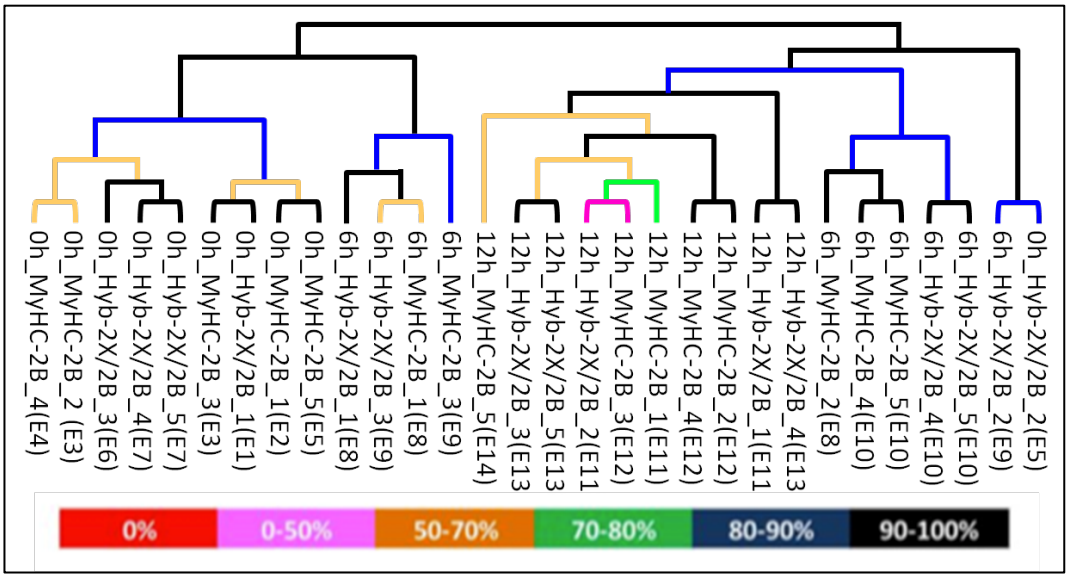

Figure 4.5: Bootstrap cluster analysis with all DE genes (FDR 0%). The 6h-stimulated fibers were divided in 2 subgroups, one most similar to unstimulated fibers and the other more similar to 12h-stimulated fibers. All 12h-stimulated fibers formed a distinct subgroup.

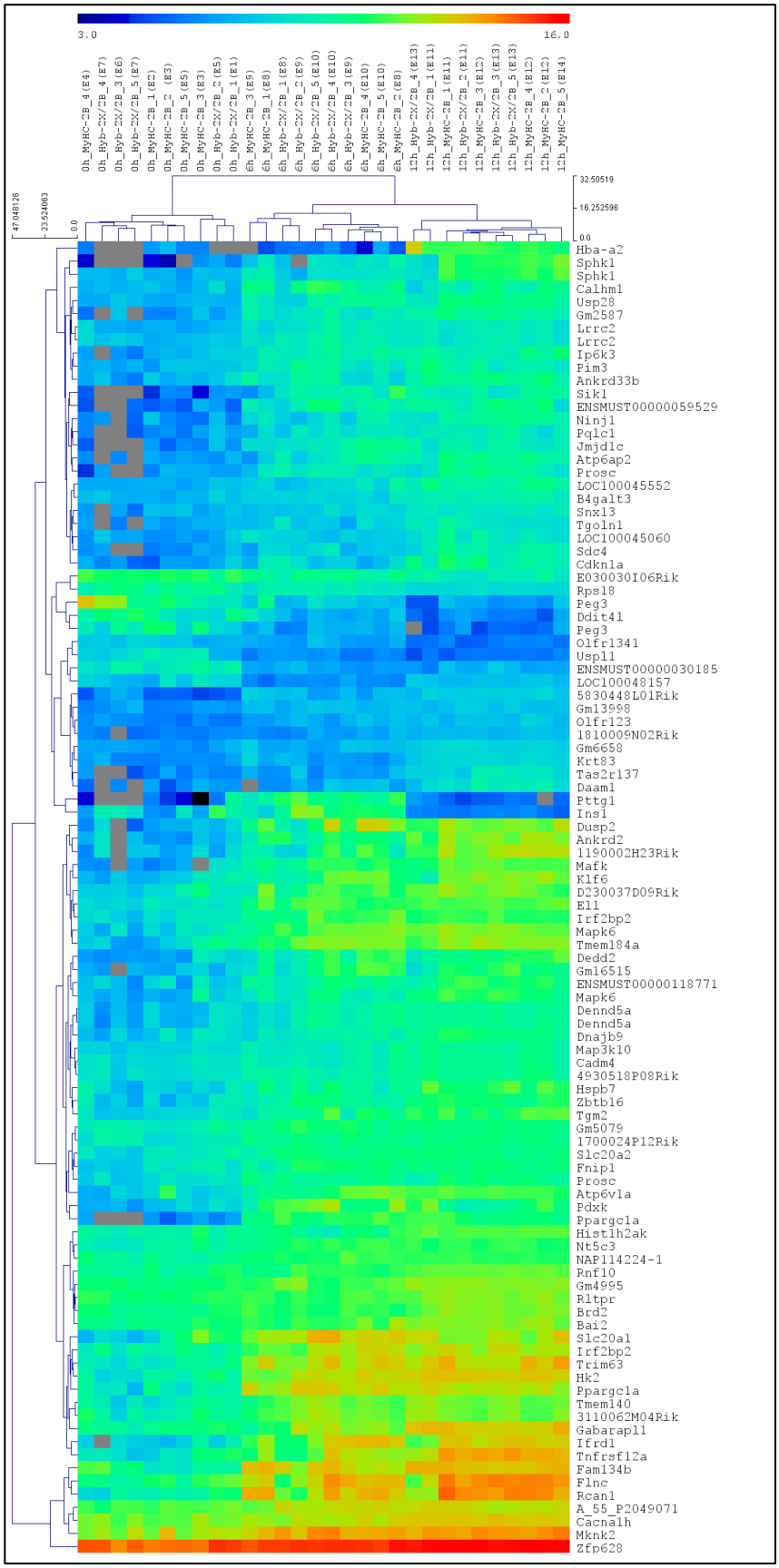

Figure 4.6: Cluster analysis with the first 100 DE genes identified by multiclass SAM analysis (FDR 0%).

Then I repeated the cluster analysis with the 100 most significant DE genes identified by a multiclass SAM analysis. In this case, all the fibers clustered according to time of stimulation (Figure 4.6). A central issue in single cell genomic analysis is the homogeneity of cell population. Even myofibers with the same MyHC isoform can express different set of genes (Chemello F. et al., 2011). So, 6h-stimulated SF may cluster with control SF because the shared genes prevail on changes induced by CLFS. After 12 h of stimulation, the number of DE genes increased about 5 times with respect to 6h, and for this reason the cluster formed by SF stimulated at this time point is more homogeneous.

4.3.3 GO enrichment

Enriched GO categories formed by DE genes identified in SF (FDR 0%) are shown in Table 4.5. Sarcomere was the first category after 6 h of CLFS, and it remained enriched also after 12 h. Regulation of transcription ranked at the first place after 12 h of stimulation, as it happens in WM (Table 4.2). It was interesting to find the category blood vessel development enriched also in SF.

As before, I queried the KEGG database to place the DE genes in biological pathways (Tab. 4.6). In this case it was sufficient to lower the threshold of the statistical test just to FDR 1% to obtain significant results (Table 4.4). In contrast with WM (Table 4.3), here more significant pathways were identified at 12h compared to the 6h time point. This result is obviously a consequence of the initial number of DE genes (602 for SF 6h and 4765 for SF 12h, respectively). However, it also suggests that myofibers had a homogeneous response to CLFS that was partially eclipsed in the analysis with the entire muscle organ.

Genes upregulated in SF after 6h of CLFS		
Category	***Number of genes***	***Score***
I band	7	3,88
Regulation of transcription	57	2,97
Body morphogenesis	22	2,66
Sequence-specific DNA binding	14	2,47
Heat shock protein	7	2,35
Genes upregulated in SF after 12h of CLFS		
Category	***Number of genes***	***Score***
Regulation of transcription	128	3,51
Blood vessel development	17	3,35
I band	9	3,31
Enzyme linked receptor protein signaling pathway	32	2,68
Translation regulation	12	2,66
Genes downregulated in SF after 12h of CLFS		
Category	***Number of genes***	***Score***
Zinc-finger	144	4,44
Ubiquitin mediated proteolysis	50	3,17
Regulation of transcription	177	2,62

Table 4.5: GO analysis of DE identified in SF. Functional Annotation Clustering of DE genes identified in SF was performed at the DAVID database. Clusters formed by enriched categories were ranked according to the relative score number (the higher, the better).

The unique significant pathway after 6h of CLFS was insulin signaling, which is involved in regulating the metabolism of glucose and lipids in muscle. It has long been known that acute exercise can improve the ability of insulin to stimulate glucose uptake (Richter E.A. et al., 1982). In mammals, several studies showed that glucose uptake capacity is greater in oxidative than in glycolytic muscle fibers (Schiaffino S. and Reggiani C., 2011). The activation of insulin pathway ultimately results in the translocation of a specific glucose transporter protein isoform (GLUT-4) to the sarcolemma and the t-tubules, where glucose transport

takes place via a facilitative diffusion process. GLUT-4 in resting cells is sequestered in intracellular membrane bound vesicles, and in response to insulin these vesicles rapidly fuse with the cell surface (Holman G.D. & Sandoval I.V., 2001). After 6 and 12h of CLFS, GLUT4 mRNA did not increase, in agreement with data in the literature showing that changes in its expression require a longer time (Hofmann S. & Pette D., 1994). Indeed, only long-term CLFS studies demonstrated the increase of GLUT4 protein expression in rat skeletal muscle (Etgen G.J. et al., 1993). By contrary, the mRNA level of hexokinase 2, which is the enzyme that phosphorylates glucose in the first step on glucose metabolism, is strongly induced already after 6h of stimulation.

Pathway identified by genes upregulated in stimulated fibers after 6h of CLFS		
Term	*Number of genes*	*PValue*
Insulin signaling pathway	11	1.92E-04
Pathway identified by genes upregulated in stimulated fibers after 12h of CLFS		
Term	*Number of genes*	*PValue*
Ribosome	22	3.85E-07
Spliceosome	22	9.24E-05
Oxidative phosphorylation	22	1.85E-04

Table 4.6: Metabolic and signaling pathways identified at the KEGG bioinformatics resource. Pathway analysis of 602 DE genes after 6 hours of CLFS and 4765 DE genes after 12 hours of CLFS identified by two-class SAM analysis using a FDR of about 1% (table 4.4). Each pathway was ranked according to the relative P-value (the lower, the better).

The up-regulation of genes involved in oxidative phosphorylation and ribosome component is a typical response of long term CLFS that is functionally related to increased protein synthesis and to changing of energy metabolism, from glycolytic to more oxidative one (Pette D. & Vrbovà G., 1992). It is interesting to note that components of oxidative phosphorylation were significantly induced already after 12 hour of CLFS (Table 4.6). This result suggests that the shift from fast glycolytic to slow oxidative fiber follows a temporal ordered series of events. While genes of oxidative phosphorylation begin to be transcribed, the induction

of typical slow isoforms of contractile proteins is not yet observed (see below, Fig. 4.12). Moreover, the significant enrichment of the category spliceosome implies that the fast to slow transition may possibly involve alternative splicing of mRNA isoforms. While preliminary analyses would confirm this assumption, more in depth examination of the expression data are necessary before drawing conclusions about this point.

4.4 Early responsive processes

The onset of slow stimulation pattern on the fast EDL muscle induced a rapid response, leading to a wide range of phenotypic adaptations. As a consequence a set of "immediate stress adaptive response" genes are quickly upregulated to values up to 10 fold higher of normal expression (La Framboise W.A. et al., 2009). To exemplify the novelty of the microgenomic approach, I first present the microarray data relative to these genes (figure 4.7). In the next figure 4.8, I then compare the foldchange values measured in SF with those of WM.

The strong upregulation of muscoloaponeurotic fibrosarcoma oncogene (Mafk), early growth response 1 (Egr1), ephrin A1 (Efna1) and activating transcription factor 3 (Atf3) was confirmed both after 6h than 12h of stimulation. However my data clearly show that MafK has a specific response in myofibers, while the higher foldchange of Egr1 and Atf3 in whole EDL muscle points to a significant contribution from other cell types (Figure 4.8). On the contrary, it seems that DmeI/homer1 and early growth response 2 (Egr2) did not change expression in myofibers. The expression trend of FBJ murine osteosarcoma viral oncogene homolog (Fos) was essentially the same in SF and WM, with a marked decrease at 12h compared to 6h. However, the early induction observed in WM do not seem muscle specific, as it is not confirmed in SF. Interestingly, JUN protooncogene related D1 (JunD) was upregulated only in myofibers, suggesting a specific role in muscle cells.

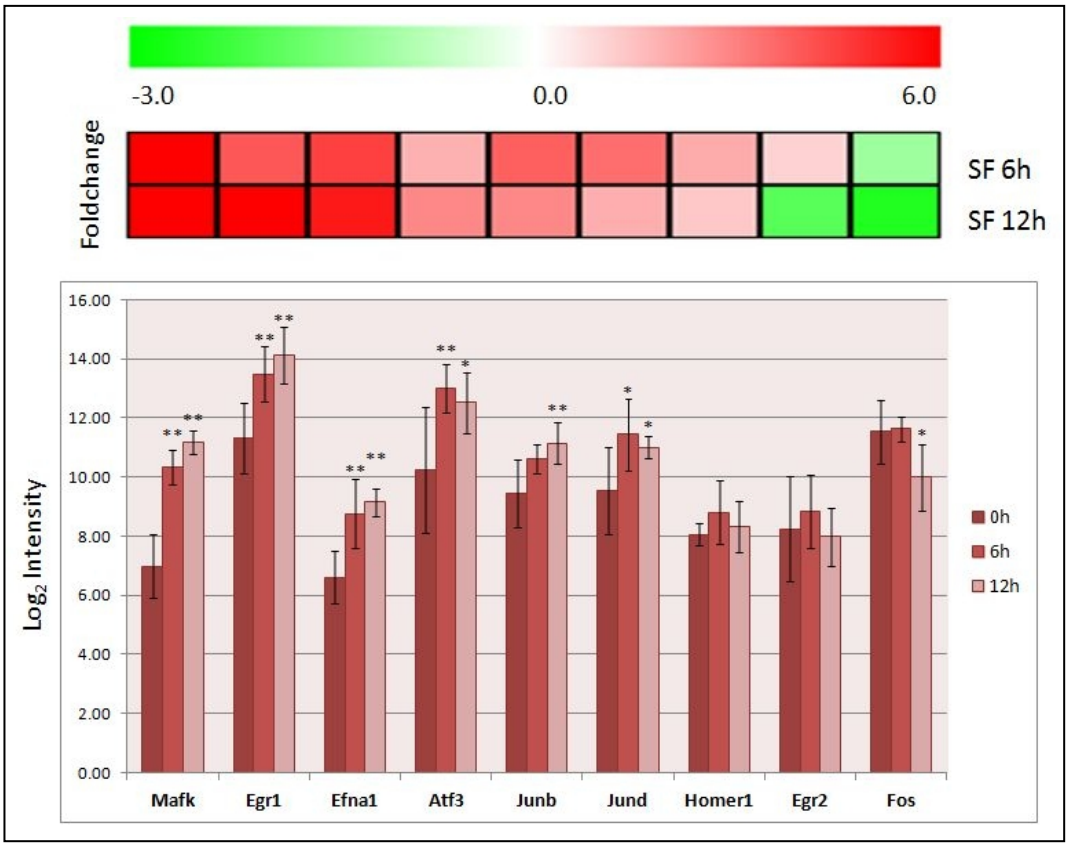

Figure 4.7: Immediate stress adaptive response genes: expression in myofibers. Each bar indicates the average Log_2 intensity values (± standard deviation) measured in SF at the three time points: 0h (control), 6h and 12h. Asterisks above the bar mark statistically significant changes (**q-value < 0.001; * q-value < 0.01). The heat map at the top visualizes the fold change variation for the same genes. The foldchange is the averaged value in stimulated fibers divided by the averaged value in unstimulated fibers at time 0 (i.e. difference between logarithms); this number is then elevated to the power of 2. The end scale was set to 6.0 to show also the smallest changes; so values for Mafk were out of scale (see Fig. 4.8).

GeneName	q-value (%)				Foldchange			
	SF 6h	SF 12h	WM 6h	WM 12h	SF 6h	SF 12h	WM 6h	WM 12h
Egr2			0.85	0.00			11.58	8.53
Homer1				0.00				2.66
Fos		0.05	0.74	0.00		-2.61	15.59	4.06
Jund	0.36	0.13			3.42	1.92		
Atf3	0.00	0.03	0.00	0.00	3.75	2.80	30.26	15.73
Junb	1.32	0.00	0.00		1.85	2.80	3.12	
Efna1	0.00	0.00	0.00	0.00	4.50	5.43	5.14	5.14
Egr1	0.00	0.00	0.00	0.00	3.96	6.09	105.57	46.68
Mafk	0.00	0.00	0.00	0.00	7.63	12.35	4.59	3.44

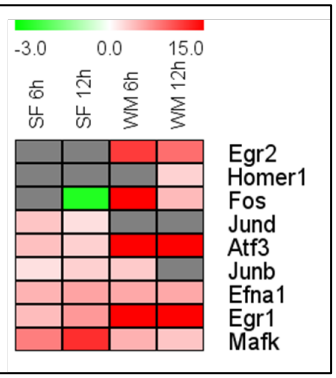

Figure 4.8: Direct comparison of significant foldchanges in myofibers (SF) and whole muscle for the same immediate stress adaptive response transcripts shown in Fig. 4.7. q-values **(%)** greater than 0.00 are highlighted. Please note that the values of Atf3 and Egr1 in WM are out of scale.

In the microarray analysis the controls are fibers from mice in normal conditions (4.3.2). To verify whether the upregulation of Egr1 in SF was influenced by other

stress factors of the stimulation method, such as fasting and anesthesia, I performed qPCR at the single fibers level (Figure 4.9). For these experiments, the control fibers were isolated from contralateral muscle of mice subjected to stimulation. Results of qPCR analysis indeed confirmed that Egr1 expression was increased in SF by CLFS, but only after 12h. A corollary of my qPCR analysis is that the strong induction of Egr1 observed at 6h in WM (105-fold increase compared to the contralateral muscle!) cannot be specific of muscle fibers.

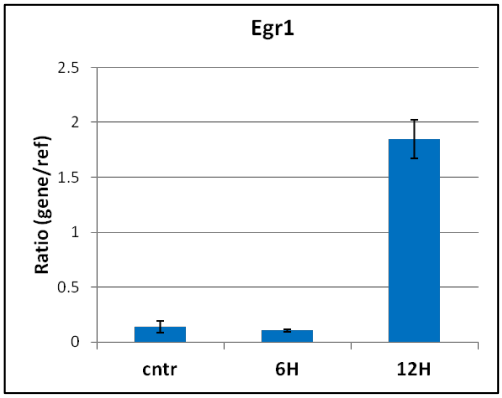

Figure 4.9: Analysis by qPCR of Egr1. Each bar is referred to the average value of Egr1 expression in 3 single fibers for each condition. Signal ratios were calculated for each fiber sample, comparing the gene expression value with the expression of the reference gene Rpl4. The error bars are referred to the standard error of the three measures. Student's t-test considered significant the differences after 12h (p-value <0.05).

4.4.1 Angiogenesis

Since microgenomics can distinguish expression in myofibers from processes occurring in other cell types, it is of particular interest to analyze the category blood vessel development that was highly enriched both in WM at 6h (Table 4.2) than in SF at 12h (Table 4.5). Figure 4.10 shows genes with significant changes, the table lists the associated q-values and the heat map allows a direct comparison of foldchanges between SF and WM in the two time points.

Angiogenesis, i.e. is the process of formation of new blood vessels, is a common adaptive response to physical activity in skeletal muscles, in order to provide additional supply of oxygen and nutrients. The capillary density differs among different types of myofibers (see introduction 1.1.2). Endurance exercise, as well as prolonged CLFS, induces an expansion of the capillary network in fast muscle

(Brown M.D. et al., 1976; Hudlicka O. et al., 1977), through a process that is mediated by a combination of growth factors, hypoxia and mechanical stresses.

GeneName	q-value (%)				Foldchange			
	SF 6h	SF 12h	WM 6h	WM 12h	SF 6h	SF 12h	WM 6h	WM 12h
Tbx3		0.22	0.00	0.28		-1.87	3.56	2.22
Vegfa		0.86	0.00	0.70		-1.79	2.67	2.44
Itgb2	0.00	0.09			1.88	1.89		
Rbpj	1.72	0.00			1.89	2.15		
Sox1	0.82	0.00			1.79	2.44		
Akt1	4.77	0.00		3.77	1.68	2.47		1.56
Qk		0.00				2.55		
Myo1e		0.00				2.65		
Tbx1	0.34	0.00	0.00	3.57	2.57	2.71	1.47	1.72
Junb	1.32	0.00	0.00		1.85	2.80	3.12	
Rapgef1	3.47	0.00			1.79	3.11		
Fgf8	4.59	0.00			1.73	3.28		
Sgpl1	0.00	0.00			3.95	3.49		
Gna13	1.45	0.00	2.57	0.00	2.12	3.95	1.63	2.35
Hs6st1		0.00		0.65		3.97		1.87
Tgfb2	0.00	0.00		0.30	2.97	4.87		3.25
Tiparp	0.00	0.00	0.72	0.71	3.72	4.89	2.07	1.88
Tgm2	0.00	0.00	0.00	0.55	3.30	5.82	1.47	2.38
Hbegf	0.00	0.00	0.97	0.00	4.46	10.04	3.13	6.18
Tnfrsf12a	0.00	0.00	0.00	0.00	5.39	15.18	6.58	9.68
Sphk1	0.21	0.00	0.00	0.00	1.33	24.62	2.93	5.11
Socs3			0.00	0.00			7.29	5.79
Pdpn	1.91			0.00	2.64			3.22
Id1			0.00	0.00			4.91	3.22
Cxcl12			3.19	0.00			1.62	3.13
Agt	0.00		1.64	0.30	3.77		1.76	2.63
Hmox1			0.00	0.71			2.26	2.39
Klf5				0.00				2.09
Acvr1			0.00	0.00			1.47	1.91
Hdac7				0.00				1.55
Eng			0.00	1.71			1.50	1.32

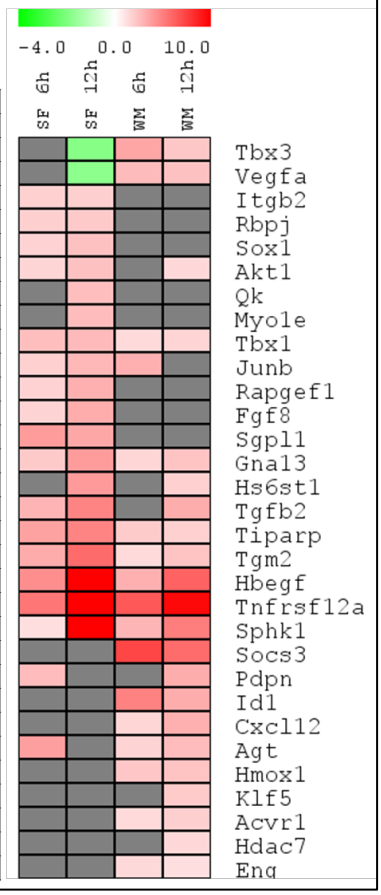

Figure 4.10: Blood vessel development. Significant genes of this category are associated with q-values (left) while the heat map (right) reveals foldchanges mearured in SF and WM samples.

It is now well established that skeletal muscle has a secretory function affecting the local muscle biology in autocrine or paracrine manner. In good agreement with this notion, genes most strongly upregulated after CLFS encode for growth factors (GF), like for example transforming GF beta 2 (Tgfb2), and other signaling molecules (Figures 4.10 and 4.11). In endothelial cells, TGFβ can propagate a signaling response via activin A receptor type I (Acvrl1), which was actually induced in WM. Binding of TGFβ to Acvrl1 activates receptor-regulated Smads (R-SMAD1/5/8) and this in turn promote transcription of target genes such as the inhibitor of DNA binding 1 (Id1) that indeed I found up-regulate only in WM. Vascular remodeling has also been described to occur through a mechanism mediated by the transmembrane protein endoglin (Eng). Interaction of TGFβ

with ACVRL1 and endoglin promotes proliferation of endothelial cells and angiogenesis (Goumans M.J. et al., 2002).

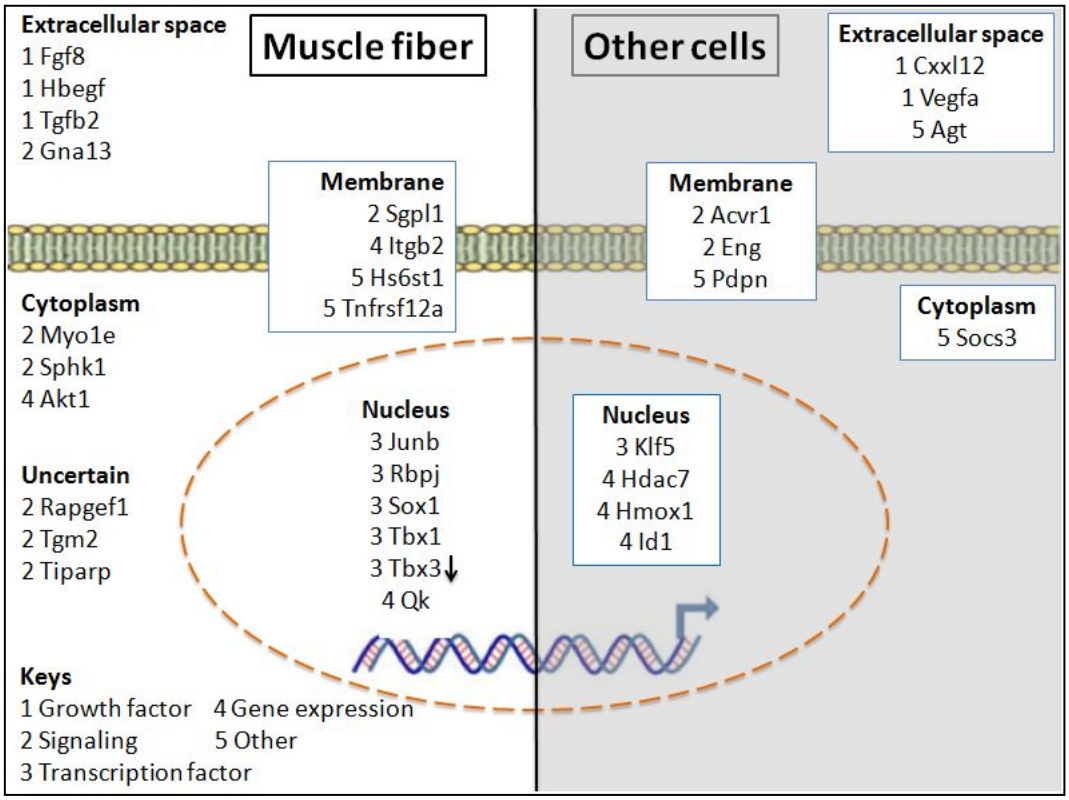

Figure 4.11: Blood vessel development. Significant genes of this category are associated with Gene Ontology terms (Cellular component). Left: genes with significant values in SF; right: genes with higher expression in WM are likely part of non-muscle cells.

Physical exercise specifically upregulates heparin-binding EGF-like GF (Hbegf) in skeletal muscle (Fukatsu Y. et al., 2009) and Hbegf was also highly induced in SF by CLFS. Transgenic mice overexpressing HB-EGF in muscle tissue were protected from obesity and insulin resistance, even when maintained on a high-fat diet. These results suggest that HB-EGF facilitates a selective use of carbohydrate rather than fat as an energy substrate. Loading experiments further showed that overexpression of HB-EGF cause substantial increases in glucose tolerance, insulin sensitivity, and glucose uptake by skeletal muscle.

Several studies have call attention to the expression of vascular endothelial growth factor A (Vegfa) in exercise-induced angiogenesis (Yan et al., 2011). Vegfa mRNA was induced after CLFS in rat hindlimb muscles (Hang J. et al., 1995; Amaral S.L. et al., 2001), but this result is not confirmed here at single fiber level,

although it is reproducible in WM (Figure 4.10). This finding would rule out that contracting myofibers are a major source of VEGF in short term CLFS.

Many studies have focused on the mechanisms of neo-vascularization in tumors. One recent report found that the proto-oncogene JunB promotes cell invasion and contributes to the development and progression of renal cell carcinoma (Kanno T. et al., 2012). However, the same TF is also a major determinant of muscle mass homeostasis and can induce muscle hypertrophy without affecting satellite cell proliferation (Raffaello A. et al., 2010). Physiologic angiogenesis has been studied much less extensively of blood vessel development occurring in tumors and other pathologic conditions. It is likely that the two processes are similar but not identical. With this respect, expression profiling in SF identified TF and proteins with nuclear localization (Fig. 4.11) that may contribute to shed light on complex events taking place in myofibers. Of note, several of these regulatory proteins have also a role in muscle cell differentiation (see below, Figures 4.16 and 4.17).

4.4.2 Sarcomere

It is now well established that changes in muscle stimulation patterns can modify structural component of thick and thin filaments (see introduction 1.1.5). Such modifications usually require weeks or months of continuous activity, due to the relatively slow turnover of these proteins (Pette D. & Vrbova G., 1992). In contrast to data reported by LaFramboise et al. 2009, the transcription of slow myosin and troponin isoforms was not activated in my experimental model, as deduced by qPCR in WM (Figure 4.2). The microarray analysis carried out in SF confirmed and extended the first qPCR data, suggesting that the induction of structural genes is likely a late process in fiber type transformation (Figure 4.12). It is possible that the TFs involved in transcription of those structural genes are not yet fully activated or the promoter of the slow genes is not accessible in fast fibers, due to a close chromatin conformation.

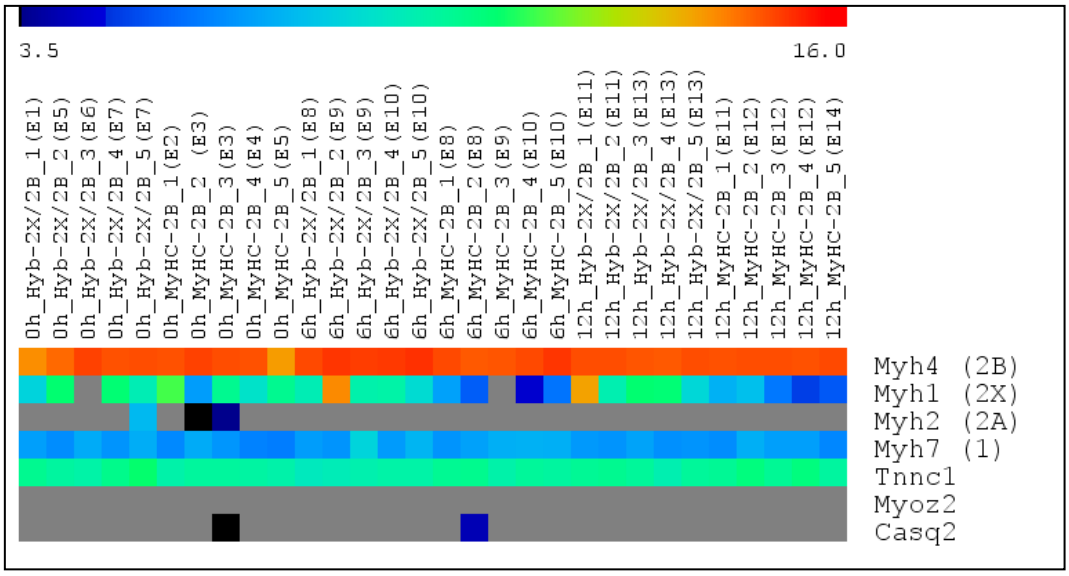

Figure 4.12: Heat map of selected sarcormere genes in SF samples. The transcription levels of slow MyHC 1 (Myh7), fast MyHC 2B (Myh4), MyHC 2X (Myh1), and MyHC 2A (Myh2) did not change in fast myofibers either after 6h or 12h of CLFS. Calsequestrin (Casq2), Myozenin (Myoz2) and MyHC 2A (Myh2) have an undetectable microarray signal in most fibers (grey color).

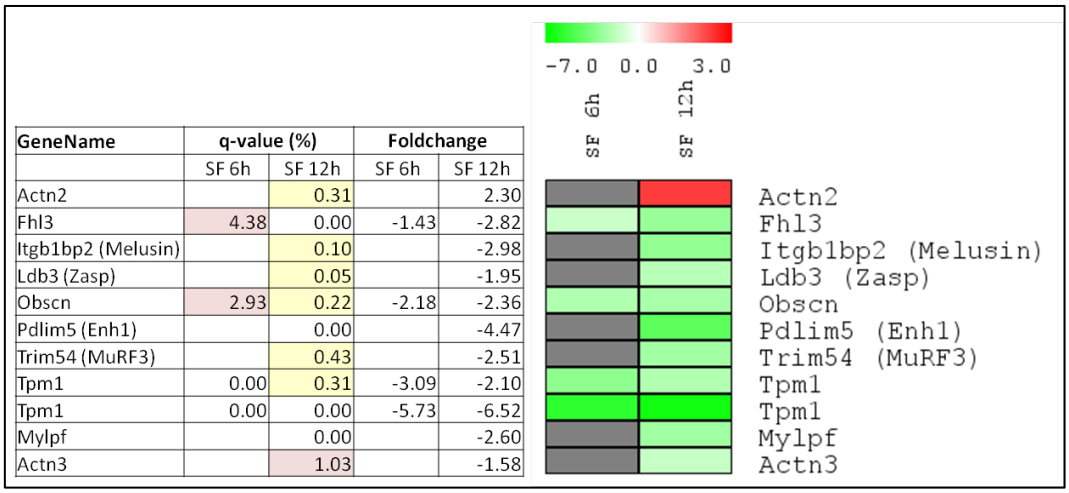

GeneName	q-value (%)		Foldchange	
	SF 6h	SF 12h	SF 6h	SF 12h
Actn2		0.31		2.30
Fhl3	4.38	0.00	-1.43	-2.82
Itgb1bp2 (Melusin)		0.10		-2.98
Ldb3 (Zasp)		0.05		-1.95
Obscn	2.93	0.22	-2.18	-2.36
Pdlim5 (Enh1)		0.00		-4.47
Trim54 (MuRF3)		0.43		-2.51
Tpm1	0.00	0.31	-3.09	-2.10
Tpm1	0.00	0.00	-5.73	-6.52
Mylpf		0.00		-2.60
Actn3		1.03		-1.58

Figure 4.13: Expression in SF of DE genes with sarcomeric localization. None of these transcripts showed significant expression changes in WM. q-values (%) greater than 0.00 are highlighted. Two different probes for the fast isoforms of tropomyosin alpha showed concordant results.

Figure 4.13 shows that the fast isoforms of tropomyosin alpha (Tpm1) was significantly downregulated in SF, as it was the regulatory myosin light chain 2f (Mylpf). Within the family of sarcomeric α-actinins, the fast isoform decreased (Actn3) with a parallel rise of the slow oxidative isoform α-Actinin-2 (Actn2). This finding is of interest, because α-actinin-3 has not only a structural importance as scaffold for the Z disc, but it also plays a role in regulation of muscle metabolism. In fact, KO mice with α-Actinin-3 deficiency show a characteristic shift from fast

glycolytic fibers toward an oxidative metabolism typical of slow muscles (Berman Y. & North KN., 2010). PDZ and LIM domain proteins possess a 100-amino acid PDZ domain at the N terminus and one to three LIM domains at the C-terminus. Through the LIM domains, Pdlim5 (also called Enigma homolog protein 1) can specifically interact with protein kinase C βI, thus regulating activities of PKC isoforms (Maturana AD et al., 2011). So the marked downregulation of Pdlim5 may also have impact on calcium signaling.

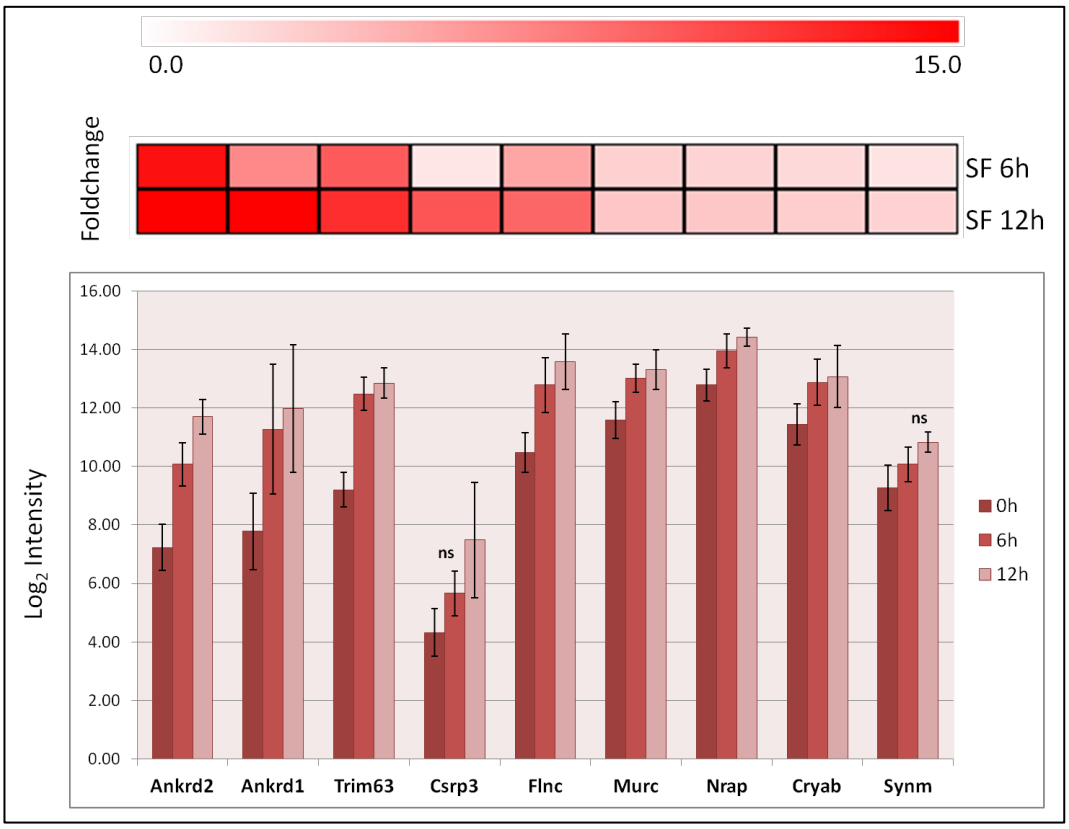

Figure 4.14: I band: expression in myofibers. Each bar indicates the average Log2 intensity values (± standard deviation) in the three time points and the heat map reports the foldchanges for the same genes (see also legend of Fig. 4.7). All changes were highly significant (**q-value < 0.001), except where specified. ns = non significant. The foldchange values of Ankrd1 and Ankrd2 after 12h are out of scale: Ankrd1 increased 23.4-fold and Ankrd-2 19.6-fold respect to unstimulated fibers (Fig. 4.15).

Several sarcomeric proteins localized in the I band are quickly recruited in response to developmental and environmental stimuli (Clark K.A. et al, 2002). In good agreement with this notion, the I band category was enriched in myofibers (Table 4.5). In particular, Ankyrin repeat domain -1 (Ankrd1) and -2 (Ankrd2), as

well as the E3 ubiquitin ligase Trim 63 (alias Murf1), were strongly upregulated in SF already after 6h of stimulation (Figure 4.14).

GeneName	q-value (%)				Foldchange			
	SF 6h	SF 12h	WM 6h	WM 12h	SF 6h	SF 12h	WM 6h	WM 12h
Ankrd1	0.00	0.00	0.00	0.00	14.07	23.40	4.64	24.39
Ankrd2	0.00	0.00			6.96	19.64		
Trim63	0.00	0.00			9.67	12.34		
Csrp3		0.00				10.05		
Flnc	0.00	0.00	0.00	2.77	5.24	9.04	1.74	1.92
Cryab	0.00	0.00			2.75	3.41		
Murc	0.00	0.00	0.00	0.21	2.59	3.32	2.00	3.70
Nrap	0.00	0.00			2.26	2.97		
Synm		0.00			1.66	2.67		

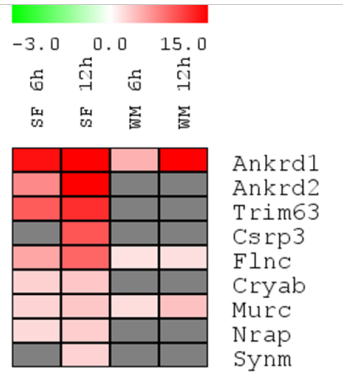

Figure 4.15: I band genes: comparison of expression levels between SF and WM for the same transcripts shown in Fig. 4.13. q-values (%) greater than 0.00 are highlighted. The foldchange value of Ankrd1 in WM after 12h is out of scale: Ankrd1 increased 24.4-fold respect to the contralateral muscle.

The situation was very different in WM: only transcripts of Ankrd1, filamin C gamma (Flnc) and muscle-related coiled-coil protein (Murc) were significantly upregulated (Figure 4.15). The discordant expression pattern of Ankrd-1 and -2 is intriguing, since they are members of a conserved muscle ankyrin repeat protein family (MARPs). Both proteins are involved in the adaptive response to mechanical perturbation, but the spatial and temporal activation is peculiar (Miller M.K. et al., 2003). Ankrd1 was originally discovered as a cytokine-inducible gene in fibroblasts (Chu W. et al., 1995); later on, it appeared to have a broad expression range with primary importance in cardiac muscle. Since Ankrd1 is also expressed by the endothelial cells of vessel (Boengler K. et al., 2003), its response to CLFS may not entirely due to myofibers.

In contrast to Ankrd1, expression of Ankrd2 is more restricted to skeletal muscle with marked preference for slow oxidative fibers (Tsukamoto Y. et al., 2002). The role of Ankrd2 as a muscle stress sensor is well documented in many different conditions from stretch to eccentric contractions but also in models of muscle unloading such as denervation. This led to the hypothesis that Ankrd2 plays a signaling role, linking the elastic I-band region of the sarcomere to transcriptional control in the nucleus (Belgrano A. et al., 2011). Since Ankrd2 is specifically

upregulated in SF, its role of muscle stretch sensor is reinforced by our data. The low induction observed in WM could be explained assuming that A) other cells composing the muscle mask Ankrd2 activation B) the averaged value is lowered by myofibers with a delayed response. In fact, the level of Ankrd2 transcript is growing with time (Figures 14.14 and 14.15). However, so far I was not able to confirm the upregulation of Ankrd2 by qPCR with the same protocol previously shown for Egr1 (Figure 4.9), using contralateral myofibers as control. Probably it will be necessary to modify some parameters of the qPCR reaction (e.g. experiments with pool of fibers) to obtain a detectable signal for this transcript.

The E3 ubiquitin ligase Trim63 is often induced as part of the atrophy-response program, which targets myofibrillar proteins to proteasome. In my experimental system, Trim63 was strongly upregulated (Fig. 4.14), but the category of ubiquitin-mediated proteolysis resulted downregulated in SF at 12h (Table 4.5). The Trim63 protein is better known as muscle-specific RING finger-1 (MURF-1) and has a high degree of homology to MURF-2 (Trim55) and MURF-3 (Trim54). The latter gene was also downregulated in SF at 12h (Fig 4.13). Further analyses are necessary in order to explain these intriguing data.

4.4.3 Regulation of transcription

In this section I will analyze only results produced in SF for two reasons: 1) more DE genes were identified (compare Table 4.2 with Table 4.5); 2) it is not possible to known in WM which cell type is responsible of the observed expression changes. As a first step, I did classify the genes into detailed subgroups using the precise vocabulary defined by the Gene Ontology (Table 4.7). However, I had to face the problem that the annotation of genes with established role in skeletal muscle is neither complete nor fully consistent (Figure 4.16). To help the discussion, I prepared a new cartoon, which shows the final conclusion of this first analysis (Figure 4.17).

Functional annotation	Genes
Transcription factor activity	a) **Known role in muscle**: Foxl2, Foxo3, Hopx, Junb, Max, Mef2a, Nfatc1, Rbpj, Tbx1, Tead1. b) Aff1, Aff3, Arid3a, Atf4, Atf5, Bach1, Cebpb, Csrnp1, E2f3, Egr1, Erf, Foxn3, Hmga1, Klf6, Mafk, , Nfil3, Nr4a1, Nr4a3, Pbx1, Smad1, Sox21, Tgif1, Tgif2, Zbtb16, Zfp628.
Regulation of gene expression	a) **Known role in muscle**: Akt1, Ankrd1, Fgf8, Murc, Musk, Ppargc1a, Qk b) Atn1, Cry2, Dedd2, Dnajb6, Efcab6, Ell, Ewsr1, Irf2bp2, Klf9, Malt1, Map3k10, Med13l, Ncoa2, Pcgf5, Per1, Ptrf, Rybp, Samd4, Scx, Sf1, Sox1, Thrap3, Ybx1, Zbtb20, Zfp652, Zfp655.
Chromatin	H3f3b, Hist1h2ag, Hist1h2ak, Hist1h2an, Hist1h3d, Hist1h3f, Hist2h2aa1, Hmga1, Hmgb3, Hmgn1.
Chromatin modification	Dot1l, Hopx, Jarid2, Jmjd1c, Kdm3a, Morf4l1, Sap30, Tlk1.
RNA binding	Cln6, Dnajb9, Exosc3, Fbl, G3bp1, Gm6506, Hnrnpa2b1, Hnrnpf, Lmna, Mbnl2, Midn, Nhp2, Snrpf, Terc, Top1, Tra2a, Zcrb1.
Cell cycle	1190002H23Rik, Cdt1, Cdkn1a, Esco1, Sik1, Sesn1.
Other	Ankrd33b, Arl4a, Brd2, Ctdp1, Dusp2, Dusp26, Ipo5, Ivns1abp, Kpna3, Mid1ip1, Mustn1, Pitpnc1, Psma1, Rabgef1, Ranbp9, Sphk1, Spop, Tnpo1, Uaca, Zfand2a.

Table 4.7: Gene Ontology classification. The 128 genes identified in SF at 12h in the broad David cluster 'Regulation of transcription' are here divided into subgroups with specific characteristics.

Among the TF and cofactors that were upregulated already after 6h, Ppargc1a, Nfatc1 and Rcan1 were implicated in fiber type transformation. In particular, a widely accepted belief assumes that peroxisome proliferator-activated receptor γ (PPARγ) coactivator-1α (Ppargc1α) mediates exercise-induced mitochondrial biogenesis, synthesis of oxidative enzymes and even fiber-type switching (Puigserver P., 2005). Ppargc1a mRNA levels are higher in slow oxidative fibers

compared to fast fibers, and can be further increased via activation of calcium dependent pathway (Handschin C. et al., 2003).

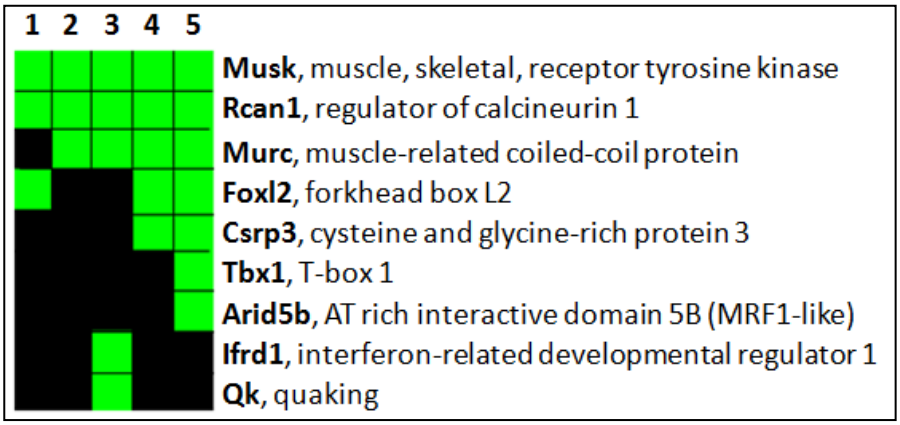

Figure 4.16 Query the Gene Ontology database for genes with known role in skeletal muscle. The 128 genes identified in SF at 12h were sent to David database. The figure shows the output cluster containing the following entries: 1) GO:0007519 skeletal muscle tissue development; 2) GO:0055001 muscle cell development; 3) GO:0042692 muscle cell differentiation; 4) GO:0060537 muscle tissue development; 5) GO:0007517 muscle organ development. As it is evident, important genes involved in muscle development and differentiation were not retrieved by this search (e.g. Ankrd2, Nfatc1, Mef2a) although they were present in the input list. Furthermore, the present status of the database is not fully consistent, as several genes are positives only to one or few terms (green squares) and negatives for the others (black squares).

The calcium/calcineurin nuclear factor of activated T cells 1(NFATc1) typically shows nuclear localization in slow fibers (Calabria E. et al., 2009). Translocation of NFATc1 from cytoplasm to nucleus and vice versa is very rapid and is totally dependent on nerve activity (Tothova J. et al., 2006). In muscles subjected to electrical stimulation, only NFATc1 respond to slow-type activity (McCullagh K.J. et al., 2004). These and other data suggest that NFATc1 play a major role in determining the expression of slow MyHC isoforms, although all 4 NFAT isoforms are necessary for active transcription (Calabria E. et al., 2009). Interestingly, the efficiency of a constitutively active NFATc1 mutant to induce transcription from the slow MyHC promoter was much lower in regenerating EDL muscle compared to regenerating denervated soleus muscle (McCullagh K.J. et al., 2004). These data show some similarities to my results and leave open the possibility that the chromatin conformation of MyHC slow promoter differs in fast and slow fibers.

It was initially suggested that NFAT alone is not sufficient for the proper activation of slow fiber specific promoters and enhancers (Chin E.R. et al., 1998; Calvo S. et al., 1999). In fact, calcium signaling triggered by calcineurin can be transduced to target genes also by myocyte enhancer factor 2 (MEF2) proteins (Wu H. et al., 2000). As said in the introduction (1.3.2), TF of this family are broadly expressed in adult fibers and are mainly regulated at the post-transcriptional level through a mechanism involving class II histone deacetylases (HDACs). In fact, the calcium- and calmodulin-dependent protein kinase (CaMK) promotes the phosphorylation dependent nuclear export of HDAC and this in turn activates transcription mediated by MEF2 (McKinsey T.A. et al., 2000a). However, in skeletal muscles of transgenic mice, both NFAT and MEF2 binding sites are necessary for properly regulated function of a slow fiber-specific enhancer (Wu H. et al., 2000). These results suggest a combinatorial control of gene expression mediated by both NFAT and MEF2 or even a direct interaction between the two proteins. In this contest, it is important to note that transcription of Mef2a was induced by CLFS, although only after 12h it became significant (Figure 4.17).

The regulator of calcineurin 1 (Rcan1) is probably the preferred target gene of NFAT in skeletal muscle and other cell types. The physiological consequence of this close relation is a negative feedback circuit where Rcan1 inhibits calcineurin-dependent signaling pathways through direct binding to the calcineurin A active site (Fuentes J.J. et al., 2000; Yang J. et al., 2000; Chakkalakal J.V. et al., 2003; Lee M.Y. et al., 2010).

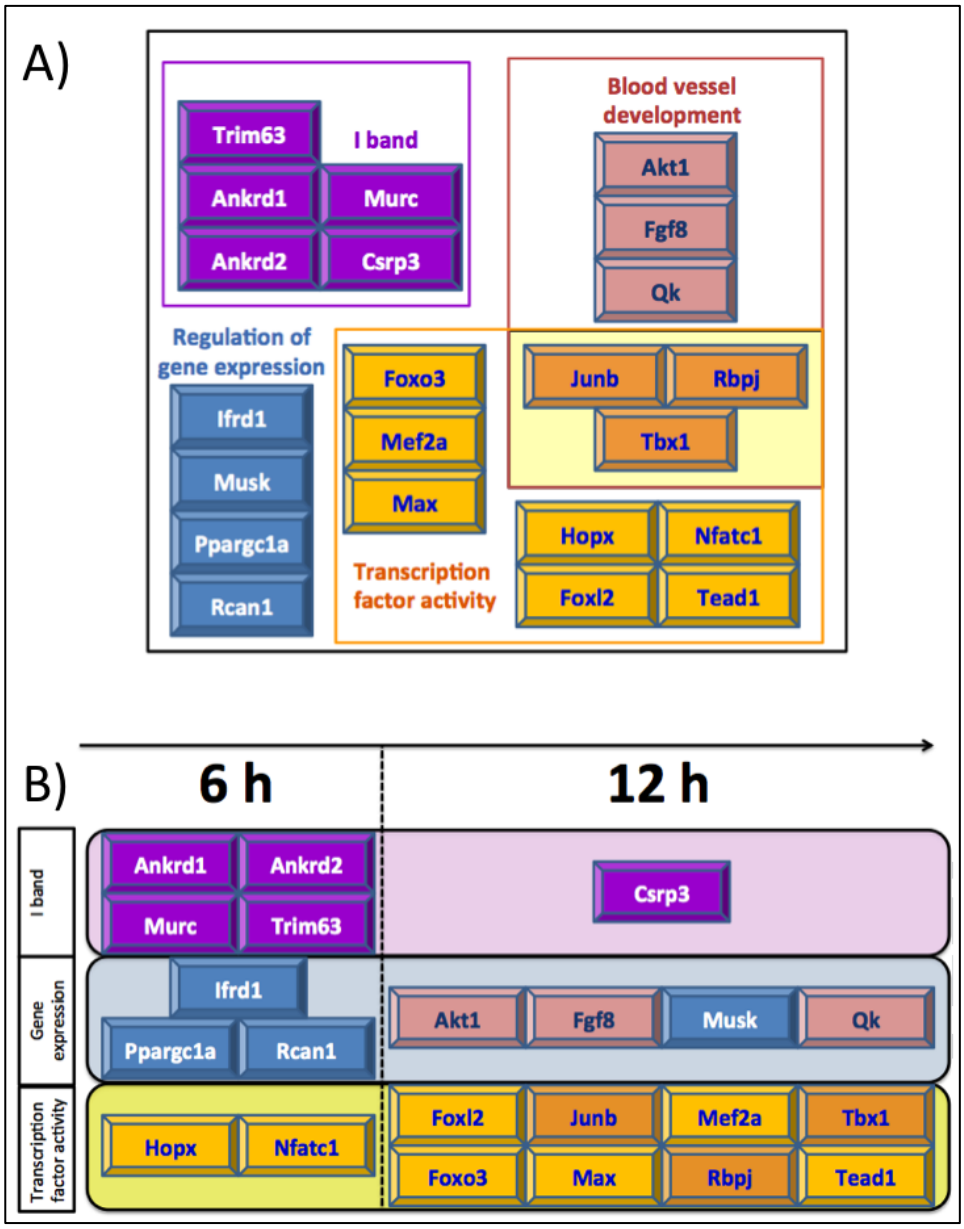

Figure 4.17: Transcription genes with known role in skeletal muscle. A) Gene listed in Table 4.7 were divided in GO categories: GO:0031674, I band (purple); GO:0001568, blood vessel development (pink); GO:0003700, transcription factor activity (yellow); GO:0010468, regulation of gene expression (blue). All of them should be annotated in the broad GO term 'muscle cell development' (GO:0055001). **B)** Simplified scheme, to put emphasis on the temporal activation of the same genes.

I just discussed sarcomeric I band proteins (4.4.2); the quick upregulation of Irfd1 and Hopx was unexpected and would merit a few comments. Irfd1, also known as Tis7 in mouse and PC4 in rat, was originally isolated as an immediate early response gene at the onset of the neuronal differentiation elicited by nerve growth factor in cultured rat astrocytes PC12 or specifically induced by chemical

compounds in mouse Swiss 3T3 cells. The finding that Irfd1 knockout mice show delayed muscle regeneration raised the interest about its possible role in skeletal muscles. Remarkably, Irfd1 is barely detectable during embryonic development, suggesting a prevalent role in terminal differentiated muscle fibers. A close inter-relationship between Irfd1, MyoD and myostatin was found as part of a differential network in bovine skeletal muscle (Hudson NJ et al., 2012). More important, functional studies have shown that the Irfd1 protein can selectively bind the MADS domain of Mef2c through displacement of histone deacetylase Hdac4 and cooperates with MyoD at inducing the transcriptional activity of Mef2c (Micheli L. et al., 2005).

The homeodomain only protein x (Hopx) is a small polypeptide named after the Hox motif that composes large part of its total 73 amino acids. Unlike other homeodomain proteins, Hopx does not bind DNA, because it lacks conserved residues that are necessary for protein-DNA interactions. In the heart, Hopx modulates the balance between growth and differentiation of myocytes by forming a complex that includes Hdac2 (Kook H et al., 2003). More specifically, Hopx acts as an adaptor that facilitates the interaction between Hdac2 and the transcription factor Gata4 (Trivedi C.M. et al., 2010). Since Gata4 activity is strongly influenced by acetylation, the Hopx-Hdac2 complex exerts a powerful effect on cardiac myocyte proliferation. Little it is known about the role of Hopx in adult skeletal muscle.

Among the other TF that were upregulated by CLFS, TEAD-1 was identified in a previous study (La Framboise W.A. et al., 2009). This protein binds to an A/T-rich element within the MyHC1 promoter and thus may function as a modulator of basal and/or inducible slow muscle gene expression (Tsika R.W. et al., 2008).

I have confirmed by qPCR at the single fibers level the strong upregulation of Rcan1 and Ppargc1a both at 6h and 12h (Figure 4.18). While trying to validate the differential expression of other TF, in most cases I was not able to obtain an amplified product from single fibers, despite several attempts. In general, regulatory proteins are expressed at lower levels compared to structural genes

and this fact without a doubt makes more challenging the qPCR reaction. To circumvent these technical problems I have planned future qPCR experiments starting from pool of fibers. I was particularly interested in the Max protein, because binding sites for this TF were enriched in many DE genes involved in angiogenesis. Unfortunately qPCR amplification with Max specific primers was unsuccessful. Max does not work alone, but it forms heterodimers with other family members, including Mad, Mxl1 and Myc. For the latter gene I could obtain a significant qPCR signal. However, the level of induction was about one order of magnitude lower of that measured for Rcan1 and Ppargc1a (Figure 4.18).

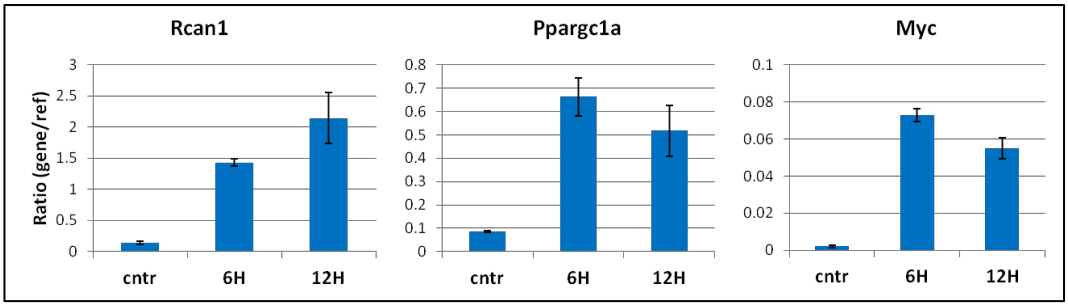

Figure 4.18: Analysis by qPCR. Each bar is referred to the average expression value of each gene in 3 single fibers for each condition. Signal ratios were calculated for each fiber sample, comparing the gene expression value with the expression of the reference gene Rpl4. The error bars are referred to the standard error of the three measures. Student's t-test considered significant all the differences (p-value <0.05).

In a second informatics approach, I searched within genes that were strongly upregulated without any a priori assumption. This type of analysis may reveal important actors of the CLFS response, not yet suggested by GO enrichment. Among the available template matching methods, I chose the one developed by Dr. Paul Pavlidis, thus referred here as PTM (Pavlidis Template Matching, see methods). Two different PTM templates were created. In the first analysis I searched for genes that were quickly upregulated at 6h and then maintained a sustained expression also at 12h (Figure 4.19). Among these genes I expected to find those of the immediate-early response. The next analysis, instead, was focused on genes of the late response (Figure 4.20). Tables 4.8 and 4.9 show the list of genes with the most significant q-values that were identified in these analyses with PTM template 011 and PTM template 001 respectively.

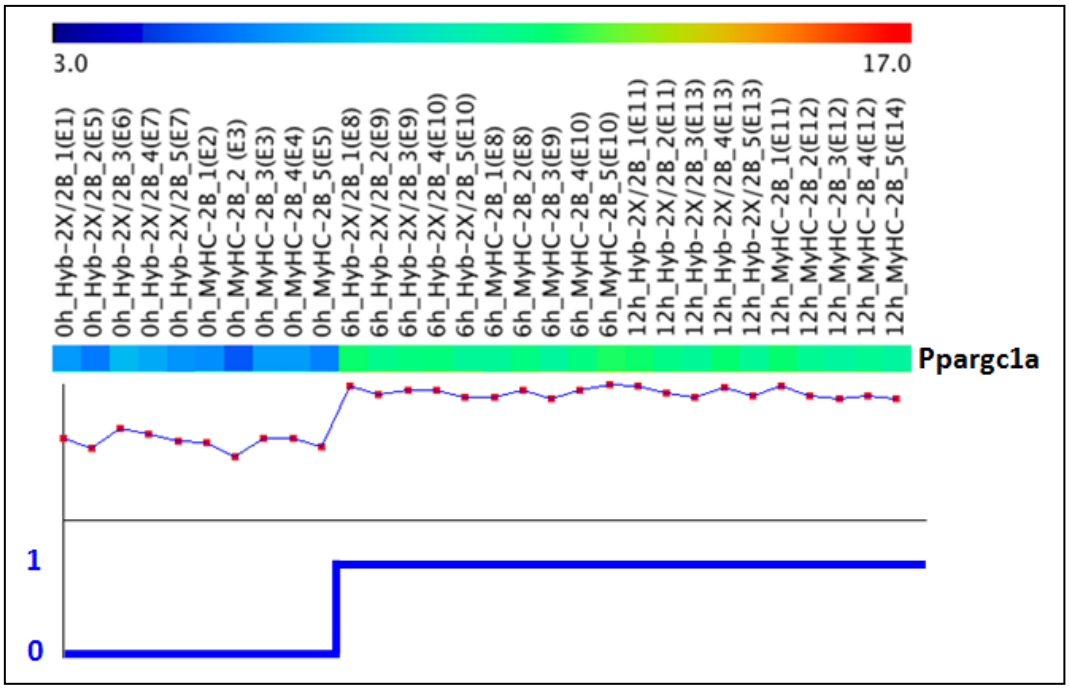

Figure 4.19: PTM template 011. Top: heat map showing expression levels in SF for the most significant gene of this analysis (Ppargc1a). Bottom: the template that was superimposed for this analysis had a very low level of expression in the control fibers at 0h, a sudden rise after 6h that is maintained also in the last time point of 12h. Genes with the highest degree of overlap with the template and associated p-values are listed in Table 4.8.

In good agreement with my expectations, Ppargc1a fitted the PTM template 011 with the highest significance (q-value 0). Other immediate-early response genes like Hk2, Ifrd1, Mafk, Rcan1 and Trim63 were also identified with PTM, showing the reliability and potential of this analysis (Table 4.8).

Interferon regulatory factor 2 binding protein 2 (Irf2bp2) immediately caught my attention, because this protein can exert a repressive function for NFAT target genes (Carneiro F.R. et al., 2011). A specific interaction between Irf2bp2 and the C-terminal domain of NFAT1 (the isoform encoded by Nfatc2) was clearly shown by experiments in cell cultures. Thus, it will be of interest to verify whether the same interaction exists in vivo in muscle fibers.

RNA polymerase II elongation factor (Ell) was discovered owing to its ability to increase the catalytic rate of transcription elongation. It belongs to a family of proteins, which also includes Ell2 and Ell3 (Eleven-nineteen Lys-rich leukaemia). Ell proteins are components of the super elongation complex that is recruited

whenever the cell requires a rapid transcriptional induction, to release RNA polymerase II from paused conformation (Luo Z. et al., 2012).

Symbol	GeneName	R value	p Value
Ppargc1a	peroxisome proliferative activated receptor, gamma, coactivator 1 alpha	0.97	0
Ell	elongation factor RNA polymerase II	0.95	1.33E-15
Trim63	tripartite motif-containing 63	0.95	2.22E-15
Hk2	hexokinase 2	0.93	6.99E-14
Ifrd1	interferon-related developmental regulator 1	0.92	7.01E-13
Irf2bp2	interferon regulatory factor 2 binding protein 2	0.92	8.62E-13
Fam134b	family with sequence similarity 134, member B	0.92	9.43E-13
Jmjd1c	jumonji domain containing 1C	0.91	2.52E-12
ENSMUST00000059529	No associated gene	0.91	2.70E-12
Mapk6	mitogen-activated protein kinase 6	0.9	6.78E-12
Tmem140	transmembrane protein 140	0.9	2.06E-11
Mafk	v-maf musculoaponeurotic fibrosarcoma oncogene family, protein K (avian)	0.9	2.18E-11
Rcan1	regulator of calcineurin 1	0.89	3.53E-11
Lrrc2	leucine rich repeat containing 2	0.89	6.52E-11

Table 4.8: PTM template 011. Significant genes for this analysis are associated with q-value (the lower the better). The R value can reach a maximum score of 1.

While acetylation is the most widely studied histone modification, the discovery of Lys and Arg methylases has shifted the interest toward this type of reaction. Jumonji domain containing proteins have the potential to remove methyl groups from Lys and Arg residues on histone tails (Kooistra S.M. & Helin K. 2012). In particular, Jmjd1c is specifically involved in demethylation of histone H3K9 and can thus mediate transcriptional activation (Kim S.M. et al., 2010).

Taken together, these observations reinforce the concept that major changes occur in the transcriptional machinery in the early phases of the CLFS response. This finding is further supported by the analysis with PTM template 001. Among the significant genes, three encoded for histone mRNA (Table 4.9). In addition, bromodomain proteins such as Brd2 are known to recognize acetylated lysine

residues on the N-terminal tails of histones, as a first step for chromatin remodeling.

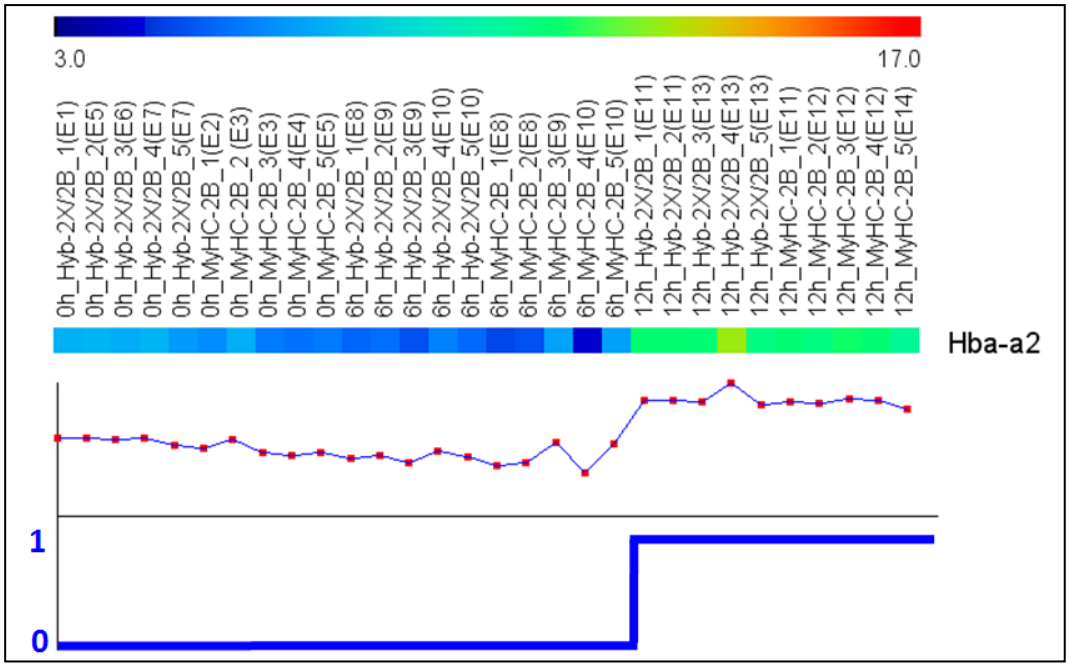

Figure 4.20: PTM template 001. Top: Hba-a2 was the most significant gene of this analysis. Bottom: the template that was superimposed had a very low level of expression in SF at 0h and 6h, with a sudden rise after 12h. Most significant genes of this analysis are listed in Table 4.8.

Symbol	Gene name	R value	p Value
Hba-a2	hemoglobin alpha, adult chain 2	0.93	5.55E-14
Tas2r137	taste receptor, type 2, member 137	0.86	1.62E-09
Rltpr	RGD motif, leucine rich repeats, tropomodulin domain and proline-rich containing	0.85	2.30E-09
NAP062746-1	No associated gene	0.85	2.87E-09
Hist1h3f	histone cluster 1, H3f	0.85	3.75E-09
Krt83	keratin 83	0.84	5.82E-09
Hist1h2ak	histone cluster 1, H2ak	0.84	6.40E-09
Hist1h2ag	histone cluster 1, H2ag	0.84	9.29E-09
Brd2	bromodomain containing 2	0.83	1.24E-08

Table 4.9: PTM template 001. Significant genes for this analysis are associated with q-value (the lower the better). The R value can reach a maximum score of 1.

5. CONCLUSIONS

During my PhD project, I used Agilent microarrays to study the transcriptional changes induced by chronic low frequency stimulation to the fast EDL muscle. Microgenomic analyses at the level of single fibers allowed distinguishing the transcriptional changes occurring in myofibers from background noise coming from other cell types. The lists of DE genes generated from SF expression profiling were much larger than those obtained from microarray experiments performed with EDL muscle. This result is likely due to heterogeneity of the whole muscle organ, although the different number of samples in the two dataset (5 for WM and 10 for SF) and the protocol of mRNA amplification (linear for WM and exponential for SF) may also influence the final results. However, my study demonstrated for the first time that it possible to apply with success the microgenomic approach in a model of muscle plasticity. This represents a big deal for future studies aimed at a better understanding the biology and physiology of skeletal muscle.

Gene Ontology analysis revealed a cross talk from myofibers to the other cell types composing the skeletal muscle, especially in the process of angiogenesis. In agreement with the recent notion of skeletal muscle as a secretory organ, I found that myofibers produces high amount of mRNA for growth factors to be secreted. Preliminary analyses suggest that TGFβ may evoke specific responses in the surrounding tissues. A real challenge is to decode the role of regulatory proteins in the process of physiologic angiogenesis (Figure 4.11).

My results clearly indicate that transcription is the first process to be regulated when myofibers respond to an extracellular stimulation. CLFS induced the early upregulation of genes that were previously implicated in fast to slow transition such as Ppargc1a, Nfatc1 and Rcan1 that I confirmed also by qPCR in SF. In agreement with the assumption that PGC-1α promotes biogenesis of mitochondria, several genes of oxidative phosphorylation were transcribed at significant levels already after 12h (Table 4.6). Vice versa, I could not see any

transcriptional activation of slow myosin and troponin isoforms (Figure 4.12), in contrast to what reported in a previous study (LaFramboise W.A. et al., 2009). These authors observed a very small level of induction for just some isoforms (MyHC1 and slow troponin C and T1) so it is possible that the observed changes occurred in muscle fibers of different types of those analyzed here (i.e. type 2X or 2A). Alternatively, contradictory effects were induced by different stimulation protocols.

Taken together, these observations lead to the conclusion that transcriptional reprogramming induced by CLFS is preparing a modification of metabolism toward more oxidative capability. In fact, both processes of blood vessel development and oxidative phosphorylation reached a significant enrichment.

In my experimental model, the specific upregulation of Rcan1 in SF indicates the transcriptional competence of NFAT transcription factors. So, why slow structural genes were not yet activated? One possible reason is that NFAT alone is not sufficient for the proper activation of slow fiber specific promoters and enhancers (Chin et al., 1998; Calvo et al., 1999). Other factors possibly implicated in this process are MEF2 and Tead1, whose expression level is slowly growing with time (Figure 4.17b). MEF2 proteins are regulated at posttranscriptional level by class II histone deacetylases (HDACs) and this step may also require a proper time for functional activation. An alternative hypothesis, which does not exclude the first, is that the promoter of slow genes is yet not accessible in fast fibers, due to a close chromatin conformation.

A novel finding of my work is that short term CLFS promote an increased expression of proteins involved in chromatin structure and remodeling (Table 4.7). The significance of this result was further supported by PTM analysis (Tables 4.8 and 4.9). The induction level of genes in this category is not lower than that observed for other regulatory proteins previously discussed (Figure 5.1).

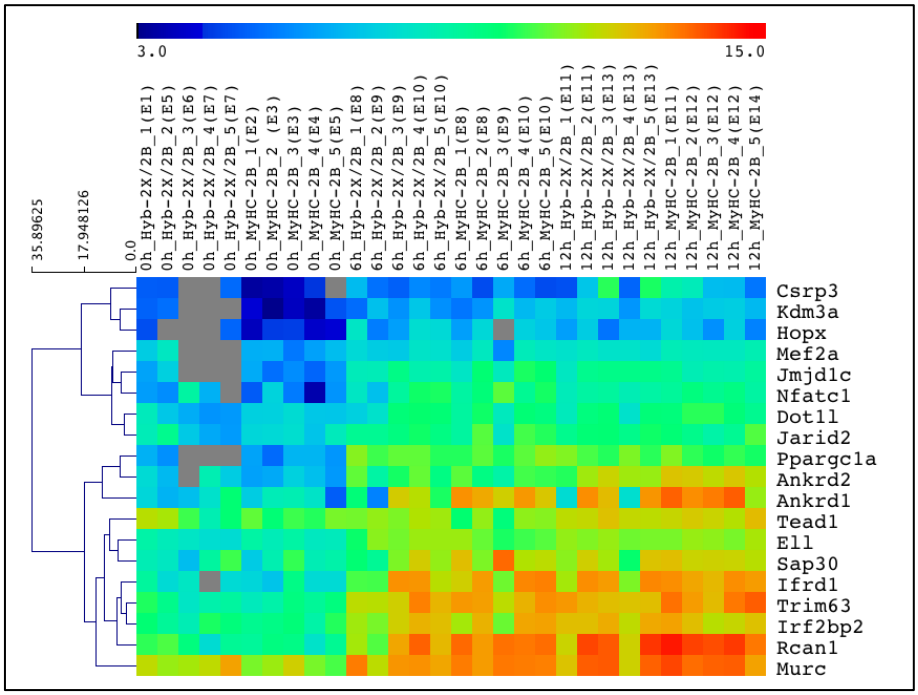

Figure 5.1: Heat map of selected chromatin genes in SF samples. Sin3 associated polypeptide (Sap30), involved in gene-specific deacetylation of histones, was highly induced in SF. After CLFS, transcription levels of Jmjd1c (histone H3K9 demethylase), Dot1l (histone H3 methyltransferase) and Jarid2 (which interact with the polycomb repressive complex 2) is not lower of other regulatory proteins like Nfatc1 or Mef2a. Kdm3a is another jumonji C domain-containing protein with histone demethylase activity.

In depth analysis of expression data generated by microarrays is a very time consuming process. In my thesis, I focused especially on genes that were strongly upregulated in SF, but other aspects of this work could be interest to investigate in the near future. First, promoter analysis of genes that are co-expressed during the time course may reveal enriched binding motif for specific transcription factors. This would help to place the DE genes within specific networks. With this respect, this set of data produced in specific fiber types is of great added value. Second and most important, functional studies on regulatory proteins that I have identified here may help to elucidate the molecular mechanism controlling the expression of specific isoform in skeletal muscle.

6. References

Amaral S.L., Linderman J.R., Morse M.M., and Greene A.S. (2001). **Angiogenesis induced by electrical stimulation is mediated by angiotensin II and VEGF.** *Microcirculation.* 8:57-67.

Aramburu J., Yaffe M.B., Lopez-Rodriguez C., Cantley L.C., Hogan P.G., and Rao A. (1999). **Affinity-driven peptide selection of an NFAT inhibitor more selective than cyclosporin A.** *Science* 285:2129-2133.

Arany Z., He H., Lin J., Hoyer K., Handschin C., Toka O., Ahmad F., Matsui T., Chin S., Wu P.H., Rybkin I.I., Shelton J.M., Manieri M., Cinti S., Schoen F.J., Bassel-Duby R., Rosenzweig A., Ingwall J.S., and Spiegelman B.M. (2005). **Transcriptional coactivator PGC-1 alpha controls the energy state and contractile function of cardiac muscle.** *Cell Metab* 1:259-271.

Arany Z., Lebrasseur N., Morris C., Smith E., Yang W., Ma Y., Chin S., and Spiegelman BM. (2007). **The transcriptional coactivator PGC-1beta drives the formation of oxidative type IIX fibers in skeletal muscle.** *Cell Metab* 5: 35-46.

Ausoni S., Gorza L., Schiaffino S., Gundersen K., and Lomo T. (1990). **Expression of myosin heavy chain isoforms in stimulated fast and slow rat muscles.** *J Neurosci* 10:153-160.

Baldwin K.M., and Haddad F. (2001). **Effects of different activity and inactivity paradigms on myosin heavy chain gene expression in striated muscle**. *J Appl Physiol* 90, 345-357.

Barnard E.A., Barnard P.J., Jarvis J.C., and Lai J. (1986). **Low frequency chronic electrical stimulation of normal and dystrophic chicken muscle.** *J. Physiol.* 376: 377-409.

Barton K.N., and MacLennan D.H. (2003). **The Proteins of the Sarcotubular System.** *In* Miology. Engel A.G. and Franzini-Armstrong C., editors. Mc Graw Hill, United States of America. 307-323.

Bassel-Duby R., and Olson E.N. (2006). **Signaling pathways in skeletal muscle remodeling**. *Annu.Rev.Biochem.* 75:19-37.

Bean C., Salamon M., Raffaello A., Campanaro S., Pallavicini A., and Lanfranchi G. (2005). **The Ankrd2, Cdkn1c and calcyclin genes are under the control of MyoD during myogenic differentiation.** *J.Mol.Biol.* 349:349-366.

Beard N.A., Laver D.R., Dulhunty A.F. (2004). **Calsequestrin and the calcium release channel of skeletal and cardiac muscle**. *Prog Biophys Mol Biol* 85: 33-69.

Belgrano A., Rakicevic L., Mittempergher L., Campanaro S., Martinelli V.C., Mouly V., Valle G., Kojic S., and Faulkner G. (2011). **Multi-Tasking Role of the Mechanosensing Protein Ankrd2 in the Signaling Network of Striated Muscle**. *PlosOne* 6:e25519

Bennett P.M., Furst D.O., and Gautel M. (1999). **The C-protein (myosin binding protein C) family: regulators of contraction and sarcomere formation?** *Rev.Physiol.Biochem.Pharmacol.* 138:203-234.

Berg, J.S., Powell B.C., and Cheney R.E. (2001). **A millennial myosin census.** *Mol.Biol.Cell.* 12:780-794.

Berman Y., and North KN. (2010) **A gene for speed: the emerging role of alpha-actinin-3 in muscle metabolism**. *Physiology (Bethesda).* 25:250-259.

Black B., and Olson E. (1998). **Transcriptional control of muscle development by myocyte enhancer factor-2 (MEF2) proteins.** Annu Rev Cell Dev Biol 14: 167-196.

Boengler K., Pipp F., Fernandez B., Ziegelhoeffer T., Schaper W., Deindl E. (2003) **Arteriogenesis is associated with an induction of the cardiac ankyrin repeat protein (carp).** *Cardiovasc. Res.* 59:573–581

Bolstad B.M., Irizarry R.A., Astrand M., and Speed T.P. (2003). **A comparison of normalization methods for high density oligonucleotide array data based on variance and bias.** *Bioinformatics* 19:185-193.

Booth F.W., Baldwin K.M. (1996). **Muscle plasticity: energy demanding and supply processes.** *In: Handbook of physiology* Peachey LD, Adrian RH, and Geiger SR, editors. Handbook of physiology,. Williams and Wilkins, Baltimore, 1075-1123.

Bottinelli R., Betto R., Schiaffino S., and Reggiani C. (1994) **Maximum shortening velocity and coexistence of myosin heavy chain isoforms in single skinned fast fibres of rat skeletal muscle.** *J Muscle Res Cell Motil* 15: 413-419.

Braissant O., Foufelle F., Scotto C., Dauca M., and Wahli, W. (1996). **Differential expression of peroxisome proliferator-activated receptors (PPARs): tissue distribution of PPAR-alpha, -beta, and -gamma in the adult rat.** *Endocrinology* 137:354-366.

Brooke M.H., and Kaiser K.K. (1970). **Muscle fiber types: how many and what kind?** *Arch Neurol* 23: 369-379.

Brown M.D., Cotter M.A., Hudlicka´ O., Vrbova´ G. (1976). **The effects of different patterns of muscle activity on capillary density, mechanical properties and structure of slow and fast rabbit muscles.** *Pflugers. Arch.* 361:241-250.

Buller A.J., Eccles J.C., Eccles R.M. (1960). **Interactions between motoneurones and muscles in respect of the characteristic speeds of their responses.** *J Physiol* 150: 417-439.

Buller A., Kean C., Ranatunga K. (1987). **Transformation of contraction speed in muscle following cross-reinnervation; dependence on muscle size**. *J Muscle Res Cell Motil* 8: 504-516.

Calabria E., Ciciliot S., Moretti I., Garcia M., Picard A., Dyar K.A., Pallafacchina G., Tothova J., Schiaffino S., and Murgia M. (2009). **NFAT isoforms control activity-dependent muscle fiber type specification.** *Proc Natl Acad Sci USA* 106: 13335-13340.

Campanaro S., Romualdi C., Fanin M., Celegato B., Pacchioni B., Trevisan S., Laveder P., De Pittà C., Pegoraro E., Hayashi Y.K., Valle G., Angelini C., and Lanfranchi G. (2002). **Gene expression profiling in dysferlinopathies using a dedicated muscle microarray.** *Hum.Mol.Genet.* 11:3283-3298.

Campbell W.G., Gordon S.E., Carlson C.J., Pattison J.S., Hamilton M.T., and Booth F.W. (2001). **Differential global gene expression in red and white skeletal muscles**. *Am J Physiol Cell Physiol* 280: C763-C768.

Calvo S., Venepally P., Cheng J. and Buonanno A. (1999) **Fiber-type-specific transcription of the troponin I slow gene is regulated by multiple elements.** *Mol Cell Biol*. 19:515-525.

Carneiro F.R., Ramalho-Oliveira R., Mognol G.P., and Viola J.P. (2011). **Interferon regulatory factor 2 binding protein 2 is a new NFAT1 partner and represses its transcriptional activity.** *Mol Cell Biol.* 31:2889-2901.

Catterall, W.A. (1991). **Functional subunit structure of voltage-gated calcium channels.** *Science.* 253:1499-1500.

Chakkalakal J.V., Harrison M.A., Carbonetto S., Chin E., Michel R.N., and Jasmin B.J. (2004). **Stimulation of calcineurin signaling attenuates the dystrophic pathology in mdx mice.** *Hum Mol Genet* 13: 379-388.

Chakkalakal J.V., Stocksley M.A., Harrison M.A., Angus L.M., Deschenes-Furry J., St-Pierre S., Megeney L.A., Chin E.R., Michel R.N., and Jasmin B.J. (2003). **Expression of utrophin A mRNA correlates with the oxidative capacity of skeletal muscle fiber types and is regulated by calcineurin/NFAT signaling.** *Proc Natl Acad Sci USA* 100: 7791-7796.

Chemello F., Bean C., Cancellara P., Laveder P., Reggiani C., and Lanfranchi G. (2011) **Microgenomic Analysis in Skeletal Muscle: Expression Signatures of Individual Fast and Slow Myofibers**. *PLoS ONE* 6(2): e16807.

Chin E.R., Olson E.N., Richardson J.A., Yang Q., Humphries C., Shelton J.M., Wu H., Zhu W., Bassel-Duby R., and Williams R.S. (1998). **A calcineurin-dependent transcriptional pathway controls skeletal muscle fiber type.** *Genes Dev* 12:2499-2509.

Chinsomboon J., Ruas J., Gupta R.K., Thom R., Shoag J., Rowe G.C., Sawada N., Raghuram S., and Arany Z. (2009) **The transcriptional coac- tivator PGC-1alpha mediates exercise-induced angiogenesis in skeletal muscle.** *Proc Natl Acad Sci USA* 106:21401–21406.

Chen, J.J. (2007). **Key aspects of analyzing microarray gene-expression data.** *Pharmacogenomics* 8:473-482.

Chu W., Burns D.K., Swerlick R.A., and Presky D.H. (1995). **Identification and characterization of a novel cytokine-inducible nuclear protein from human endothelial cells.** *J Biol Chem* 270:10236-10245.

Clark K.A., McElhinny A.S., Beckerle M.C., and Gregorio C.C. (2002). **Striated muscle cytoarchitecture: an intricate web of form and function.** *Annu.Rev.Cell Dev.Biol.* 18:637-706.

Crabtree G.R. and Olson E.N. (2002). **NFAT signaling. Choreographing the social lives of cells.** *Cell* 109 Suppl, S67-79.

Craig R.W., and Padròn R. (2003). **Molecular Structure of the Sarcomere.** *In* Miology. Engel A.G. and Franzini-Armstrong C., editors. Mc Graw Hill, United States of America. 129-166.

Damiani E., and Margreth A. (1994). **Characterization study of the ryanodine receptor and of calsequestrin isoforms of mammalian skeletal muscles in relation to fibre types.** *JMuscle Res Cell Motil* 15: 86-101.

Davies K.E., and Nowak K.J. (2006) **Molecular mechanisms of muscular dystrophies: old and new players.** *Nature Reviews Molecular Cell Biology* 7:762-773

DeNardi C., Ausoni S., Moretti P., Gorza L., Velleca M., Buckingham M., and Schiaffino S. (1993) **Type 2X-myosin heavy chain is coded by a muscle fiber type-specific and developmentally regulated gene**. *J Cell Biol* 123: 823-835.

Donoghue P, Doran P, Wynne K, Pedersen K, Dunn MJ, Ohlendieck K. Proteomic profiling of chronic low-frequency stimulated fast muscle. Proteomics 7: 3417–3430, 2007.

Dubowitz V., and Pearse A.G. (1960). **Reciprocal relationship of phosphorylase and oxidative enzymes in skeletal muscle**. *Nature.* 185:701-702.

Elvidge G. (2006). **Microarray expression technology: from start to finish.** *Pharmacogenomics.* 7:123-134.

English A.W., Eason J., Schwartz G., Shirley A., and Carrasco D.I. (1999). **Sexual dimorphism in the rabbit masseter muscle, Myosin heavy chain composition of neuromuscular compartments.** *Cells Tissues Organs* 164, 179-191.

Etgen G.J., Farrar R.P., and Ivy J.L. (1993) **Effect of chronic electrical stimulation of GLUT4 protein content in fast-twitch muscle.** *Am. J. Physiol.* 264:R816-R819.

Everts M.E., Andersen J., Clausen T., Hansen O. (1989). **Quantitative determination of Ca2+-dependent Mg2+-ATPase from sarcoplasmic reticulum in muscle biopsies**. *Biochem* J 260:443-448.

Faulkner G., Lanfranchi G., and Valle G. (2001). **Telethonin and other new proteins of the Z-disc of skeletal muscle.** *IUBMB Life.* 51:275-282.

Felder E., Protasi F., Hirsch R., Franzini-Armstrong C., and Allen P.D. (2002). **Morphology and molecular composition of sarcoplasmic reticulum surface junctions in the absence of DHPR and RyR in mouse skeletal muscle.** *Biophys.J.* 82:3144-3149.

Flück M. & Hoppeler H. (2003), **Molecular basis of skeletal muscle plasticity-from gene to form and function.** *Rev Physiol Biochem Pharmacol.* 146:159-216.

Frey N., Barrientos T., Shelton J.M., Frank D., Rutten H., Gehring D., Kuhn C., Lutz M., Rothermel B., Bassel-Duby R., Richardson J.A., Katus H.A., Hill J.A., and Olson E.N. (2004). **Mice lacking calsarcin-1 are sensitized to calcineurin signaling and show accelerated cardiomyopathy in response to pathological biomechanical stress.** *Nat Med* 10:1336-1343.

Frey N., Frank D., Lippl S., Kuhn C., Kogler H., Barrientos T., Rohr C., Will R., Muller O.J., Weiler H., Bassel-Duby R., Katus H.A., and Olson E.N. (2008). **Calsarcin-2 deficiency increases exercise capacity in mice through calcineurin/NFAT activation.** *J Clin Invest* 118:3598-3608.

Froemming G.R., Murray B.E., Harmon S., Pette D., and Ohlendieck K. (2000). **Comparative analysis of the isoform expression pattern of the Ca^{2+}-regulatory membrane protein in fast-twitch, slow-twitch, cardiac, neonatal, and chronic low-frequency stimulated muscle fibers.** *Biochim. Biophys. Acta* 1466:151-168.

Fuentes J.J., Genesca L., Kingsbury T.J., Cunningham K.W., Perez-Riba M., Estivill X., and de la Luna S. (2000) **DSCR1, overexpressed in Down syndrome, is an inhibitor of calcineurin-mediated signaling pathways.** *Hum Mol Genet* 9: 1681-1690.

Fukatsu Y., Noguchi T., Hosooka T., Ogura T., Kotani K., Abe T., Shibakusa T., Inoue K., Sakai M., Tobimatsu K., Inagaki K., Yoshioka T., Matsuo M., Nakae J., Matsuki Y., Hiramatsu R., Kaku K., Okamura H., Fushiki T., Kasuga M. (2009). **Muscle-specific overexpression of heparin-binding epidermal growth factor-like growth factor increases peripheral glucose disposal and insulin sensitivity.** *Endocrinology.* 150:2683-2691.

Furst D.O., Obermann W.M., and van der Ven P.F. (1999). **Structure and assembly of the sarcomeric M band.** *Rev.Physiol.Biochem.Pharmacol.* 138:163-202.

Gauthier G.F., and Padykula H.A. (1966). **Cytological studies of fiber types in skeletal muscle. A comparative study of the mammalian diaphragm.** *J.Cell Biol.* 28:333-354.

Goldspink G., Scutt A., Loughna P.T., Wells D.J., Jaenicke T., and Gerlach G.F. (1992). **Gene expression in skeletal muscle in response to stretch and force generation**. *Am J Physiol* 262:R356-R363

Gorza L. (1990) **Identification of a novel type 2 fiber population in mammalian skeletal muscle by combined use of histochemical myosin ATPase and anti-myosin monoclonal antibodies.** *J Histochem Cytochem* 38: 257-265.

Goumans M.J., Valdimarsdottir G., Itoh S., Rosendahl A., Sideras P., and ten Dijke P. (2002) **Balancing the activation state of the endothelium via two distinct TGF-β type I receptors.** *EMBO J.* 21:1743-1753.

Granit R., Henatsch H.D., and Steg G. (1956). **Tonic and phasic ventral horn cells differentiated by post-tetanic potentiation in cat extensors**. *Acta Physiol Scand* 37: 114-126.

Grichko V.P., Heywood-Cooksey A., Kidd K.R., and Fitts R.H. (2000). **Substrate profile in rat soleus muscle fibers after hindlimb unloading and fatigue**. *J Appl Physiol* 88: 473-478.

Grifone R., Laclef C., Spitz F., Lopez S., Demignon J., Guidotti J.E., Kawakami K., Xu P.X., Kelly R., Petrof B.J., Daegelen D., Concordet J.P., and Maire P. (2004) **Six1 and Eya1 expression can reprogram adult muscle from the slow-twitch phenotype into the fast-twitch phenotype.** *Mol Cell Biol* 24:6253-6267.

Gutmann E., Hanzlikova V., and Lojda Z. (1970). **Effect of androgens on histochemical fibre type. Differentiation in the temporal muscle of the guinea pig**. *Histochemie* 24: 287-291.

Haddad F., Pandorf C.E., Giger J.M., and Baldwin K.M. (2006). **Striated Muscle Plasticity: Regulation of the Myosin Heavy Chain Genes**. *In* Skeletal Muscle Plasticity in Health and Disease: From Genes to Whole Muscle. Bottinelli R. and Reggiani C., editors. Springer, Dordrecht, The Netherlands. 55-89.

Handschin C., Rhee J., Lin J., Tarr P.T., and Spiegelman B.M. (2003). **An autoregulatory loop controls peroxisome proliferator-activated receptor gamma coactivator 1alpha expression in muscle.** *Proc Natl Acad Sci U S A* 100:7111-7116.

Hang J., Kong L., Gu J.W., Adair T.H. (1995) **VEGF gene expression is upregulated in electrically stimulated rat skeletal muscle.** *Am J Physiol.* 269:H1827-H1831.

Hartner K.T., Kirschbaum B.J., and Pette D. (1989). **The multiplicity of troponin T isoforms. Normal rabbit muscles and effects of chronic stimulation.** *Eur J Biochem* 179:31-38.

Helliwell T.R. (1999). **Muscle: Part 1 - Normal structure and function.** *Current Orthopaedics.* 13:33-41.

Hennig R., and Lomo T. (1985) **Firing patterns of motor units in normal rats**. *Nature* 314: 164-166.

Hicks A., Ohlendieck K., Gopel S.O., and Pette D. (1997). **Early functional and biochemical adaptations to low-frequency stimulation of rabbit fast-twitch muscle.** *Am J Physiol* 273:C297-C305.

Hofmann S., and Pette D. (1994). **Low-frequency stimulation of rat fast- twitch muscle enhances the expression of hexokinase II and both the translocation and expression of glucose transporter 4 (GLUT-4).** *Eur J Biochem* 219:307-315.

Holman G. D., and Sandoval I. V. (2001). **Moving the insulin- regulated glucose transporter GLUT4 into and out of storage.** *Trends in Cell Biology* 11:173-179.

Hood DA, and Pette D. (1989). **Chronic long-term stimulation creates a unique metabolic enzyme profile in rabbit fast-twitch muscle.** *FEBS Lett* 247:471-474.

Hood D.A., Zak R., and Pette D. (1989). **Chronic stimulation of rat skeletal muscle induces coordinate increases in mitochondrial and nuclear mRNAs of cytochrome c oxidase subunits.** *Eur J Biochem* 179:275-280.

Hoh J.F. (1975). **Selective and non-selective reinnervation of fast-twitch and slow-twitch rat skeletal muscle.** *J Physiol* 251: 791-801.

Horowits R. (1999). **The physiological role of titin in striated muscl**e. *Rev.Physiol.Biochem.Pharmacol.* 138:57-96.

Huang da, W., Sherman B.T., and Lempicki R.A. (2009). **Systematic and integrative analysis of large gene lists using DAVID bioinformatics resources.** *Nat.Protoc.* 4:44-57.

Huber B., and Pette D. (1996) **Dynamics of parvalbumin expression in low-frequency-stimulated fast-twitch rat muscle.** *Eur J Biochem* 236:814-819.

Hudlickaʹ O., Brown M., Cotter M., Smith M., and Vrbovaʹ G. (1977). **The effect of long-term stimulation of fast muscles on their blood flow, metabolism and ability to withstand fatigue.** *Pflugers Arch* 369:141-149.

Hudson N.J., Dalrymple B.P., and Reverter A. (2012). **Beyond differential expression: the quest for causal mutations and effector molecules.** *BMC Genomics.* 13:356.

Hughes S.M., Chi M.M., Lowry O.H., and Gundersen K. (1999) **Myogenin induces a shift of enzyme activity from glycolytic to oxidative metabolism in muscles of transgenic mice.** *J Cell Biol* 145:633-642.

Hulshizer R., and Blalock E.M. (2007) **Post hoc pattern matching: assigning significance to statistically defined expression patterns in single channel microarray data.** *BMC Bioinformatics*.

Huxley H.E. (1957). **The double array of filaments in cross-striated muscle.** *J.Biophys.Biochem.Cytol.* 3:631-648.

Irrcher I., Adhihetty P.J., Sheehan T., Joseph A.M., and Hood D.A. (2003). **PPARgamma coactivator-1alpha expression during thyroid hormone and contractile activity induced mitochondrial adaptations.** *American Journal of Physiology* 284:C1669-C1677.

Izumo S., Nadal-Ginard B., Mahdavi V. (1986). **All members of the MHC multigene family respond to thyroid hormone in a highly tissue-specific manner.** *Science* 231:597-600.

Jäger S., Handschin C., St-Pierre J., and Spiegelman B.M. (2007). **AMP- activated protein kinase (AMPK) action in skeletal muscle via direct phosphorylation of PGC-1alpha.** *Proc Natl Acad Sci USA* 104:12017-12022.

Kandarian S.C. (2006) **Large Scale Gene expression profiles as tools to study skeletal muscle adaptation.** *In* Skeletal Muscle Plasticity in Health and Disease: From Genes to Whole Muscle. Bottinelli R. and Reggiani C., editors. Springer, Dordrecht, The Netherlands. 29-54.

Kanno T., Kamba T., Yamasaki T., Shibasaki N., Saito R., Terada N., Toda Y., Mikami Y., Inoue T., Kanematsu A., Nishiyama H., Ogawa O., and Nakamura E. (2012). **JunB promotes cell invasion and angiogenesis in VHL-defective renal cell carcinoma**. **Oncogene**. 31:3098-3110.

Kaufmann M., Simoneau J.A., Veerkamp J.H., and Pette D. (1989). **Electro- stimulation-induced increases in fatty acid-binding protein and myoglobin in rat fast-twitch muscle and comparison with tissue levels in heart.** *FEBS Lett* 245:181-184.

Khatri P., and Draghici S. (2005). **Ontological analysis of gene expression data: current tools, limitations, and open problems.** *Bioinformatics.* 21:3587-3595.

Kim S.M., Kim J.Y., Choe N.W., Cho I.H., Kim J.R., Kim D.W., Seol J.E., Lee S.E., Kook H., Nam K.I., Kook H., Bhak Y.Y., Seo S.B. (2010). **Regulation of mouse steroidogenesis by WHISTLE and JMJD1C through histone methylation balance.** *Nucleic Acids Res.* 38:6389-403.

Kitamura T., Kitamura Y.I., Funahashi Y., Shawber C.J., Castrillon D.H., Kollipara R., De-Pinho R.A., Kitajewski J., and Accili D. (2007) **A Foxo/Notch pathway controls myogenic differen- tiation and fiber type specification.** *J Clin Invest* 117:2477-2485.

Kliewer S.A., Forman B.M., Blumberg B., Ong E.S., Borgmeyer U., Mangelsdorf D.J., Umesono K., and Evans R.M. (1994). **Differential expression and activation of a family of murine peroxisome proliferator-activated receptors.** *Proceedings of the National Academy of Sciences USA* 91:7355-7359.

Kooistra S.M., and Helin K. (2012). **Molecular mechanisms and potential functions of histone demethylases.** *Nat Rev Mol Cell Biol.* 13:297-311.

Kook H., and Epstein J.A. (2003). **Hopping to the beat. Hop regulation of cardiac gene expression.** *Trends Cardiovasc Med.* 13:261-264.

Kruger M., Wright J., and Wang K. (1991). **Nebulin as a length regulator of thin filaments of vertebrate skeletal muscles: correlation of thin filament length, nebulin size, and epitope profile.** *J.Cell Biol.* 115:97-107.

Kurimoto K., and Saitou M. (2010). **Single-cell cDNA microarray profiling of complex biological processes of differentiation.** *Curr.Opin.Genet.Dev*. 20:470-477.

Kushmerick M.J. (1998). **Energy balance in muscle activity: simulations of ATPase coupled to oxidative phosphorylation and to creatine kinase.** *Comp.Biochem.Physiol.B.Biochem.Mol.Biol.* 120:109-123.

LaFramboise W. A., Jayaraman R. C., Bombach K. L., Ankrapp D. P., Krill-Burger J. M., Sciulli C. M., Petrosko P., and Wiseman R. W. (2009). **Acute molecular response of mouse hindlimb muscles to chronic stimulation**. *Am J Physiol Cell Physiol* 297:C556-C570

Leberer E., Härtner K.T., Brandl C.J., Fujii J., Tada M., MacLennan D.H., Pette D. (1989) **Slow/cardiac sarcoplasmic reticulum Ca-ATPase and phospholamban mRNAs are expressed in chronically stimulated rabbit fast-twitch muscle.** *Eur J Biochem* 185:51-54.

Leberer E., Härtner K.T., and Pette D. (1988). **Postnatal development of Ca2+-sequestration by the sarcoplasmic reticulum of fast and slow muscles in normal and dystrophic mice.** *Eur J Biochem* 174: 247-253.

Lee M.Y., Garvey S.M., Baras A.S., Lemmon J.A., Gomez M.F., Schoppee Bortz P.D., Daum G., LeBoeuf R.C., and Wamhoff B.R. (2010). **Integrative genomics identifies DSCR1 (RCAN1) as a novel NFAT-dependent mediator of phenotypic modulation in vascular smooth muscle cells.** *Hum Mol Genet*. 19:468-79.

Leeuw T., and Pette D. (1993) **Coordinate changes in the expression of troponin subunit and myosin heavy chain isoforms during fast-to-slow transition of low-frequency stimulated rabbit muscle.** *Eur J Biochem* 213:1039-1046.

Lin J., Handschin C., and Spiegelman B.M. (2005). **Metabolic control through the PGC-1 family of transcription coactivators.** *Cell Metabolism* 1:361-370.

Lin J., Wu H., Tarr P.T., Zhang C.Y., Wu Z., Boss O., Michael L.F., Puigserver P., Isotani E., Olson E.N., Lowell B.B., Bassel-Duby R., and Spiegelman B.M. (2002). **Transcriptional co-activator PGC-1 alpha drives the formation of slow-twitch muscle fibres.** *Nature* 418:797-801.

Liu Y., Randall W.R., and Schneider M.F. (2005) **Activity-dependent and independent nuclear fluxes of HDAC4 mediated by different kinases in adult skeletal muscle.** *J Cell Biol* 168:887-897.

Luo Z., Lin C., Shilatifard A. (2012). **The super elongation complex (SEC) family in transcriptional control.** *Nat Rev Mol Cell Biol.* 13:543-547.

Lunde I.G., Ekmark M., Rana Z.A., Buonanno A., and Gundersen K. (2007). **PPAR{delta} expression is influenced by muscle activity and induces slow muscle properties in adult rat muscles after somatic gene transfer.** *Journal of Physiology* 582:1277-1287.

Luquet S., Lopez-Soriano J., Holst D., Fredenrich A., Melki J., Rassoulzadegan M., and Grimaldi P.A. (2003) **Peroxisome proliferator-activated receptor delta controls muscle de- velopment and oxidative capability.** *FASEB J* 17: 2299-2301.

Luther P.K., Padron R., Ritter S., Craig R., and Squire J.M.. (2003). **Heterogeneity of Z-band structure within a single muscle sarcomere: implications for sarcomere assembly.** *J.Mol.Biol.* 332:161-169.

Lytton J., Westlin M., Burk S.E., Shull G.E., and MacLennan D.H. (1992). **Functional comparisons between isoforms of the sarcoplasmic or endoplasmic reticulum family of calcium pumps.** *J.Biol.Chem.* 267:14483-14489.

Marty I., Robert M., Villaz M., De Jongh K., Lai Y., Catterall W.A., and Ronjat M. (1994). **Biochemical evidence for a complex involving dihydropyridine receptor and ryanodine receptor in triad junctions of skeletal muscle.** *Proc.Natl.Acad.Sci.U.S.A.* 91:2270-2274.

Maturana A.D., Nakagawa N., Yoshimoto N., Tatematsu K., Hoshijima M., Tanizawa K., and Kuroda S. (2011). **LIM domains regulate protein kinase C activity: a novel molecular function**. *Cell Signal.* 23:928-34.

McCullagh K.J., Calabria E., Pallafacchina G., Ciciliot S., Serrano A.L., Argentini C., Kalhovde J.M., Lomo T., Schiaffino S. (2004) **NFAT is a nerve activity sensor in skeletal muscle and controls activity-dependent myosin switching**. *Proc Natl Acad Sci USA* 101:10590-10595.

McElhinny A.S., Kakinuma K., Sorimachi H., Labeit S., and Gregorio C.C. (2002) **Muscle-specific RING finger-1 interacts with titin to regulate sarcomeric M-line and thick filament structure and may have nuclear functions via its interaction with glucocorticoid modulatory element binding protein-1**. *J Cell Biol* 157: 125–136.

McKinsey T.A., Zhang C.L., Lu J., Olson E.N. (2000a). **Signal-dependent nuclear export of a histone deacetylase regulates muscle differentiation.** *Nature* 408:106-111.

McKinsey T.A., Zhang C.L. and Olson E.N. (2000b). **Activation of the myocyte enhancer factor-2 transcription factor by calcium/calmodulin-dependent protein kinase-stimulated binding of 14-3-3 to histone** deacetylase 5. *Proc Natl Acad Sci U S A* 97:14400-14405.

Mejat A., Ramond F., Bassel-Duby R., Khochbin S., Olson E. N., and Schaeffer L. (2005). **Histone deacetylase 9 couples neuronal activity to muscle chromatin acetylation and gene expression.** *Nature Neuroscience* 8, 313–321.

Melzer W., Herrmann-Frank A., and Luttgau H.C. (1995). **The role of Ca2+ ions in excitation-contraction coupling of skeletal muscle fibres**. *Biochim.Biophys.Acta.* 1241:59-116.

Michael L.F., Wu Z., Cheatham R.B., Puigserver P., Adelmant G., Lehman J.J., Kelly D.P., and Spiegelman B.M. (2001). **Restoration of insulin-sensitive glucose transporter (GLUT4) gene expression in muscle cells by the transcriptional coactivator PGC-1.** *Proc Natl Acad Sci USA* 98:3820-3825.

Micheli L., Leonardi L., Conti F., Buanne P., Canu N., Caruso M., and Tirone F. (2005). **PC4 coactivates MyoD by relieving the histone deacetylase 4-mediated inhibition of myocyte enhancer factor 2C.** *Mol Cell Biol.* 25:2242-2259.

Miller M.K., Bang M.L., Witt C.C.2, Labeit D., Trombitas C., Watanabe K., Granzier H., McElhinny A.S., Gregorio C.C. and Labeit S. (2003). **The Muscle Ankyrin Repeat Proteins: CARP, ankrd2/Arpp and DARP as a Family of Titin Filament- based Stress Response Molecules** *J. Mol. Biol.* 333:951-964

Murgia M., Serrano A.L., Calabria E., Pallafacchina G., Lomo T., and Schiaffino S. (2000). **Ras is involved in nerve-activity-dependent regulation of muscle genes.** *Nat Cell Biol* 2:142-147.

Naya F.J., Mercer B., Shelton J., Richardson J.A., Williams R.S., and Olson E.N. (2000). **Stimulation of slow skeletal muscle fiber gene expression by calcineurin in vivo.** *J Biol Chem* 275: 4545-4548.

Obermann W.M., Gautel M., Steiner F., van der Ven P.F., Weber K., and Furst D.O. (1996). **The structure of the sarcomeric M band: localization of defined domains of myomesin, M-protein, and the 250-kD carboxy-terminal region of titin by immunoelectron microscopy.** *J.Cell Biol.* 134:1441-1453.

Oh M., Rybkin I.I., Copeland V., Czubryt M.P , Shelton J.M., vanRooij E., Richardson J.A., Hill J.A., De Windt L.J., Bassel-Duby R., Olson E.N., and Rothermel B.A. (2005). **Calcineurin is necessary for the maintenance but not embryonic development of slow muscle fibers.** *Mol Cell Biol* 25: 6629-6638.

Ohlendieck K., Murray B.E., Froemming G.R., Maguire P.B., Leisner E., Traub I., and Pette D. (1999). **Effects of chronic low-frequency stimulation on Ca2+-regulatory membrane proteins in rabbit fast muscle.** *Pflugers Arch.* 438:700-708.

Rayment I., Smith C., and R.G. Yount R.G. (1996). **The active site of myosin.** *Annu.Rev.Physiol.* 58:671-702.

Parsons S.A., Millay D.P., Wilkins B.J., Bueno O.F., Tsika G.L., Neilson J.R., Liberatore C.M., Yutzey K.E., Crabtree G.R., Tsika R.W., and Molkentin J.D. (2004). **Genetic loss of calcineurin blocks mechanical overload-induced skeletal muscle fiber type switching but not hypertrophy.** *J Biol Chem* 279:26192-26200.

Pattison J.S., Folk L.C., Madsen R.W., Childs T.E., Spangenburg E.E., and Booth F.W. (2003). **Expression profiling identifies dysregulation of myosin heavy chains IIb and IIx during limb immobilization in the soleus muscles of old rats.** *J.Physiol.* 553:357-368.

Pattullo M.C., Cotter M.A., Cameron N.E., and Barry J.A. (1992) **Effects of lengthened immobilization on functional and histochemical properties of rabbit tibialis anterior muscle.** *Exp Physiol* 77: 433-442.

Pavlidis P., and Noble WS. (2001). **Analysis of strain and regional variation in gene expression in mouse brain.** *Genome Biol. 2001*;2:RESEARCH0042.

Payne, A.M., and Delbono O. (2006). **Plasticity of Excitation-Contraction Coupling in Skeletal Muscle.** *In* Skeletal Muscle Plasticity in Health and Disease: From Genes to Whole Muscle. Bottinelli R. and Reggiani C., editors. Springer, Dordrecht, The Netherlands. 173-211.

Periasamy M., and Kalyanasundaram A. (2007) **SERCA pump isoforms: their role in calcium transport and disease.** *Muscle Nerve* 35: 430–442.

Peter J.B., Barnard R.J., Edgerton V.R., Gillespie C.A., and Stempel K.E. (1972) **Metabolic profiles of three fiber types of skeletal muscle in guinea pigs and rabbits.** *Biochemistry* 11: 2627-2633.

Pette D. (2001). **Historical Perspectives, Plasticity of mammalian skeletal muscle.** *J Appl Physiol* 90:1119-1124.

Pette D. (2006). **Skeletal Muscle Plasticity – History, Facts and Concepts.** *In* Skeletal Muscle Plasticity in Health and Disease: From Genes to Whole Muscle. Bottinelli R. and Reggiani C., editors. Springer, Dordrecht, The Netherlands. 1-27.

Pette D., Smith M.E., Staudte H.W., Vrbová G. (1973). **Effects of long-term electrical stimulation on some contractile and metabolic characteristics of fast rabbit muscles**. *Pflugers Arch.* 338:257-272.

Pette D., and Staron R.S. (1990). **Cellular and molecular diversities of mammalian skeletal muscle fibers.** *Rev. Physiol. Biochem. Pharmacol.* 116: 1-76.

Pette D, and Staron R.S. (1997). **Mammalian skeletal muscle fiber type transitions.** *Int Rev Cytol* 170: 143-223.

Pette D., and Staron R.S. (2001). **Transitions of muscle fiber phenotypic profiles.** *Histochem.Cell Biol.* 115:359-372.

Pette D, Vrbová G. (1992). **Adaptation of mammalian skeletal muscle fibers to chronic electrical stimulation.** *Rev Physiol Biochem Pharmacol* 120:116-202.

Pette D., and Vrbovà G. (1999). **What does chronic electrical stimulation teach us about muscle plasticity?** *Muscle Nerve* 22: 666-677.

Potthoff M.J., Wu H., Arnold M.A., Shelton J.M., Backs J., McAnally J., Richardson J.A., Bassel-Duby R., and Olson E.N. (2007). **Histone deacetylase degradation and MEF2 activation promote the formation of slow-twitch myofibers.** *J Clin Invest* 117: 2459-2467.

Puigserver P. (2005). **Tissue-specific regulation of metabolic pathways through the transcriptional coactivator PGC1-α.** *Int J Obes*. 29:S5–S9.

Puigserver P., and Spiegelman BM. (2003). **Peroxisome proliferator-activated receptor-gamma coactivator 1 alpha (PGC-1 alpha): transcriptional coactivator and metabolic regulator.** *Endocr Rev* 24:78-90.

Raffaello A., Laveder P., Romualdi C., Bean C., Toniolo L., Germinario E., Megighian A., Danieli-Betto D., Reggiani C., and Lanfranchi G. (2006). **Denervation in murine fast-twitch muscle: short-term physiological changes and temporal expression profiling.** *Physiol.Genomics.* 25:60-74.

Raffaello A., Milan G., Masiero E., Carnio S., Lee D., Lanfranchi G., Goldberg A.L., and Sandri M. (2010). **JunB transcription factor maintains skeletal and promotes hypertrophy.** *J Cell Biol.* 191:101-113.

Rana Z.A., Gundersen K., and Buonanno A. (2008). **Activity-dependentrepressionofmusclegenes by NFAT.** *Proc Natl Acad Sci USA* 105: 5921-5926.

Reggiani C., and Kronnie G.T. (2004). **Muscle plasticity and high throughput gene expression studies.** *Journal of Muscle Research and Cell Motility* 25: 231-234.

Reichmann H., Hoppeler H., Mathieu-Costello O., von Bergen F., and Pette D. (1985). **Biochemical and ultrastructural changes of skeletal muscle mitochondria after chronic electrical stimulation in rabbits.** *Pflugers Arch* 404:1-9.

Reid M.B. (2005). **Response of the ubiquitin-proteasome pathway to changes in muscle activity.** *Am J Physiol Regul Integr Comp Physiol* 288:R1423-R1431.

Richter E.A., Garetto L.P., Goodman M.N., Ruderman N.B. (1982) **Muscle glucose metabolism following exercise in the rat: increased sensitivity to insulin.** *J Clin Invest* 69:785-793.

Rios E., and Brum G. (1987). **Involvement of dihydropyridine receptors in excitation-contraction coupling in skeletal muscle.** *Nature.* 325:717-720.

Rose A.J., Kiens B., and Richter E.A. (2006) **Ca2+-calmodulin-dependent protein kinase expression and signalling in skeletal muscle during exercise.** *J Physiol* 574:889-903.

Russell A.P., Feilchenfeldt J., Schreiber S., Praz M., Crettenand A., Gobelet C., Meier C.A., Bell D.R., Kralli A., Giacobino J.P., and Deriaz O. (2003). **Endurance training in humans leads to fiber type-specific increases in levels of peroxisome proliferator-activated receptor-gamma coactivator-1 and peroxisome proliferator-activated receptor-alpha in skeletal muscle.** *Diabetes* 52:2874-2881.

Saeed A.I., Bhagabati N.K., Braisted J.C., Liang W., Sharov V., Howe E.A., Li J., Thiagarajan M., White J.A., and Quackenbush J. (2006). **TM4 microarray software suite.** *Methods Enzymol.* 411:134-193.

Salmons S., Vrbová G. (1969). **The influence of activity on some contractile characteristics of mammalian fast and slow muscles.** *J Physiol (Lond)* 201:535-549.

Sandow, A. (1965). **Excitation-contraction coupling in skeletal muscle.** *Pharmacol.Rev.* 17:265-320.

Sanes J.R. (2003). **The Extracellular Matrix.** *In* Miology. Engel A.G. and Franzini-Armstrong C., editors. Mc Graw Hill, United States of America. 471-487.

Schachat F.H., Williams R.S., and Schnurr C.A. (1988). **Coordinate changes in fast thin filament and Z-line protein expression in the early response to chronic stimulation.** *J Biol Chem* 263: 13975-13978.

Schiaffino S., Gorza L., Sartore S., Saggin L., Ausoni S., Vianello M., Gundersen K., and Lomo T. (1989). **Three myosin heavy chain isoforms in type 2 skeletal muscle fibres.** *J.Muscle Res.Cell.Motil.* 10:197-205

Schiaffino S., Hanzlikova V., and Pierobon S. (1970). **Relations between structure and function in rat skeletal muscle fibers**. *J Cell Biol* 47: 107-119.

Schiaffino S, and Reggiani C. (1996) **Molecular diversity of myofibrillar proteins: gene regulation and functional significance.** *Physiol Rev* 76: 371-423.

Schiaffino S., and Reggiani C. (2011) **Fiber Types In Mammalian Skeletal Muscles.** *Physiol Rev* 91: 1447-1531.

Schiaffino S., Sandri M., and Murgia M. (2006). **Signaling pathways controlling muscle fiber size and type in response to nerve activity.** *In* Skeletal Muscle Plasticity in Health and Disease: From Genes to Whole Muscle. Bottinelli R. and Reggiani C., editors. Springer, Dordrecht, The Netherlands. 91-119.

Schiaffino S. and Serrano A. (2002). **Calcineurin signaling and neural control of skeletal muscle fiber type and size.** *Trends Pharmacol Sci* 23:569-575.

Schuler M., Ali F., Chambon C., Duteil D., Bornert J.M., Tardivel A., Desvergne B., Wahli W., Chambon P., and Metzger D. (2006). **PGC1alpha expression is controlled in skeletal muscles by PPARbeta, whose ablation results in fiber-type switching, obesity, type 2 diabetes.** *Cell Metab* 4: 407-414.

Schwaller B., Dick J., Dhoot G., Carroll S., Vrbova G., Nicotera P., Pette D., Wyss A., Bluethmann H., Hunziker W., and Celio M.R. (1999). **Prolonged contraction-relaxation cycle of fast-twitch muscles in parvalbumin knockout mice.** *Am J Physiol Cell Physiol* 276: C395-C403.

Serysheva I.I., Schatz M., van Heel M., Chiu W., and Hamilton S.L. (1999). **Structure of the skeletal muscle calcium release channel activated with Ca2+ and AMP-PCP.** *Biophys.J.* 77:1936-1944.

Seward D.J., Haney J.C., Rudnicki M.A., and Swoap S.J. (2001) **bHLH transcription factor MyoD affects myosin heavy chain expression pattern in a muscle-specific fashion.** *Am J Physiol Cell Physiol* 280:C408-C413.

Sharan R., Maron-Katz A., and Shamir R. (2003). **CLICK and EXPANDER: a system for clustering and visualizing gene expression data.** *Bioinformatics.* 19:1787-1799.

Shen T., Cseresnyes Z., Liu Y., Randall W.R., and Schneider M.F. (2007). **Regulation of the nuclear export of the transcription factor NFATc1 by protein kinases after slow fibre type electrical stimulation of adult mouse skeletal muscle fibres.** *J Physiol* 579: 535-551.

Simoneau J-A, Kaufmann M., Pette D. (1993). **Asynchronous in- creases in oxidative capacity and resistance to fatigue of electrostimulated muscles of rat and rabbit**. *J Physiol*. 460: 573-580.

Simoneau J-A, and Pette D. (1988). **Species-specific effects of chronic nerve stimulation upon tibialis anterior muscle in mouse, rat, guinea pig, and rabbit.** *Pflügers Arch* 412: 86-92.

Smerdu V., Karsch-Mizrachi I., Campione M., Leinwand L., and Schiaffino S. (1994). **Type IIx myosin heavy chain transcripts are expressed in type IIb fibers of human skeletal muscle.** *Am.J.Physiol.* 267:C1723-8.

Sparrow J.C., and Schöck F. (2009) **The initial steps of myofibril assembly: integrins pave the way.** *Nature Reviews Molecular Cell Biology* 10:293-298.

Sreter F.A., Lopez J.R., Alamo L., Mabuchi K., and Gergely J. (1987). **Changes in intracellular ionized Ca concentration associated with muscle fiber type transformation.** *Am J Physiol* 253:C296-C300.

Staron, R.S., and Pette D. (1986). **Correlation between myofibrillar ATPase activity and myosin heavy chain composition in rabbit muscle fibers**. *Histochemistry.* 86:19-23.

St-Pierre J., Drori S., Uldry M., Silvaggi J.M., Rhee J., Jäger S., Handschin C., Zheng K., Lin J., Yang W., Simon D.K., Bachoo R., Spiegelman B.M. (2006). **Suppression of reactive oxy- gen species and neurodegeneration by the PGC-1 transcriptional coactivators.** *Cell* 127:397-408.

Sugiura T., Miyata H., Kawai Y., Matoba H., and Murakami N. (1993). **Changes in myosin heavy chain isoform expression of overloaded rat skeletal muscles.** *Int J Biochem* 25, 1609-1613.

Takahashi M., McCurdy D.T., Essig D.A. and Hood D.A. (1993). **Delta-Aminolaevulinate synthase expression in muscle after contraction and recovery.** *Biochem. J.* 291:219-223.

Takeshima H., Nishimura S., Matsumoto T., Ishida H., Kangawa K., Minamino N., Matsuo H., Ueda M., Hanaoka M., Hirose T., et al. (1989). **Primary structure and expression from complementary DNA of skeletal muscle ryanodine receptor.** *Nature.* 339:439-45.

Terada S., Goto M., Kato M., Kawanaka K., Shimokawa T., and Tabata I. (2002). **Effects of low-intensity prolonged exercise on PGC-1 mRNA expression in rat epitrochlearis muscle.** *Biochem Biophys Res Commun* 296: 350-354.

Tothova J., Blaauw B., Pallafacchina G., Rudolf R., Argentini C., Reggiani C., and Schiaffino S. (2006). **NFATc1 nucleocytoplasmic shuttling is controlled by nerve activity in skeletal muscle.** *J Cell Sci* 119: 1604–1611.

Trivedi C.M., Zhu W., Wang Q., Jia C., Kee H.J., Li L., Hannenhalli S., Epstein J.A. (2010). **Hopx and Hdac2 interact to modulate Gata4 acetylation and embryonic cardiac myocyte proliferation.** *Dev Cell.* 19:450-459.

Tsika R.W., Schramm C., Simmer G., Fitzsimons D.P., Moss R.L., Ji J. (2008). **Overexpression of TEAD-1 in transgenic mouse striated muscles produces a slower skeletal muscle contractile phenotype.** *J Biol Chem.* 283:36154-36167.

Tsukamoto Y., Senda T., Nakano T., Nakada C., Hida T., Ishiguro N., Kondo G., Baba T., Sato K., Osaki M., Mori S., Ito H., and Moriyama M. (2002). **Arpp, a new homolog of carp, is preferentially expressed in type 1 skeletal muscle fibers and is markedly induced by denervation.** *Lab Invest* 82:645-655.

Tusher, V.G., Tibshirani R., and Chu G. (2001). **Significance analysis of microarrays applied to the ionizing radiation response.** *Proc.Natl.Acad.Sci.U.S.A.* 98:5116-5121.

Vale R.D., and Milligan. R.A. (2000). **The way things move: looking under the hood of molecular motor proteins.** *Science.* 288:88-95.

Wang D., and Bodovitz S. (2010). **Single cell analysis: the new frontier in 'omics'.** *Trends Biotechnol.* 28:281-290.

Wang Y.X., Zhang C.L., Yu R.T., Cho H.K., Nelson M.C., Bayuga-Ocampo C.R., Ham J., Kang H., and Evans R.M. (2004). **Regulation of muscle fiber type and running endurance by PPARdelta.** *PLoS Biol* 2: e294.

Welle S., Brooks A.I., Delehanty J.M., Needler N., and Thornton C.A. (2003). **Gene expression profile of aging in human skeletal muscle.** *Physiol Genomics.* 14:149-159.

Welle S., Tawil R., and Thornton CA. (2008). **Sex-related differences in gene expression in human skeletal muscle.** *PLoS ONE* 3: e1385.

Wright D.C., Han D.H., Garcia-Roves P.M., Geiger P.C., Jones T.E., and Holloszy J.O. (2007). **Exercise induced mitochondrial biogenesis begins before the increase in muscle PGC-1α expression.** *J Biol Chem* 282: 194-199.

Wu H., Gallardo T., Olson E.N., Williams R.S., and Shohet R.V. (2003). **Transcriptional analysis of mouse skeletal myofiber diversity and adaptation to endurance exercise.** *J Muscle Res Cell Motil* 24:587-592.

Wu H., Kanatous S.B., Thurmond F.A., Gallardo T., Isotani E., Bassel-Duby R., and Williams R.S. (2002). **Regulation of Mitochondrial Biogenesis in Skeletal Muscle by CaMK.** *Science* 296:349-352.

Wu H., Naya F.J., McKinsey T.A., Mercer B., Shelton J.M., Chin E.R., Simard A.R., Michel R.N., Bassel-Duby R., Olson E.N., and Williams R.S. (2000). **MEF2 responds to multiple calcium-regulated signals in the control of skeletal muscle fiber type.** *EMBO J* 19: 1963-1973.

Wu H., Rothermel B., Kanatous S., Rosenberg P., Naya F.J., Shelton J.M., Hutcheson K.A., DiMaio J.M., Olson E.N., Bassel-Duby R. and Williams R.S. (2001). **Activation of MEF2 by muscle activity is mediated through a calcineurin- dependent pathway.** *Embo J* 20:6414-6423.

Wu K.D., and Lytton J. (1993). **Molecular cloning and quantification of sarcoplasmic reticulum Ca2+-ATPase isoforms in rat muscles**. *Am J Physiol Cell Physiol* 264: C331-C341.

Wu Z., Puigserver P., Andersson U., Zhang C., Adelmant G., Mootha V., Troy A., Cinti S., Lowell B., Scarpulla R.C., and Spiegelman B.M. (1999). **Mechanisms controlling mitochondrial biogenesis and respiration through the thermogenic coactivator PGC-1.** *Cell* 98: 115-124.

Yan Z., Okutsu M., Akhtar Y.N., and Lira VA. (2011) **Regulation of exercise-induced fiber type transformation, mitochondrial biogenesis, and angiogenesis in skeletal muscle.** *J Appl Physiol.* 110:264-74.

Yang J., Rothermel B., Vega R.B., Frey N., McKinsey T.A., Olson E.N., Bassel-Duby R., and Williams R.S. (2000). **Independent signals control expression of the calcineurin inhibitory proteins MCIP1 and MCIP2 in striated muscles.** *Circ Res.* 87:E61-68.

7. ACKNOWLEDGMENTS

Firstly, I would like to thank Prof. Gerolamo Lanfranchi for giving me the opportunity to work in his lab. I specifically thank Paolo Laveder for his constant guidance and for his help in writing this thesis. I thank Camilla Bean and Francesco Chemello for their support in my research work. I wish also to thank Prof. Carlo Reggiani for his suggestions, Bert Blaauw for stimulation experiments, and Lina Cancellara for myofibers characterization.

Finally, I thank all those people who helped me in the laboratory during these years, in particular the staff of the MicroCribi Microarray Service (http://microcribi.cribi.unipd.it) for their assistance in microarray experiments and Chiara Romualdi for her help in data analysis.